

THE ROLE OF AMPK ACTIVATION IN THE ATTENUATION OF CHRONIC PAIN

by

Kufreobong Inyang



APPROVED BY SUPERVISORY COMMITTEE:

Theodore Price, Chair

Gregory Dussor

Christa McIntyre

Tres Thompson

Copyright 2019

Kufreobong Inyang

All rights Reserved

To my family

THE ROLE OF AMPK ACTIVATION IN THE ATTENUATION OF CHRONIC PAIN

by

KUFREOBONG INYANG, BA, MS

DISSERTATION

Presented to the Faculty of

The University of Texas at Dallas

in Partial Fulfillment

of the Requirements

for the Degree of

DOCTOR OF PHILOSOPHY IN

COGNITION AND NEUROSCIENCE

THE UNIVERSITY OF TEXAS AT DALLAS

December 2019

ACKNOWLEDGMENTS

Throughout my doctorate, I have received a great deal of support and assistance from a great number of people and I would like to take this chance to thank some of them. I would first like to thank my supervisor and mentor, Dr. Theodore Price, who provided much needed guidance that was instrumental to my success in this program. I am eternally grateful for his decision to take a chance on me despite my limited neuroscience background going into the program. You taught me a lot about how to be a scientist and how to empower someone that you're mentoring.

Besides my advisor, I would like to also thank the members of my committee (Dr. Gregory Dussor, Dr. Tres Thompson and Dr. Christa McIntyre) for their great support and invaluable advice. It's really easy to get caught up in my own relatively narrow world of AMPK. All of you have divergent areas of research expertise and have helped me think about my project as a neuroscientist rather than just a pain researcher. I would also like to thank you all for your cooperation with me and each other. I know it's not easy to fit reading this dissertation and my defense into your busy schedules.

I would also like to acknowledge all of my colleagues in the Price lab. I appreciate all the support that I've gotten from each of you over the years. Particularly, I would like to thank Galo Mejia and Dr. Michael Burton, our lab manager and former post-doc respectively, for teaching me many of the techniques used in my project and always being there to listen to my random experiment ideas as well as my long rants about sports. I wouldn't be the scientist I am today without y'all. I would also like to thank my

undergrads: Thomas Szabo-Pardi, Emma Wentworth, Eric Ramirez and Tim McDougal. Each of you contributed to my project greatly, and it was a pleasure mentoring and working with each of you. All of you are great scientists and I know you will all go on to do great things.

Next, I would like to thank my family and friends. I would like to start by thanking my parents for always pushing and challenging me to be the best they knew I could be. You were always there to give me the love and support that I needed, whether that be comfort when I was down or tough love when I needed to persevere. Thank you for never letting me give up and for setting greatness as the default expectation. I would also like to thank my sisters: Nya, Meyene and Ibet. Thanks for always being there to support me and your unwavering confidence in me even when I lost confidence in myself. There's no way I could fail with you guys as my support system and I hope that you are as proud of me as I am of each of you. I would also like to thank all of my friends who have supported me throughout this process and who have patiently listened to me talk about my project and my complaints about writing my dissertation.

Last but definitely not least, I would like to thank God. Everything I do is for the glory of God. Without Him, there is no way that I would have been able to make it through this program or through the various trials and tribulations that I've experienced in my personal life during the time of my PhD. I can do all things through Christ who strengthens me.

November 2019

THE ROLE OF AMPK ACTIVATION IN THE ATTENUATION OF CHRONIC PAIN

Kufreobong Inyang, PhD
The University of Texas at Dallas, 2019

Supervising Professor: Theodore Price

Chronic pain is a serious medical condition that impacts over 100 million Americans each year. Metformin is a widely prescribed drug used in the treatment of type II diabetes that has been repurposed as an analgesic. While the drug has many mechanisms of action, most of these converge on AMP activated protein kinase (AMPK), which metformin activates. AMPK is a multifunctional kinase that is a negative regulator of mechanistic target of rapamycin (mTOR) and mitogen activated protein kinase (MAPK) signaling. Activating AMPK decreases the excitability of dorsal root ganglion neurons and AMPK activators are effective in reducing chronic pain in inflammatory, post-surgical and neuropathic rodent models. We explored the behavioral effects of metformin in the SNI model in males and females. We are also aware of potential sex differences in microglia, immune cells of the CNS that play a key role in pain. We conducted experiments to investigate the effects of metformin on SNI-induced microglial activation, a process implicated in the maintenance of neuropathic pain that has recently been shown to be sexually dimorphic. Metformin cause a decrease in

mechanical hypersensitivity, cold allodynia and microglial activation in male mice but not in females. We then explored the effects of positive allosteric modulators of AMPK and indirect upstream activators of AMPK in male and female mice to treat incision-induced and paclitaxel-induced mechanical hypersensitivity. We used metformin as well as other structurally distinct AMPK activators, narciclasine (NCLS), ZLN 024 and MK 8722, to treat incision-induced and mechanical hypersensitivity and hyperalgesic priming in male and female mice. We found that metformin was the only AMPK activator to have sex specific effects. Indirect AMPK activators metformin and NCLS were able to reduce mechanical hypersensitivity and block hyperalgesic priming, direct AMPK activators, ZLN 024 and MK 8722 only blocked priming. Direct and indirect AMPK activators stimulated AMPK in DRG cultures to a similar degree. These AMPK activators were also tested for their ability to prevent and reverse paclitaxel-induced mechanical hypersensitivity. Drugs were given concurrently with paclitaxel then after the completion of paclitaxel treatment to test whether they prevent and reverse established mechanical hypersensitivity respectively. Unlike metformin, narciclasine also reversed mechanical hypersensitivity in established chemotherapy-induced peripheral neuropathy (CIPN). Both metformin, narciclasine and MK8722 prevented the development of hyperalgesic priming induced by paclitaxel treatment. MK8722 had no effect on mechanical hypersensitivity caused by paclitaxel in either the prevention or reversal treatment paradigms. Incision and CIPN decreased phosphorylated AMPK (p-AMPK) in DRG. Because AMPK phosphorylation is required for kinase activity, we concluded that indirect AMPK activators are more effective for treating pain hypersensitivity after

incision or paclitaxel treatment because they can drive increased p-AMPK through upstream kinases like liver kinase B1 (LKB1). Conversely, direct allosteric modulators of AMPK have decreased efficacy due to this injury-induced decrease in p-AMPK. From this, we concluded that indirect AMPK activators are more effective than positive allosteric modulators in producing disease modifying effects in chronic pain models. Moreover, the lack of sex-differences seen with narciclasine make it a particularly attractive candidate for subsequent preclinical pain research.

TABLE OF CONTENTS

ACKNOWLEDGMENTS.....	v
ABSTRACT.....	vii
LISTS OF FIGURES.....	xi
LIST OF TABLES.....	xix
CHAPTER 1 INTRODUCTION.....	1
CHAPTER 2 THE ANTIDIABETIC DRUG METFORMIN PREVENTS AND REVERSES NEUROPATHIC PAIN AND SPINAL CORD MICROGLIAL ACTIVATION IN MALE BUT NOT FEMALE MICE.....	24
CHAPTER 3 INDIRECT AMPK ACTIVATORS PREVENT INCISION-INDUCED HYPERALGESIA AND BLOCK HYPERALGESIC PRIMING WHILE POSITIVE ALLOSTERIC MODULATORS ONLY BLOCK PRIMING IN MICE.....	64
Appendix Supplementary Figures.....	108
CHAPTER 4 ALLEVIATION OF PACLITAXEL-INDUCED MECHANICAL HYPERSENSITIVITY AND HYPERALGESIC PRIMING WITH AMPK ACTIVATORS IN MALE AND FEMALE MICE.....	113
CHAPTER 5 DISCUSSION.....	142
BIBLIOGRAPHY.....	161
BIOGRAPHICAL SKETCH.....	174
CURRICULUM VITAE.....	175

LIST OF FIGURES

Figure 1.1: eIF4F and AMPK activation. Cap-dependent translation initiation requires the formation of the eIF4F complex comprised of the 4A, 4E and 4G subunits. AMPK activators inhibit the formation of the eIF4F complex and subsequent translation through the downregulation of the mTOR and ERK pathways.....	13
Figure 1.2: Types of AMPK activators. AMPK can be activated by positive allosteric modulators like ZLN 024 and MK 8722 that cause conformational changes or by modulating upstream targets metformin and narciclasine.....	14
Figure 2.1: Metformin treatment reverses SNI-induced mechanical and cold hypersensitivity in male mice: A-C. SNI surgery caused mechanical hypersensitivity in male mice as measured using the withdrawal frequency test. After treatment with Metformin, the response frequency was decreased for all filament weights. D. Cold hypersensitivity was induced by SNI and the effect was reduced after metformin administration. *p < 0.05; **p < 0.01; ***p < 0.001; ****p < 0.0001; ###p<0.001 versus BL; N= 9 for all groups.....	45
Figure 2.2: Metformin treatment does not influence SNI-induced mechanical or cold hypersensitivity in female mice: A-C. In female mice metformin failed to resolve mechanical hypersensitivity. Surgery (sham or SNI) induced a statistically significant difference from baseline for both groups ###p<.0001. D. A statistically significant increase in cold hypersensitivity was observed in the female SNI and the SNI + metformin group when compared to the vehicle group. *p < 0.05; **p < 0.01; ***p < 0.001; ****p < 0.0001; N= 6 per group.....	46
Figure 2.3: Metformin reverses microglial activation in SNI male mice: A-D. Representative immunohistochemistry images of the dorsal horn of male lumbar spinal cord at 20X magnification. Quantification of images shown in E. Metformin decreased SNI-induced microglia activation. SNI caused a loss of IB4 staining in the dorsal horn (A) that was reversed by metformin treatment (B) *p < 0.05; **p < 0.01; N= 5 per group.....	47
Figure 2.4: Metformin does not reverse microglial activation in SNI female mice: A-D. Representative immunohistochemistry images of the dorsal horn of female lumbar spinal cord at 20X magnification. Quantification of images shown in E. SNI robustly stimulated microglial activation in female SNI mice, but metformin had no effect. A loss of IB4 staining was not observed in female SNI mice (A-B). ***p < 0.001; N= 5 per group.....	48

Figure 2.5: Metformin does not reverse astrocyte proliferation in SNI male mice: A-D. Representative immunohistochemistry images of the dorsal horn of male lumbar spinal cord at 20X magnification. Quantification of images shown in E. SNI robustly stimulated astrocyte proliferation in male mice, but metformin had no effect. ***p < 0.01; N= 5 per group.....49

Figure 2.6: SNI did not result in an increase in astrocytes in the spinal dorsal horn of female mice: A-D. Representative immunohistochemistry images of the dorsal horn of female lumbar spinal cord at 20X magnification. Quantification of images shown in E. SNI did not cause an increase in the number of astrocytes seen in the dorsal horn of female mice. N= 5 per group.....50

Figure 2.7: Preemptive treatment with metformin for 7 days prior to SNI inhibits neuropathic pain in male mice: Male mice were given metformin for 7 days prior to SNI. Mechanical hypersensitivity was inhibited at indicated time points after SNI. *p < 0.05; **p < 0.01; #p<0.05 versus BL. N= 6.....51

Figure 2.8: Treatment with metformin for the first 7 days after SNI inhibits neuropathic pain in male mice: Male mice were given metformin for 7 days starting at the day of SNI surgery. Mechanical hypersensitivity was inhibited at the indicated time points after SNI. D. Metformin also decreased in cold hypersensitivity after SNI. *p < 0.05; **p < 0.01; ***p < 0.001; ****p < 0.0001; N= 6 per group.....52

Figure 2.9: Early treatment with metformin blocks SNI-induced microglial activation in male mice: A-B. Representative immunohistochemistry images of the dorsal horn of male lumbar spinal cord at 20X magnification. Quantification of images shown in C. Metformin decreased SNI-induced microglia activation. SNI caused a loss of IB4 staining in the dorsal horn (A) that was reversed by metformin treatment for the first 7 days after surgery (B). *p < 0.05; N= 5 per group.....53

Figure 2.10: Treatment with metformin for the first 7 days after SNI failed to inhibit neuropathic pain in female mice: A-C. Female mice were given metformin for 7 days starting at the day of SNI surgery. Mechanical hypersensitivity was not inhibited at the indicated time points after SNI. D. Metformin also did not decrease cold hypersensitivity after SNI. N= 4 per group.....54

Figure 2.11: Early treatment with metformin does not block SNI-induced microglial activation in female mice: A-B. Representative immunohistochemistry images of the dorsal horn of female lumbar spinal cord. Quantification of images shown in C. Metformin did not decrease SNI-induced microglia activation. Again, SNI did not cause a loss in IB4 staining in female mice that was seen in males following SNI. N= 6 per group.....55

Figure 2.12: Metformin induces AMPK activity in male and female DRG neurons *in vitro*. Male and female neuron cultures were treated with metformin (20 mM) for 1 hr. A-B (male), D-E (female). Representative immunohistochemistry images of the DRG neurons at 40X magnification. Quantification of images shown in C (male) and F (female). Metformin increased p-ACC intensity in male and female neuron cultures. Only neurons that were positive for peripherin staining were analyzed. Maximum fluorescence refers to the maximum fluorescence intensity per neuron analyzed. **p < 0.01; ***p < 0.001. N= 20 images analyzed per group.....56

Figure 2.13: Metformin induces AMPK activity in male and female microglia *in vitro*. Male and female microglia cultures were treated with metformin (20 mM) for 1 hr. A-B (male), D-E (female). Representative immunohistochemistry images of the DRG neurons at 40X magnification. Quantification of images shown in C and F. Metformin increased p-ACC intensity in male and female microglia cultures. Only microglia that were positive for Iba1 staining were analyzed. Maximum fluorescence refers to the maximum fluorescence intensity per microglial cell analyzed. *p < 0.05. N= 20 images analyzed per group.....57

Figure 3.1: Metformin treatment attenuates incision-induced mechanical hypersensitivity and blocks hyperalgesic priming in male mice. A-C. Metformin treatment starting immediately after baseline measurements, which were done 3 days prior to plantar incision, decreased mechanical hypersensitivity following plantar incision surgery and prevented plantar incision-induced hyperalgesic priming precipitated by PGE2 injection. D-F: In female mice, metformin treatment failed to decrease mechanical hypersensitivity compared to vehicle treated mice. Metformin also failed to prevent plantar incision-induced hyperalgesic priming precipitated by PGE2 injection. ***p < 0.001; treatment effect; N= 6 for the metformin groups and N= 5 for the vehicle groups.....87

Figure 3.2: Male and female mice recover from plantar incision surgery at the same rate. A-C. Plantar incision surgery in male and female mice caused an increase in mechanical hypersensitivity that resolved at the same rate with no significant differences in mechanical hypersensitivity. N= 21 males and N= 18 females.....88

Figure 3.3: Narciclasine treatment attenuates surgery-induced mechanical hypersensitivity and blocks hyperalgesic priming in male and female mice. A-C. Narciclasine treatment starting immediately after baseline measurements dose-dependently decreased mechanical hypersensitivity following plantar incision surgery and prevented plantar incision-induced hyperalgesic priming precipitated by PGE2 injection at all doses. *p < 0.05; **p < 0.01; ***p < 0.001; N= 4 for the NCLS groups and N= 3 for the vehicle group. D-F. Narciclasine treatment also decreased mechanical hypersensitivity following plantar incision surgery and prevented surgery-induced hyperalgesic priming precipitated by PGE2 injection. *p < 0.05; **p < 0.01; ***p < 0.001; N= 6 for the NCLS group and N= 6 for the vehicle group.....89

Figure 3.4: Narciclasine induces AMPK activity in male DRG neurons in vitro. Male neuron cultures were treated with vehicle (A), 100 nM (B) or 1 μ M narciclasine (NCLS) (C) for 1 hr. Representative immunohistochemistry images of the DRG neurons at 40X magnification. Quantification of images shown in D. 1 μ M NCLS increased p-ACC intensity in neuron cultures. Only neurons that were positive for peripherin staining were analyzed. Maximum florescence refers to the maximum florescence intensity per neuron analyzed. **p < 0.01. N= 39 images analyzed per group.....90

Figure 3.5: Narciclasine increases AMPK signaling in male and female DRGs. A single dose of NCLS (3 mg/kg) caused a significant increase in AMPK signaling in DRGs for male (A) and female (C) mice 1 hr post-injection while not effecting AMPK signaling in liver for male (B) or females (D). NCLS treatment increased the ratio of p-AMPK to total-AMPK in male (E) and females (G) DRGs but not in male (F) or female (H) liver. *p < 0.05; students t-test; N= 4 per condition in male mice; N= 4 for female NCLS treatment and N=3 for female vehicle.....91

Figure 3.6: ZLN-024 treatment blocks hyperalgesic priming in male and female mice but had no effect on acute incision-induced mechanical hypersensitivity. A-F. While ZLN-024 treatment starting immediately after baseline measurements had no effect on initial mechanical hypersensitivity following plantar incision surgery, drug treatment was effective in prevention of plantar incision-induced hyperalgesic priming precipitated by PGE2 injection in male (A-C) and female (D-F) mice. *p < 0.05; **p < 0.01; ***p < 0.001; ****p < 0.0001; N= 6 for the ZLN-024 group and N= 6 for the vehicle group.....92

Figure 3.7: MK8722 treatment blocks hyperalgesic priming in male and female mice but had no effect on acute incision-induced mechanical hypersensitivity. A-F. While MK8722 treatment starting immediately after baseline measurements had no effect on initial mechanical hypersensitivity following plantar incision surgery, drug treatment was effective in prevention of plantar incision-induced hyperalgesic priming precipitated by PGE2 injection in male (A-C) and female (D-F) mice. *p < 0.05; **p < 0.01; ***p < 0.001; ****p < 0.0001; N= 6 for the MK8722 group and N= 5 for the vehicle group.....93

Figure 3.8: Local MK8722 treatment attenuates hyperalgesic priming in male and female mice but had no effect on acute incision-induced mechanical hypersensitivity. Local injection of MK8722 at the time of incision and again 24 hrs later (red arrows) had no effect on initial mechanical hypersensitivity following plantar incision surgery in males or females. However, drug treatment was effective in prevention of plantar incision-induced hyperalgesic priming precipitated by PGE2 injection in male (A-C) and female (D-F) mice. *p < 0.05; **p < 0.01; ***p < 0.001; N= 4 for the MK8722 group and N= 4 for the vehicle group in both males and females.....94

Figure 3.9: MK8722 induces AMPK activation in DRG neurons in vitro. Neuron cultures were treated with vehicle (A), 100 nM (B) or 10 μ M MK 8722 (C) for 1 hr. Representative immunohistochemistry images of the DRG neurons at 40X

magnification. Quantification of images shown in D. 100 nM and 10 μ M NCLS increased p-ACC intensity in male neuron cultures. Only neurons that were positive for peripherin staining were analyzed. Maximum florescence refers to the maximum florescence intensity per neuron analyzed. ** $p < 0.01$; *** $p < 0.001$. N= 39 images analyzed per group. E) Shows a full concentration-response curve of MK8722 with an approximate EC50 of 900 nM (95% confidence interval 253 nM – 2.62 μ M).....95

Figure 3.10: Incision decreases AMPK signaling in injured lumbar DRGs. A) Plantar incision caused a decrease in p-AMPK signaling in ipsilateral lumbar DRGs 2 hrs post-surgery measured by Western blot. B) Incision decreased the ratio between p-AMPK and total-AMPK in the ipsilateral DRGs compared to the side contralateral from the injury. ** $p < 0.01$; students t-test; N= 5 per condition in male mice.....96

Figure 3.11: Effects of metformin on sham male mice. A-C. Metformin treatment had no effect on the mechanical sensitivity of sham male mice and did not induce hyperalgesic priming. D. Metformin also had no effect on locomotor activity and coordination as indicated by their performance on the rotarod compared to the vehicle group. N = 4 for the metformin (200 mg/kg) group and N = 4 for the vehicle group.....108

Figure 3.12: Lower doses of metformin treatment failed to attenuate incision-induced mechanical hypersensitivity or blocks hyperalgesic priming in female mice. A-C. Metformin treatment at 100 and 50 mg/kg failed to decrease mechanical hypersensitivity compared to vehicle treated mice. Metformin also failed to prevent plantar incision-induced hyperalgesic priming precipitated by PGE2 injection. N= 4 for the metformin groups and N= 4 for the vehicle group.....109

Figure 3.13: Sex differences in pharmacokinetics of metformin. Male and female mice were given metformin (200 mg/kg, i.p.) and then plasma (A) and brain (B) were taken at the indicated time points. (C) Brain to plasma ratios were calculated at each time point per sex and were not different between sexes. Two-way ANOVA with Bonferroni post hoc test. * $p < 0.05$, ** $p < 0.01$; *** $p < 0.001$. N= 3 per group.....110

Figure 3.14: Effects of narciclasine on sham male mice. A-C. NCLS treatment had no effect on the mechanical sensitivity of sham male mice and did not induce hyperalgesic priming. D. NCLS also had no effect on locomotor activity and coordination as indicated by their performance on the rotarod compared to the vehicle group. N= 4 for the NCLS group and N= 4 for the vehicle group.....111

Figure 3.15: Effects of MK8722 on sham male mice. A-C. MK8722 treatment had no effect on the mechanical sensitivity of sham male mice and did not induce hyperalgesic priming. D. MK8722 also had no effect on locomotor activity and coordination as indicated by their performance on the rotarod compared to the vehicle group. N= 4 for the MK8722 group and N= 4 for the vehicle group.....112

Figure 4.1: Paclitaxel induced hyperalgesic priming in male mice. A-C. Paclitaxel treatment caused an increase in mechanical hypersensitivity. Following resolution of this hypersensitivity, PGE₂ was able to cause an increase in response frequency indicating the presence of hyperalgesic priming. ***p < 0.001; N = 4 per group.....131

Figure 4.2: Metformin attenuated paclitaxel-induced hyperalgesic priming in male and female mice. A-F. In male and female mice, metformin treatment immediately following a 7-day paclitaxel treatment failed to reverse CIPN but blocked attenuated subsequent hyperalgesic priming precipitated by PGE₂. *p < 0.05, **p < 0.01, ***p < 0.001; N = 4 per group.....132

Figure 4.3: Narciclasine (NCLS) blocks attenuated paclitaxel-induced mechanical hypersensitivity and hyperalgesic priming in males and females. A-C. NCLS blocked attenuated the development of CIPN in male mice when give concurrently with paclitaxel and blocked attenuated hyperalgesic priming precipitated by PGE₂. *p < 0.05; **p < 0.01; ***p < 0.001; N = 6 for NCLS group and vehicle group. D-F. NCLS prevented CIPN in female mice when given concurrently with paclitaxel treatment and blocked attenuated hyperalgesic priming precipitated by PGE₂. *p < 0.05; **p < 0.01; ***p < 0.001; N = 6 for NCLS group and N = 6 for vehicle group.....133

Figure 4.4: Narciclasine partially reverses paclitaxel-induced mechanical hypersensitivity and blocks priming in male and females. A-C. NCLS reverses CIPN in male mice when give immediately following paclitaxel treatment and blocked hyperalgesic priming precipitated by PGE₂. *p < 0.05; **p < 0.01; ***p < 0.001; N = 6 for the NCLS group and N = 6 for the vehicle group. D-F. NCLS reversed CIPN in female mice when given immediately following 7-day paclitaxel treatment and blocked attenuated hyperalgesic priming precipitated by PGE₂. *p < 0.05; **p < 0.01; ***p < 0.001; N = 5 for the NCLS group and N = 5 for the vehicle group.....134

Figure 4.5: MK8722 attenuates paclitaxel-induced hyperalgesic priming in male and female mice when given concurrently with paclitaxel. A-C. MK8722 did not block attenuate the development of CIPN in male mice when give concurrently with paclitaxel but was effective in blocking attenuating hyperalgesic priming precipitated by PGE₂. ***p < 0.001; N=6 for MK8722 group and vehicle group. D-F. MK8722 failed to prevent CIPN in female mice when given concurrently with paclitaxel treatment but again attenuated hyperalgesic priming precipitated by PGE₂. *p < 0.05; **p < 0.01; ***p < 0.001; N= 4 for NCLS and vehicle group.....135

Figure 4.6: MK8722 attenuates paclitaxel-induced hyperalgesic priming in male and female mice when given after paclitaxel treatment. A-C. MK8722 did not reverse CIPN in male mice when given following paclitaxel but was effective in reducing hyperalgesic priming precipitated by PGE₂. *p < 0.05; **p < 0.01; N = 6 for MK8722 group and vehicle group. D-F. MK8722 failed to reverse CIPN in female mice when given immediately following 7-day paclitaxel treatment but again inhibited hyperalgesic priming precipitated by PGE₂. *p < 0.05; **p < 0.01; ***p < 0.001; N = 4 for MK8722 and vehicle group.....136

Figure 5.1: Narciclasine reduced SNI-induced cold allodynia. Two weeks post-SNI, 7-day narciclasine treatment failed to reduce mechanical hypersensitivity (A) but caused a reduction in cold allodynia (B).....159

LIST OF TABLES

Table 1.1: AMPK activators in Pain.....	15
Table 2.1: Statistical tests and values.....	58
Table 3.1: Statistical test values given by figure number and panel.....	97
Table 3.2: Metformin PK study.....	106
Table 4.1: Statistical test values given by figure number and panel.....	137
Table 5.1: Systemic AMPK activators in the incision model.....	160

CHAPTER 1

INTRODUCTION

Chronic Pain is a problem

Chronic pain is a rapidly growing national health crisis that impacts over 100 million Americans with a yearly cost of \$600 billion in lost productivity and healthcare expenditures (Simon 2012). Pain is defined as an unpleasant sensory or emotional experience usually from actual or potential tissue damage (Merskey H 1986). Chronic pain is recognized as pain that lasts longer than normal healing time (Bonica and Hoffman) to the point where it no longer has physiological benefit. Pain is usually considered chronic when it lasts or is recurring for at least 3 months (Merskey H 1994). This pain is typically characterized by persistent physical pain, disability, emotional disturbance, and social withdrawal symptoms (Hylands-White, Duarte et al. 2017). According to a 2011 Institute of Medicine report, treatment of chronic pain is largely unsuccessful despite the extreme costs (Simon 2012). In addition to the financial cost, chronic pain also has an enormous psychological impact on those suffering from it.

Treatment of chronic pain is largely ineffective

Treatment of chronic pain typically involves a mixture of medical, physical and psychological components (Hylands-White, Duarte et al. 2017). Some forms of chronic pain require surgical intervention (Min et al. 2019; Best et al. 2019) which has shown very limited effectiveness in alleviating symptoms (Jonas et al. 2018). This is typically reserved for pain caused by degenerative diseases such as disk degeneration

(Takaishi, Okada et al. 2019). Additionally, post-surgical pain is one of the most common forms of chronic pain (Haroutiunian et al. 2013) causing impairment in nearly 10% of surgical patients which contributes to the limited efficacy of surgical intervention of pain (Kehlet, Jensen et al. 2006). The forms of chronic pain we used in this study are the spared nerve injury model for neuropathic pain from trauma, the plantar incision model for post-surgical pain and the paclitaxel model for chemotherapy induced peripheral neuropathy.

The first model of chronic pain that we used was the spared nerve injury (Decosterd, 2000) model. In this model, the sciatic nerve was isolated and the common peroneal and tibial nerve branches were severed leaving the sural nerve intact (Decosterd and Woolf 2000). This surgery produced robust mechanical and cold hypersensitivity on the area of the hindpaw innervated by the sural nerve as well as a guarding of the affected paw (Xie, Strong et al. 2017) that is permanent if left untreated. The purpose of this model is to mimic neuropathic pain from major trauma such as the removal of a limb. Gabapentin and pregabalin are considered first line pharmaceutical options while capsaicin patches and opioids are considered second- and third-line option respectively (Gilron, Baron et al. 2015).

The second model for chronic pain that we used was the plantar incision model for post-surgical pain. The purpose of this model is to examine acute post-surgical pain as well as pain plasticity because this model creates a state in which animals are more susceptible to hypersensitivity from subthreshold insults following the resolution of an initial injury (Reichling and Levine 2009, Price and Inyang). In this model, a 5-mm

incision was made in the hindpaw 2 mm below the heel and the wound was sutured using coated Vicryl sutures (Banik et al. 2006). This caused a short term acute mechanical hypersensitivity that resolves in about 2 weeks. Following the resolution of this initial injury, hyperalgesic priming was tested by giving each animal an intraplantar injection of prostaglandin E2 (PGE2) (Dina, Green et al. 2008, Reichling and Levine 2009) as a preclinical way of mimicking aspects of the transition from acute to chronic pain. Post-operative pain is generally managed and prevented using opioids and local nerve blocks with varying efficacy (Lovich-Sapola, Smith et al. 2015). Creation of non-opioid analgesics for post-surgical pain would benefit patients and caretakers.

The final model that we used was the paclitaxel model for chemotherapy-induced peripheral neuropathy (Areti et al.). CIPN presents itself in 30-40% of chemotherapy patients (Pachman et al. 2011) and is characterized by a glove-and-stocking distribution of pain (Seretny et al. 2014). We induced CIPN using the chemotherapy drug paclitaxel. CIPN was induced using paclitaxel given via intraperitoneal injection every other day for one week for a cumulative dose of 16 mg/kg (Megat et al. 2019). As with the post-surgical pain model, we also test hyperalgesic priming using intraplantar PGE2 to assess the transition from acute to chronic pain. Hyperalgesic priming has not been tested in the paclitaxel model, so we first planned to test whether this model produces a priming effect like what has previously been shown in the incision model (Tillu et al. 2012). As with injury induced neuropathy, gabapentin is one of the most commonly prescribed drugs for CIPN, but it shows limited efficacy (Hu et al. 2019).

Therapeutic exercises are often part of prescribed chronic pain treatments.

Conventional therapeutic exercises as well as various forms of yoga are effective in treatment of chronic pain when done over an extended period of time (Wieland, Skoetz et al. 2017, Neyaz, Sumila et al. 2019). Exercise regiments that include aerobics and resistance training under the supervision of a professional can have robust effects on chronic musculoskeletal pain (Mee-Inta, Zhao et al. 2019). While things like yoga can be effective at times, the analgesic benefits seem to be largely specific to lower back pain (Goode, Coeytaux et al. 2016, Wieland, Skoetz et al. 2017) and largely contingent on the patient's ability to be able to perform the necessary exercises. It is not fully understood how exercise causes an analgesic effect. Exercise has been linked to the activation of 5' adenosine monophosphate-activated protein kinase or AMPK (Areti et al.) (Narkar et al. 2008). Although exercise can be very effective in humans, not all people are able to exercise and there are situations where it cannot be used, such as right after surgery. The efficacy of exercise and its known connection to AMPK activation suggests that AMPK activation may be part of the mechanism that links exercise to pain relief. While we did not study exercise in this dissertation, we do focus on AMPK as a potential pain relief target.

Opioids have been part of chronic pain management for centuries and has emerged as a solution to non-cancer pain particularly over the past few decades (Dart, Severtson et al. 2015). There have been several comprehensive reviews of the effects of opioids in chronic pain treatment (Chou et al. 2015; Kalso et al. 2004; Noble et al. 2010) that suggest opioids have limited efficacy and many adverse effects including sedation,

dizziness, nausea and respiratory depression (Camilleri, Lembo, and Katzka 2017; Chen and Ashburn 2015; Benyamin et al. 2008). Opioids also have a strong addictive component. In America, there is a well-documented opioid addiction epidemic (Thapa et al. 2019; Salsitz and Wiegand 2016; Stoicea et al. 2019) that has led to deaths at an alarming rate (Rudd et al. 2016). This has necessitated the exploration of new pharmaceuticals as the amount of opioids being prescribed continues to skyrocket (Dorn, Meek et al. 2011, Szigethy, Knisely et al. 2018).

One of the leading opioid alternatives being prescribed for chronic pain is gabapentin (Rai et al. 2017; Senderovich and Jeyapragasan 2018). While gabapentin has shown to be effective particularly in combating neuropathic pain specifically (Cavalli et al. 2019), there is evidence that the drug causes cognitive impairments (Shiers et al. 2018) greater than those caused by neuropathic pain (Moriarty et al. 2017). Gabapentin also does not appear to be as effective for other forms of pain (Eloy et al. 2017) making it less than ideal as chronic pain analgesic. Similar to opioids, gabapentin has been shown several incidences of abuse, withdrawal and dependence (Victorri-Vigneau, Guerlais et al. 2007, Mersfelder and Nichols 2016). An ideal chronic pain analgesic would have the effectiveness of gabapentin without the negative cognitive effects while showing effectiveness across several different forms of chronic pain.

eIF4F and its modulation through AMPK activation

Despite the presence of various analgesics that vary in their ability to relieve pain, there is a need for more effective drugs. Several labs in the pain field are currently working

with drugs that prevent and inhibit pain through the inhibition of translation of genes related to pain. As with most forms of long-lasting neuroplasticity, chronic pain requires protein synthesis (Costa-Mattioli et al. 2009). Some of the key kinases involved in the initiation of neural plasticity in relation to pain are mammalian target of rapamycin (Atef et al.) and extracellular regulated kinase (Asiedu, Han et al. 2017), which signal to eukaryotic initiation factors (Seifarth, Schehler et al. 2013) eIF4E, eIF4G and the eIF4E binding protein (Atef, El-Sayed et al. 2019). (Sonenberg and Hinnebusch 2009) which together form the eIF4F complex. Local translation initiated by the eIF4F complex on the axons of primary afferent neurons is essential for the initiation and maintenance of elevated levels of pain (Jimenez-Diaz, Geranton et al. , Price and Geranton). While pain conditions cause an increase in eIF4F signaling (Melemedjian et al. 2010), the formation of the eIF4F complex can be inhibited through the concurrent inhibition of the mTOR and ERK signaling pathways through the activation of adenosine monophosphate kinase (Areti et al.) as shown in figure 1 (Tillu et al. 2012). AMPK is a heterotrimer kinase consisting of a catalytic subunit, α , and 2 regulatory subunits, β and γ (Hardie , Hardie, Ross et al. 2012). This kinase is involved in intercellular energy homeostasis as well as cell migration and proliferation (Zhao et al. 2018). In order to be activated, AMPK α must be phosphorylated at the threonine 172 (Zhang, Xu et al. 2013) (Stein et al. 2000). While our early experiments were done with resveratrol, there are some major issues with this compound that likely limits its applicability to most patients. The biggest issue with resveratrol is that it has very limited oral bioavailability so it

cannot likely be used to engage AMPK in people that have neuropathic, visceral or certain post-surgical pain types.

Types of AMPK activators

In general, AMPK activators broadly fall into 2 categories: direct positive allosteric modulators and indirect AMPK activators. Positive allosteric modulators cause conformational changes to the structure of AMPK resulting in greater activation through the phosphorylation of Thr-172 in the AMPK α subunit as previously described. Indirect AMPK activators cause an activation in AMPK by modulation of upstream kinases. In the case of the plant-derived compound narciclasine, that upstream target that acts on AMPK is cAMP (Zhang, Zhou et al. 2009) while LKB1 is involved with AMPK activation for metformin (Shaw et al. 2005). While both direct and indirect AMPK activators have shown to be effective in vitro (Marrone et al. 2018; Myers et al. 2017; Rarova et al. 2019; Asiedu et al. 2017), most of the work our lab that was done with AMPK in pain involves indirect AMPK activators (Mejia et al. 2016; Burton et al. 2017). In the incision model, we have seen indirect AMPK activators are effective in attenuating acute mechanical hypersensitivity as well as blocking hyperalgesic priming (Burton et al. 2017; Mejia et al. 2016). Table 1 displays a comprehensive list of the preclinical publications that have used AMPK activators in rodent pain models. Metformin is the most commonly used AMPK activator in preclinical models but has predominantly been used in males. We compared some of these indirect AMPK activators to direct AMPK activators in the incision and paclitaxel models. Our initial hypothesis was that the direct

AMPK activators will have a stronger anti-hyperalgesic effect since they more directly impact AMPK rather than going through other kinases that could dampen their effects.

Metformin as the imperfect premier AMPK activator

Metformin is a commonly prescribed type II diabetes drug. This drug activates AMPK in a liver kinase B1 (Dasgupta and Milbrandt 2007) dependent manner classifying it as an indirect AMPK activator since it does not directly act on AMPK (Shaw et al. 2005).

Because of its AMPK related activity, metformin is being repurposed as a pain drug.

Metformin has shown to be effective in reversing surgery-induced neuropathic pain in mice and rat models (Melemedjian OK 2011; Ge et al. 2018) as well as models of post-surgical pain prevention (Burton et al. 2017). Metformin is also effective in the prevention of chemotherapy-induced peripheral neuropathy from paclitaxel and cisplatin (Mao-Ying, Kavelaars et al. 2014). While metformin appears to be a very promising AMPK activator that can be used as an analgesic, there are still a lot of unknowns and potential issues with the drug. Metformin's mechanism of action is still largely unknown and not very specific to AMPK (Ikhlas and Ahmad 2017, Rena, Hardie et al. 2017). This has led to the additional investigation of other AMPK activators. Narciclasine (Inyang et al.) is a natural compound from the plant Amaryllidaceae (Dumont et al. 2007) that activates AMPK (Julien SG 2017) indirectly through a mechanism that involves cAMP (Zhang, Zhou et al. 2009) and has shown an ability to combat inflammation (Yui et al. 2001). While this is the only published mechanism, we do not believe that it is likely to be the relevant AMPK related mechanism of NCLS. Activating cAMP causes an increase in protein kinase A (Aley and Levine 1999, Pierce, Premont et al. 2002). PKA is known to

play a role in the establishment (England, Bevan et al. 1996) and maintenance of inflammatory pain (Aley and Levine 1999). We also looked at positive allosteric modulators MK8722 (Feng et al. 2018; Weihrauch and Handschin 2018) and ZLN-024 (Zhang, Xu et al. 2013) that work directly on AMPK. These drugs cause conformational changes in the structure of AMPK but are dependent on phosphorylation of Thr-172 in the AMPK α subunit (Hawley et al. 1996; Stein et al. 2000). We explored these AMPK activators of different mechanisms of action across several different pain models to determine what the direction of subsequent research for AMPK as an analgesic. One of the key advantages of metformin over the other AMPK activators is that it is an FDA approved drug without many significant negative side effects. Our initial hypothesis was that all these AMPK activators will be effective without major side effects.

Metformin effects in people- not much evidence of sex differences

Metformin has long been used in humans as a type II diabetes drug. The mechanism of action for diabetes treatment is relatively well understood. Metformin decreases fasting insulin concentrations (Turner R 1998), enhancing glucose sensitivity, and decreases hepatic glucose output (Cusi, Consoli et al. 1996). In years of clinical trials and metformin treatment of diabetes, there is considerable evidence that this drug is equally effective in both men and women at preventing type II diabetes and causing weight loss (Glechner et al. 2015; Gillett et al. 2012) despite sex differences in age of onset, detection and burden of the disease (Glechner et al. 2015). Considering this lack of sex difference in metformin treatment, we did not expect there to be sex differences in pain treatment with metformin. In addition to being able to prevent and/or treat diabetes,

metformin also showed an ability to reverse existing diabetic symptoms (Gow et al. 2017). This leads us to the hypothesis that metformin should be able to prevent chronic pain as well as reverse it which our lab has already established to be true for neuropathic pain in mice (Melemedjian OK 2011).

Sex differences in pain

Until recently, sex was an underexplored variable in clinical and preclinical research (Clayton and Collins 2014). Some studies have shown that there are some sex differences in the development and maintenance of chronic pain (Mapplebeck, Beggs et al. 2017). One of the key differences between chronic pain in males and females are the immune cells involved in its maintenance. While microglia appear to have a very important role in male mice (Tsuda 2016), they do not appear to play the same role in females (Sorge et al. 2015). Rather T cells have been shown to be the key immune cells for female chronic pain (Sorge and Totsch 2017; Laumet et al. 2019). This is further complicated by the fact that male and female mice have comparable levels of microglial activation following injury (Sorge et al. 2015). It has been suggested that while males and females have a similar microglial pain maintenance system, females default to using T-cell as a main method of cytokine release following injury (Sorge and Totsch 2017). We plan to explore the effects of metformin on microglia in male and female mice. We hypothesize that metformin will influence microglia in male but female mice. In addition to microglia, male mice also show a more robust astrocyte response to neuropathic pain (Bennett and Xie 1988).

There is also evidence of sex differences in the way that pain is experienced and reported. Women generally tend to report have lower pain thresholds (Riley, Gilbert et al. 1998) and report more pain from similar stimuli than men (Miller and Newton 2006). Similar behavioral sex differences have been observed in mouse models. Female mice show greater allodynia and a longer recovery time in multiple neuropathic pain models (Vacca et al. 2014; Nicotra et al. 2014). It is unclear why there is a difference between male and female pain. One obvious potential cause of this difference between male and female pain relates to the difference in sex hormones. One of the main differences between males and females is that males have more testosterone while females have more estrogen. While this may contribute to sex differences to some extent, this does not provide a through explanation. In children while there are far fewer instances of sex differences in pain, girls still showed a lower pain threshold and higher sensitivity (Boerner, Birnie et al. 2014).

There is also a link between some of the immune cells implicated in pain and sex hormones. Testosterone has been shown to decrease T cell activity through decreasing T-helper cell function (Grossman, Roselle et al. 1991) and CD4+ T-cell differentiation (Kissick et al. 2014). Higher levels of testosterone in men causing a downregulation in CD4+ T cells has also been linked to the lower incidence of autoimmune diseases in males compare to females (Trigunaite, Dimo et al. 2015). Auto immune diseases have many different presentations, autoreactive T cells is a common underlying theme in all of these conditions (Mifflin and Kerr 2017). Some of these sex differences in T cells function such as differences in morphine analgesia are absent in neutered male and

female mice (Rosen et al. 2019). This is relevant because many autoimmune diseases are associated with chronic pain in the peripheral nervous system (Morrison et al. 2013; Green, Krishnareddy, and Lebowhl 2015) and these diseases are roughly 3 times more common in women compared to men (Hayter and Cook 2012). Opioids are often used to treat pain associated with a wide variety these autoimmune disease such as rheumatic diseases (Lang et al. 2010; Somers et al. 2019), diabetic neuropathy (Peltier, Goutman et al. 2014) and fibromyalgia (Clauw 2015) which are more common in women than in men (Ngo, Steyn et al. 2014).

So far, our lab has shown that metformin is effective for treating neuropathic pain in (Melemedjian OK 2011) as well as incisional pain (Burton et al. 2017) males. In the work in this dissertation, we plan to explore potential sex differences with metformin as well as other AMPK activators. Specifically, we plan to look at the anti-hyperalgesic effects of these drugs and potential sex differences in the SNI model, the plantar incision model and the paclitaxel model of CIPN. Our hypothesis was that AMPK activators will be equally effective in males and females for treating pain. This overarching hypothesis turned out to be true for some AMPK activators and not for others. The following chapters describe our work on optimizing and furthering our understanding of how AMPK activators might best be used for the treatment of pain.

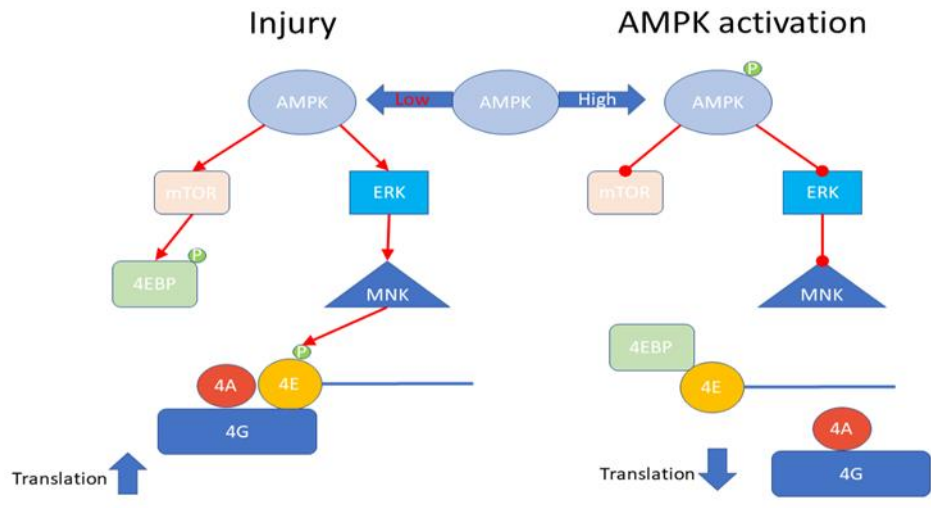


Figure 1.1: eIF4F and AMPK activation. Cap-dependent translation initiation requires the formation of the eIF4F complex comprised of the 4A, 4E and 4G subunits. AMPK activators inhibit the formation of the eIF4F complex and subsequent translation through the downregulation of the mTOR and ERK pathways.

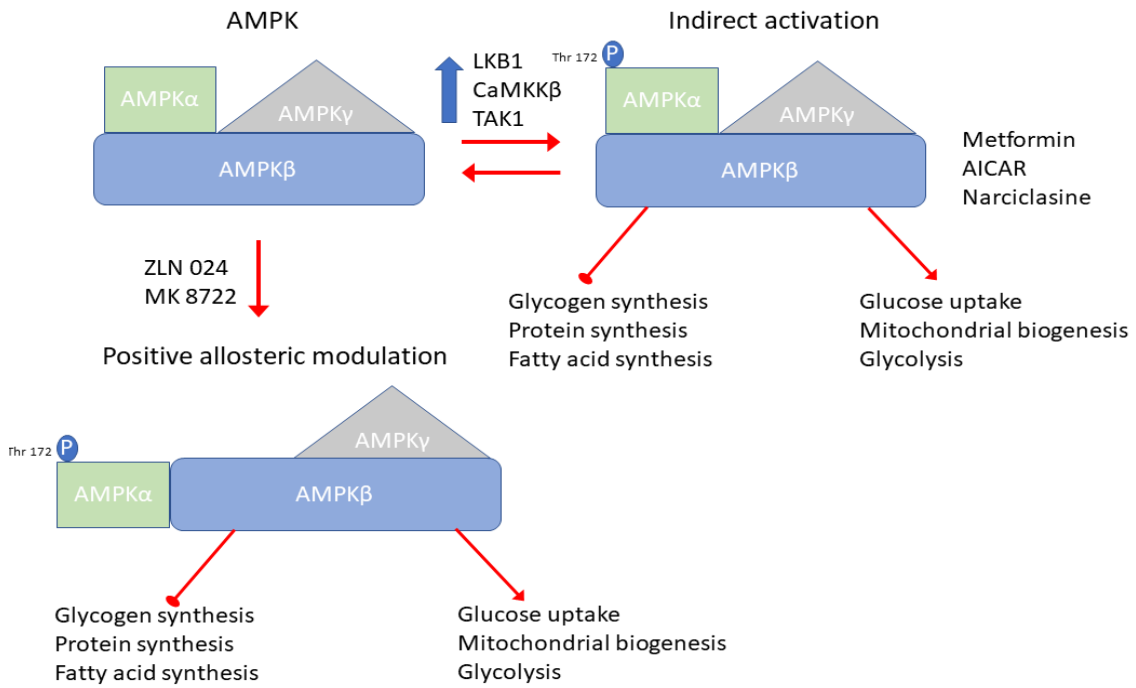


Figure 1.2: Types of AMPK activators. AMPK can be activated by positive allosteric modulators like ZLN 024 and MK 8722 that cause conformational changes or by modulating upstream targets metformin and narciclasine.

Table 1.1: AMPK activators in Pain

Title	Authors	Model	Compound	Sex	Time of administration
Resveratrol engages AMPK to attenuate ERK and mTOR signaling in sensory neurons and inhibits incision-induced acute and chronic pain	Tillu DV et al. (Tillu, Melemedjian et al. 2012)	Plantar incision	Resveratrol (1 and 10 µg intraplantar)	Male	Immediately following and 1-day post-incision
Activation of the AMP-activated protein kinase reduces inflammatory nociception	Russe OQ et al. (Russe, Moser et al. 2013)	Formalin and zymosan-induced paw inflammation model	Metformin (100 mg/kg i.p) and AICAR (400 mg/kg i.p)	Male	10 min post-formalin
Adenosine Monophosphate-activated Protein Kinase Regulates Interleukin-1β Expression and Glial Glutamate Transporter Function in Rodents with Neuropathic Pain	Maixner et al. (Maixner, Yan et al. 2015)	Spared nerve ligation	AICAR (30 µM i.t)	Male	10 days post-SNL
Metformin attenuates hyperalgesia and allodynia in rats with painful diabetic	Ma et al. (Ma, Yu et al. 2015)	Streptozotocin-induced diabetic neuropathy	Metformin (30 mg/kg, 200 mg/kg or 500 mg/kg)	Male	21 days post-STZ

Table 1.1: AMPK activators in Pain

Title	Authors	Model	Compound	Sex	Time of administration
neuropathy induced by streptozotocin					
Activation of Adenosine Monophosphate-activated Protein Kinase Suppresses Neuroinflammation and Ameliorates Bone Cancer Pain: Involvement of Inhibition on Mitogen-activated Protein Kinase	Song H et al. (Song, Han et al. 2015)	Tumor cell implantation (bone cancer pain)	Resveratrol (300 mg/kg) intragastrically and AICAR (10 and 30 µg i.t.)	Females	14 days post-TCI
The potent, indirect adenosine monophosphate-activated protein kinase activator R419 attenuates mitogen-activated protein kinase signaling, inhibits nociceptor excitability, and reduces pain hypersensitivity in mice	Mejia et al. (Mejia, Asiedu et al. 2016)	NGF-induced mechanical hypersensitivity and plantar incision	R419 (10 µg i.pl.)	Male	At the time of injection or incision
Targeting adenosine	Melemedjian et al.	Spared Nerve Injury	Metformin (200	Male	14 days post-SNI

Table 1.1: AMPK activators in Pain

Title	Authors	Model	Compound	Sex	Time of administration
monophosphate-activated protein kinase (AMPK) in preclinical models reveals a potential mechanism for the treatment of neuropathic pain	al. (Melemedjan, Asiedu et al. 2011)		mg/kg/day i.p.) and A769662 (30 mg/kg/day i.p.)		
The anti-diabetic drug metformin protects against chemotherapy-induced peripheral neuropathy in a mouse model	Mao-Ying QL et al. (Mao-Ying, Kavelaars et al. 2014)	Chemotherapy-induced peripheral neuropathy	Metformin (200 mg/kg/day i.p.)	Male and female	24 hrs prior to cisplatin treatment
The inhibition of spinal synaptic plasticity mediated by activation of AMP-activated protein kinase signaling alleviates the acute pain induced by oxaliplatin	Ling YZ et al. (Ling, Li et al. 2017)	Chemotherapy-induced peripheral neuropathy	Metformin (25 µg i.t.)	Male	Prior to oxaliplatin

Table 1.1: AMPK activators in Pain

Title	Authors	Model	Compound	Sex	Time of administration
Pharmacological activation of AMPK inhibits incision-evoked mechanical hypersensitivity and the development of hyperalgesic priming in mice	Burton MD et al. (Burton, Tillu et al. 2017)	Plantar incision	Metformin (30, 100, 150, or 200 mg/kg i.p.)	Male	4 days starting 2 days prior to surgery
Methyl cinnamate alleviated CCI-induced upregulation of spinal AMPA receptors and pain hypersensitivity by targeting AMPK	Gui Y et al. (Gui, Chen et al. 2018)	Chronic Constriction Injury-neuropathic pain	Methyl cinnamate (100 mg/kg p.o.)	Male	7 day starting 7 days post CCI
Effects of metformin on the expression of AMPK and STAT3 in the spinal dorsal horn of rats with neuropathic pain	Ge A et al. (Ge, Wang et al. 2018)	Chronic Constriction Injury-neuropathic pain	Metformin (200 mg/kg i.p.)	Male	5 days starting 5 days post CCI

Table 1.1: AMPK activators in Pain

Title	Authors	Model	Compound	Sex	Time of administration
Rosmarinic Acid Mitigates Mitochondrial Dysfunction and Spinal Glial Activation in Oxaliplatin-induced Peripheral Neuropathy	Areti A et al. (Areti, Komirishetty et al. 2018)	Chemotherapy-induced peripheral neuropathy	Rosmarinic Acid (25 and 50 mg/kg p.o.)	Male	Following oxaliplatin injections
Metformin inhibits visceral allodynia and increased gut permeability induced by stress in rats	Nozu T et al. (Nozu, Miyagishi et al. 2019)	Lipopolysaccharide-induced visceral allodynia	Metformin (5-50 mg/kg for 3 days)	Male	48 h, 24 h, and 30 min before injection of LPS
AMPK activation attenuates inflammatory pain through inhibiting NF- κ B activation and IL-1 β expression	Xiang HC et al. (Xiang, Lin et al. 2019)	complete Freund's adjuvant	AICAR (5, 15, and 20 μ g/20 μ l subq)	Male	4 days post-CFA
AMP-Activated Protein Kinase Activation in Dorsal Root Ganglion Suppresses mTOR/p70S6K Signaling and Alleviates Painful Radiculopathies in Lumbar	Liu Y et al. (Liu, Li et al. 2019)	lumbar disc herniation (LDH) induced painful radiculopathies	Metformin (250mg/kg/day)	Male	1 week prior to surgery for 3 weeks

Table 1.1: AMPK activators in Pain

Title	Authors	Model	Compound	Sex	Time of administration
Disc Herniation Rat Model					
Metformin antinociceptive effect in models of nociceptive and neuropathic pain is partially mediated by activation of opioidergic mechanisms	Augusto PSA et al. (Augusto, Braga et al. 2019)	Chronic Constriction Injury - neuropathic pain and hot plate	Metformin (250, 500 and 1000 mg/kg)	Male	8 days post-CCI
Resveratrol attenuates bone cancer pain through regulating the expression levels of ASIC3 and activating cell autophagy	Zhu H et al. (Zhu, Ding et al. 2017)	MRMT-1 Bone cancer model	Resveratrol (0.3, 1, and 3 mg/kg i.p.)	Female	21 days post-operation
Resveratrol attenuates neuropathic pain through balancing pro-inflammatory	Tao L et al. (Tao, Ding et al. 2016)	Chronic Constriction Injury	Resveratrol (5, 10, 20 and 40 mg/kg i.p.)	Female	7 consecutive days prior to CCI

Table 1.1: AMPK activators in Pain

Title	Authors	Model	Compound	Sex	Time of administration
and anti-inflammatory cytokines release in mice					
Resveratrol alleviates inflammatory hyperalgesia by modulation of reactive oxygen species (ROS), antioxidant enzymes and ERK activation.	Singh AK et al. (Singh and Vinayak 2017)	complete Freund's adjuvant	Resveratrol (20 mg/kg i.p.)	Male	Immediately following CFA
Antihyperalgesia effect of AMP-activated protein kinase (AMPK) activators in a mouse model of postoperative pain	Das V et al. (Das, Kroin et al. 2019)	Plantar incision	Metformin (200 mg/kg p.o.)	Male and Female	4 hrs post-surgery repeated for 3 days
Metformin relieves neuropathic pain after spinal nerve ligation via autophagy flux stimulation	Weng W et al. (Weng, Yao et al. 2019)	Spared nerve ligation (SNL)	Metformin (50 mg/kg/d i.p.)	Male	Immediately following surgery

Table 1.1: AMPK activators in Pain

Title	Authors	Model	Compound	Sex	Time of administration
Anti-inflammatory effects of Metformin improve the neuropathic pain and locomotor activity in spinal cord injured rats: introduction of an alternative therapy	Afshari K et al. (Afshari, Dehdashtian et al. 2018)	Spinal cord injury	Metformin (10, 50 and 100 mg/kg i.p.)	Male	Immediately following surgery
Evaluation of the neonatal streptozotocin model of diabetes in rats: Evidence for a model of neuropathic pain	Barragán-Iglesias P et al. (Barragan-Iglesias, Oidor-Chan et al. 2018)	streptozotocin model of diabetes	Metformin (200mg/kg/day, p.o.)	Male	For 2 weeks starting 14 weeks post-STZ
Metformin Synergizes With Conventional and Adjuvant Analgesic Drugs to Reduce Inflammatory Hyperalgesia in Rats	Pecikoza UB et al. (Pecikoza, Tomic et al. 2017)	Carrageenan-induced hyperalgesia	Metformin (50-200 mg/kg i.p.)	Male	Concurrent with carrageenan

Table 1.1: AMPK activators in Pain

Title	Authors	Model	Compound	Sex	Time of administration
Neuropathic Pain Creates an Enduring Prefrontal Cortex Dysfunction Corrected by the Type II Diabetic Drug Metformin But Not by Gabapentin	Shiers S et al. (Shiers, Pradhan et al. 2018)	Spared nerve injury	Metformin (200 mg/kg i.p.)	Male and female	7 days starting 2 weeks post-SNI
Puerarin Attenuates Osteoarthritis via Upregulating AMP-Activated Protein Kinase/Proliferator-Activated Receptor-γ Coactivator-1 Signaling Pathway in Osteoarthritis Rats	Wang L et al. (Wang, Shan et al. 2018)	Osteoarthritis	Puerarin		
Involvement of AMPK/SIRT1 pathway in anti-allodynic effect of troxerutin in CCI-induced neuropathic pain	Gui Y et al. (Gui, Li et al. 2015)	Chronic Constriction Injury	Troxerutin (150 mg/kg p.o.)	Male	

Table 1.1: AMPK activators in Pain

Title	Authors	Model	Compound	Sex	Time of administration
Impaired AMPK-CGRP signaling in the central nervous system contributes to enhanced neuropathic pain in high-fat diet-induced obese rats, with or without nerve injury.	Guo X et al. (Guo, Tao et al. 2019)	Spared Nerve Injury	AICAR (0.2 μ mol/kg i.t.)	Male	7 days starting 14 days post-SNI
Analgesic effect of resveratrol on colitis-induced visceral pain via inhibition of TRAF6/NF- κ B signaling pathway in the spinal cord	Lu Y et al. (Lu, Xu et al. 2019)	Trinitrobenzene sulfonic acid (TNBS)-induced colonic inflammation	Resveratrol (4.5 or 45 nM i.t.)	Male	4 days starting 4 days post-enema

CHAPTER 2

THE ANTIDIABETIC DRUG METFORMIN PREVENTS AND REVERSES

NEUROPATHIC PAIN AND SPINAL CORD MICROGLIAL ACTIVATION IN MALE

BUT NOT FEMALE MICE

Kufreobong E Inyang¹, Michael D Burton¹, Thomas Szabo-Pardi¹, Emma Wentworth¹,
Gregory Dussor¹, Theodore J Price^{1*}

¹School of Behavioral and Brain Sciences,

School of Behavioral and Brain Sciences

The University of Texas at Dallas

800 W Campbell Rd

Richardson TX 75080

Abstract

Metformin is a widely prescribed drug used in the treatment of type II diabetes. While the drug has many mechanisms of action, most of these converge on AMP activated protein kinase (AMPK), which metformin activates. AMPK is a multifunctional kinase that is a negative regulator of mechanistic target of rapamycin (Atef, El-Sayed et al. 2019) and mitogen activated protein kinase (MAPK) signaling. Activation of AMPK decreases the excitability of dorsal root ganglion neurons and AMPK activators are effective in reducing chronic pain in inflammatory, post-surgical and neuropathic rodent models. We have previously shown that metformin leads to an enduring resolution of neuropathic pain in the spared nerve injury (Myers, Guan et al.) model in male mice and rats. The precise mechanism underlying this long-lasting effect is not known. We conducted experiments to investigate the effects of metformin on SNI-induced microglial activation, a process implicated in the maintenance of neuropathic pain that has recently been shown to be sexually dimorphic. We find that metformin is effective at inhibiting development of neuropathic pain when treatment is given around the time of injury and that metformin is likewise effective at reversing neuropathic mechanical hypersensitivity when treatment is initiation weeks after injury. This effect is linked to decreased Iba-1 staining in the dorsal horn, a marker of microglial activation. Importantly, these positive behavioral and microglia effects of metformin were only observed in male mice. We conclude that the neuropathic pain modifying effects of metformin are sex-specific supporting a differential role for microglial activation in male and female mice.

Introduction

Chronic pain affects over 100 million Americans, more than the number of people suffering from heart disease, diabetes and cancer combined (Institute of Medicine Committee on Advancing Pain Research and Education 2011). The problem of this epidemic of chronic pain is compounded by the fact that available analgesics are not efficacious for many patients over the long-term (Finnerup, Attal et al. 2015). Among the many chronic pain types, neuropathic pain is common, affecting up to 10% of the population, and is particularly hard to treat. Front-line neuropathic pain medications have numbers needed to treat for 50% efficacy of between 5 and 10 (Finnerup, Attal et al. 2015). New, more efficacious treatments for chronic pain in general, and neuropathic pain, are urgently needed (Price, Basbaum et al. 2018). Adenosine monophosphate-activated protein kinase (AMPK) is a fuel-sensing enzyme present in all mammals (Hardie 2007). AMPK is a kinase that detects changes in the AMP/ATP ratio in all cells to regulate anabolic processes when cellular energy status is low (Kahn BB 2005). Activation of AMPK decreases mTORC1 signaling as well as MAPK signaling leading to a general suppression of cap-dependent protein synthesis (Hardie). Peripheral nerve injury (PNI) leads to an induction of increased mTORC1 (Terenzio, Koley et al. 2018) and MAPK signaling in DRG neurons and activation of these signaling pathways has been linked to increased nociceptor excitability (Melemedjian, Asiedu et al. 2010, Melemedjian OK 2011, Melemedjian, Khoutorsky et al. 2013, Moy, Khoutorsky et al. 2017). Many studies have now demonstrated that AMPK activation in nociceptive DRG neurons leads to a decrease in mTORC1 and MAPK signaling and a decrease in

nociceptor excitability (Price, Das et al. 2015, Asiedu, Dussor et al. 2016). AMPK activators are also effective at reducing behavioral signs of pain in rodent models (Price, Das et al. 2015, Asiedu, Dussor et al. 2016) and this is at least partially dependent on nociceptor-expressed AMPK because specific deletion of an α subunit of AMPK in these cells abrogates that anti-hyperalgesic effects of AMPK activators (Russe, Moser et al. 2013).

Metformin is a widely prescribed drug for type II diabetes. The drug activates AMPK in a liver kinase B1 (LKB1) dependent fashion and is therefore an indirect AMPK activator (Shaw, Lamia et al. 2005). The precise mechanism through which metformin acts is still an area of controversy, however, the drug is widely viewed as safe, is effective for type II diabetes and could potentially be repurposed for the treatment of neuropathic pain. Metformin is effective in reversing SNI- and chronic constriction injury- (Kola, Hubina et al.) induced neuropathic pain in male mice and rats (Melemedjian OK 2011, Ge, Wang et al. 2018), is effective in reducing pain produced by surgical incision in male mice (Burton, Tillu et al. 2017) and is also effective in preventing the development of inflammatory pain (Russe, Moser et al. 2013). Metformin treatment can also prevent, but not reverse, the development of chemotherapy-induced peripheral neuropathy in female mice (Mao-Ying, Kavelaars et al. 2014).

Microglia activation in the spinal dorsal horn has been linked to many types of chronic neuropathic pain in rodents (Watkins, Milligan et al. 2001, Milligan and Watkins 2009). Interestingly, a series of recent studies suggest that the effects of microglia on neuropathic pain in mice and rats are male sex-specific (Sorge, Mapplebeck et al. 2015,

Taves, Berta et al. 2016). We hypothesized that the enduring effects of metformin that are observed in neuropathic pain models may be dependent on a reversal of microglial activation in the dorsal horn. This hypothesis would be consistent with recent findings in the CCI model in rats (Ge, Wang et al. 2018). A corollary of this hypothesis is that metformin may be effective in male but not female mice. Our experiments demonstrate that metformin prevents, and reverses SNI-induced mechanical and cold hypersensitivity and that this effect is paralleled by decreased microglial activation. These effects were only observed in male mice. Our experiments have important implications for the potential repurposing of metformin as an anti-neuropathic pain drug as well as for understanding the mechanisms driving neuropathic pain.

Methods

Laboratory Animals

Animal procedures were approved by The University of Texas at Dallas Institutional animal care and use committee and were in accordance with National Institutes of Health Guidelines. All the experiments were performed male or female ICR mice obtained from Envigo at 4 weeks of age. Mice were housed in the University of Texas at Dallas Animal Care Facility for at least one week prior to the start of behavior testing and surgery. Animals had ad libitum access to food and water and were on a 12 hr non-inverted light/dark cycle. Experimenters were blinded to treatment groups in behavioral experiments. Mice were randomized to treatment groups using a random number generator and in such a manner that multiple treatment groups were always found

within any individual cage of animals. Male and female mice were housed separately in groups of 4 per cage.

Behavioral Testing

Mechanical sensitivity was assessed using stimulation of the hindpaw of the mouse with calibrated von Frey filaments from Stoelting. We used 0.6, 1.0 and 1.4-gram filaments and measured the response frequency to 10 consecutive stimulations of the hindpaw with each filament with stimulations spaced by at least 5 sec following 45 minutes of habituation to the testing boxes. The number of responses for each filament force was recorded. Following this baseline testing, neuropathic pain was induced in half of the mice using the SNI surgery model. This surgery consisted of exposing and cutting the Peroneal and Tibial branches of the Sciatic nerve while leaving the Sural nerve intact (Decosterd 2000). The remaining mice received a sham surgery where the nerve was exposed but not cut. Two-weeks post-surgery, the withdrawal frequency test was repeated to ensure that mechanical hypersensitivity had indeed been produced.

Following this test, groups of SNI mice and sham mice were treated with 200 mg/kg of Metformin (LKT Laboratories Inc.) dissolved in 0.9% saline through intraperitoneal (I.P.) injections once a day at 10 am for 7 consecutive days. For the prophylactic metformin treatment experiment, mice were given 200 mg/kg of metformin following baseline testing then SNI was performed after the 7th day of treatment. In another prophylactic experiment mice were treated with metformin for 7 days with injections starting on the day of SNI surgery. Vehicle treated mice for each experiment received daily injections of 0.9% saline solution for 7 consecutive days as well. Following injections, the withdrawal

frequency test was performed at indicated time points post-SNI to determine persistent effects of metformin treatment. Cold allodynia was also measured using the acetone test (Allchorne, Broom et al. 2005). To do this, the left hindpaw of the mouse was sprayed with 0.1 mL of acetone using a needle and syringe and the duration of reaction to the evaporative cooling stimulus was measured over the course of a minute.

Behavioral tests were done in the same way for male and female mice.

Immunohistochemistry

After the end of behavioral testing in SNI or sham mice, the lumbar spinal cords and DRGs were removed, placed in 4% formalin overnight and transferred to 30% sucrose for cryoprotection for 24 hrs then mounted in Optimal Cutting Temperature (OCT) compound. Lumbar spinal cord and DRG sections were cut into 20 μ m slices using a cryostat and mounted onto positively charged (Superfrost plus) slides for immunohistochemistry. An antigen retrieval step was performed using a 10 mM Citric Acid buffer solution pH 6.0 with .05% Tween 20 for 45 minutes at room temperature. Following 3 5-minute washes in 1X phosphate buffered saline (PBS), the slides were then put into a permeabilization solution containing 10% normal goat serum (Gabrielsen, Monath et al. 1992) and 0.2% Triton X 100 in PBS for 30 minutes. This was followed by another series of 5-minute washes in PBS and 1.5 hrs in a blocking solution containing 10% NGS and 0.01% Na azide in PBS. Following another PBS wash, the slides were incubated overnight in a primary antibody solution made from the blocking solution. The next day, the slides were washed again in PBS then incubated in a secondary antibody solution also made from the blocking solution for 1 hr. Following 3

more PBS washes and a wash in deionized H₂O, Prolong Gold mounting media was used to mount coverslips. The primary antibodies used were Ionized calcium binding adaptor molecule 1 (IBA1) from Wako Chemicals (Cat 019-19741) for activated microglia for the spinal cord sections and at a concentration of 1:1000 with Alexa Fluor 488 goat anti-rabbit (GAR-488) secondary (1:1000) and isolectin B4 (IB4) conjugated to alexfluor-567 (1:300) from Life Technologies (Cat I21412) for non-peptidergic central projection labeling. Imaging of the tissue sections was done using an Olympus Fluoview FV1200 laser scanning confocal microscope with scale bars indicating the level of magnification. Images were analyzed using the cell counter tool in ImageJ.

Neuron Culture

Dorsal root ganglia (DRG) were extracted aseptically from 5 to 12 4-week old male ICR mice per cell culture plate for each cellular imaging experiment and placed in Hank's Buffered Salt Solution (HBSS, Invitrogen) on ice. The DRGs were dissociated enzymatically at 37 °C; first with collagenase A (1 mg/ml, Roche) for 25 min, then collagenase D (1 mg/ml, Roche) that included papain (30 µg/ml, Roche) for 20 min. Afterward, a trypsin inhibitor (1 mg/ml, Roche) that contained bovine serum albumin (BSA, Fisher, 1 mg/ml) was applied and the ganglia were mixed to allow for further dissociation with a polished Pasteur pipette. The tissue was then filtered through 70-µm nylon cell strainer (Falcon) and re-suspended in DMEM F-12 GlutaMax media (Invitrogen) that contained 10% fetal bovine serum (FBS, Hyclone) and 1× penicillin streptomycin (Pen-Strep). The media also contained NGF (10 ng/ml, Millipore) and 5-fluoro-2'-deoxyuridine + uridine (FRDU-U, 3.0 µg/ml + 7.0 µg/ml, Sigma) to reduce

proliferation of glia and fibroblasts. Neurons were cultured for 7 days on 12-mm glass coverslips (#1 thickness, Chemglass) in a 24-well tissue culture plate (Falcon) coated with poly-d-lysine (Sigma) at 37 °C with 95% air and 5% CO₂. On the day of the experiment, metformin was diluted into DMEM F-12 plus GlutaMax media and added directly onto the neurons at a concentration 20 mM for 1 hr.

Microglia isolation, Culture, and Treatment

Microglia from whole brain and spinal cord were isolated and cultured as described previously, with few modifications (Norden, Fenn et al. 2014, Burton, Rytych et al. 2016). Mice were euthanized and whole brains and spinal cords were collected, placed in sterile dulbecco's phosphate-buffered saline (DPBS), and then homogenized by passage through a 70- μ m cell strainer in Dulbecco's PBS (DPBS) supplemented with 0.2% glucose. Homogenates were centrifuged at 600 \times g for 6 minutes at 10°C and resulting pellets were resuspended in sterile 70% isotonic Percoll (GE-Healthcare) at room temperature. A discontinuous sterile Percoll density gradient was layered on top of the 70% isotonic Percoll at 50%, 35%, and 0% (DPBS). The suspension was centrifuged at 2000 \times g for 20 minutes and microglia were collected from the interphase between the 70% and 50% Percoll layers. Cells were washed with sterile DPBS and then resuspended in DMEM F-12 GlutaMax media (Invitrogen) that contained 5% fetal bovine serum (FBS, Hyclone) and 2 \times penicillin streptomycin (Pen-Strep). Each isolation yielded $\sim 5 \times 10^5$ viable cells from each mouse brain and spinal cord and roughly 100,000 – 150,000 cells per well were plated and cultured for two-three days on 12mm glass coverslips (#1 thickness, chemglass) in a 24-well tissue culture plate

(Falcon) coated with poly-D-lysine (Sigma-Aldrich) at 37°C with 95% oxygen and 5% CO₂. The day before the experiment, cells were serum-starved overnight (0% FBS media). On the day of the experiment, metformin (20mM) was diluted into DMEM F-12 Glutamax and added directly onto the cells for 1 hour.

Immunocytochemistry (ICC) and digital image analysis

Following metformin treatment, the cells were washed with DPS and fixed with 10% formalin in phosphate buffered saline (PBS) for 30 minutes. Cells were blocked with 10% normal goat serum and labelled with Iba-1-635 (1:500; Wako Chemicals) and phospho-ACC (p-ACC, 1:1000; Cell Signaling Technologies) overnight at 4° C. Next, cells were washed and incubated with a fluochrome-conjugated secondary antibody (Alexa Fluor, anti-rabbit 488, invitrogen) and counterstained with a DNA stain, 4',6-diamidino-2-phenylindole (DAPI) (Invitrogen) and mounted with Prolong Gold (Invitrogen). Images were taken on an Olympus Fluoview FV1200 laser scanning confocal microscope and analyzed using the co-localization tool within Olympus' FV software. The intensity of each channel was adjusted so that only areas that contained a strong signal of 488 nm and 405 nm were visible. This adjusted imaged contained distinct puncta that could then be counted and analyzed using Graphpad prism 7xx. Results were reported as the average percent area in the positive threshold for all representative pictures.

Statistics

Data are shown as mean +/- standard error of the mean (SEM) and the number of animals or samples used in each analysis are given in figure legends. GraphPad Prism 7 was used to analyze data. Two-way ANOVAs were used to analyze von Frey data, one-way ANOVAs were used for acetone data and two tailed t-tests or one-way ANOVAs were used to analyze imaging data. Post-hoc tests used are described in figure legends. Significance level was set at $\alpha < 0.05$.

Results

Metformin reverses SNI-induced mechanical and cold hypersensitivity in male mice.

To assess the effects of metformin on established SNI-induced mechanical and cold hypersensitivity in male and female mice we obtained baseline responses for von Frey filament strengths of 0.6, 1.0 and 1.4 grams and then performed SNI or sham surgery. Mice were allocated to metformin (200 mg/kg) or saline treatment groups and then given injections via the I.P. injection route starting on day 14 after surgery. Starting at 21 days after surgery (after 7 days of metformin or vehicle treatment) and continuing at time points out to 56 days post-surgery, we monitored mechanical hypersensitivity weekly and then assessed cold hypersensitivity with the acetone test at day 56 post-surgery. Mice were then euthanized and tissues were taken for immunohistochemistry. In male mice, metformin reversed SNI-induced mechanical hypersensitivity to 0.6, 1.0 and 1.4 gram von Frey filaments and this effect persisted out to 56 days after SNI (32 days after the end of metformin treatment, **Fig 2.1A-C**). Additionally, we observed an

increase in acetone response in SNI male mice that received saline treatment (**Fig 2.1D**) but this effect was not seen in SNI mice treated with metformin. These results suggest, as we have previously reported using different behavioral end-points (Melemedjian OK 2011, Melemedjian, Khoutorsky et al. 2013), that metformin has an enduring effect on neuropathic mechanical and cold pain in male mice. We also compared the baseline response frequency to other timepoints for both the vehicle treated SNI and sham mice. For the sham mice, there was no difference between the baseline and the post-surgery timepoints. In the SNI vehicle treated mice there was a strong induction of neuropathic mechanical and cold hypersensitivity when compared to baseline, as expected. Therefore, in male mice, we do not observe any persistent changes in mechanical or cold sensitivity that are associated with the sham surgery.

Female mice show robust responses to PNI but do not respond to metformin treatment.

We obtained baseline measures of mechanical sensitivity in female mice then performed SNI or sham surgery and confirmed the development of mechanical hypersensitivity 14 days after treatment. On day 14 mice were treated with metformin (200 mg/kg) or vehicle for 7 days and tested over the same time course that was used for male mice. Strikingly, 200 mg/kg metformin failed to reduce mechanical hypersensitivity in female mice at any time point (**Fig 2.2A-C**). Metformin also had no positive effect on cold hypersensitivity in female mice. Surprisingly, metformin exacerbated the acetone response in female mice with SNI (**Fig 2.2D**) but had no effect in sham mice demonstrating that this effect is not produced by metformin treatment alone. We also compared the baseline response frequencies for both the vehicle treated

SNI and female sham mice. Unlike in male mice, female sham mice showed a significant mechanical hypersensitivity that persisted over the time course of the experiment (**Fig 2.2A-C**). This effect was slightly reduced by metformin treatment at the 1.4-gram filament strength.

Metformin treatment reverses microglial staining intensity in the spinal cord in male but not female mice.

Following behavioral testing we removed spinal cords from male and female SNI and sham mice treated with metformin or vehicle 30 days earlier. Immunohistochemistry was performed to examine Iba-1 and IB4 staining. In male SNI mice treated with vehicle we observed a clear increase in Iba-1 positive cells compared to sham vehicle treated mice (**Fig 2.3A-E**). Metformin treatment strongly reduced the number of Iba-1 positive cells in SNI mice (**Fig 2.3B-C**). This finding is consistent with recent data from male CCI rats treated with metformin (Ge, Wang et al. 2018) although the time courses of treatment and persistence of the reversal are different between these experiments. We also observed a loss of IB4 staining in the dorsal horn in SNI male mice treated with vehicle, as originally described in rats (Bailey and Ribeiro-da-Silva 2006). This absent band of staining in the male SNI vehicle group averaged 96.32 μm in length. This loss of IB4 staining was not evident in SNI male mice treated with metformin suggesting that this histochemical sign of PNI is also reversed by metformin treatment. It is notable that this change in IB4 staining in the dorsal horn induced by SNI was consistent with the time course of similar findings in a nerve constriction model in male rats (Lorenzo, Magnussen et al. 2014).

Results in female mice were strikingly different. While the number of Iba-1 positive cells was increased by SNI (**Fig 2.4A-C**) there was no effect of metformin treatment. We also did not observe any loss of IB4 staining in female SNI mice suggesting that this change does not occur in female mice. The absolute number of Iba-1 positive cells in the dorsal horn of female mice was higher than in male mice in the sham condition, consistent with the development of mechanical hypersensitivity to sham surgery in female mice. Therefore, while metformin is able to reverse neuropathic mechanical and cold hypersensitivity and microglial reactivity in male mice, the same drug was without effect on all of these measures in female mice.

SNI caused an increase in GFAP-positive cells in male mice but not females that was not affected by metformin treatment.

In addition to examining Iba-1, we also examined GFAP staining in the dorsal horn of male and female SNI mice following the behavioral experiments. Immunohistochemistry was performed to examine GFAP and IB4 staining in males and females. In male SNI mice treated with vehicle we observed a clear increase in GFAP positive cells compared to sham vehicle treated mice (**Fig 2.5A-E**). Metformin did not have an effect in reducing the amount of GFAP positive cells in SNI males (**Fig 2.5B-D**).

As with the Iba-1 staining, we saw different results in the female tissue. While we did not see an effect of metformin on the number of GFAP-positive cells in female mice either, SNI also failed to cause a significant increase in the number of GFAP-positive cells when compared to sham mice (**Fig 2.6A-E**). These results are consistent with recent

data from GFAP staining done in virgin female SNL mice (Gutierrez, Hayashida et al. 2013) although the time courses of treatment and neuropathic model used are different between these experiments.

Prophylactic metformin treatment partially prevents development of neuropathy and microglial activation in male mice.

Having established that metformin reverses neuropathic pain selectively in male mice, we tested whether metformin could prevent development of SNI-induced neuropathic pain in male mice and whether any behavioral changes were correlated with spinal microglia. Naïve male ICR mice were treated with metformin (200 mg/kg) or saline for 7 days using two paradigms. In the first treatment paradigm male mice were given metformin starting 7 days prior to surgery and treatment was stopped the day of surgery. The rationale for the approach was to create a steady state plasma level of metformin to achieve strong AMPK activation at the time of injury. In the other paradigm, metformin treatment was started at the time of surgery and then continued for the ensuing 7 days. Following drug treatment, all mice were tested for mechanical hypersensitivity 14 days post-surgery and at ensuing time points. Cold allodynia was also assessed. The first prophylactic treatment group showed decreased mechanical hypersensitivity at several time points after SNI (**Fig 2.7A-C**) but the magnitude of the effect was not as large as in the reversal treatment paradigm. Another set of male mice were treated in the second prophylactic treatment paradigm metformin (200 mg/kg) starting the day of surgery. We observed a significant decrease in mechanical hypersensitivity in the metformin treated mice when compared to the vehicle group (**Fig**

2.8A-C). We also tested cold allodynia using the acetone test in this cohort of mice and observed a significant decrease in response duration (**Fig 2.8D**) indicating that prophylactic treatment with metformin prevents the full development of mechanical and cold hypersensitivity but this treatment is most effective when given over the duration of neuropathic pain development rather than simply at the time of surgical injury.

At 42 days post-SNI, in the second prophylactic metformin treatment paradigm, mice were sacrificed and their spinal cords were stained with Iba1 and IB4 as in the reversal experiment. We used the 7-day treatment starting at the time of surgical injury paradigm for this experiment because the behavioral effect was more robust. Metformin treatment caused a decrease in the number of Iba-1 cells in the dorsal horn compared to vehicle treatment (**Fig 2.9A-C**). Moreover, the loss of IB4 staining in the dorsal horn was evident in the vehicle treated mice but not in the metformin treated mice, consistent with our observations in the reversal treatment paradigm.

Prophylactic metformin treatment had no effect on the development of neuropathy and microglial activation in female mice.

To further examine the apparent sexual dimorphism of metformin, we tested whether metformin could prevent development of SNI-induced neuropathic pain in male mice and whether any behavioral changes were correlated with spinal microglia. Naïve female ICR mice were treated with metformin (200 mg/kg) or saline for 7 days using the second prophylactic treatment paradigms previously described in which treatment began starting the day of surgery. Following drug treatment, all mice were tested for

mechanical hypersensitivity 14 days post-surgery and at ensuing time points. Cold allodynia was also assessed. We observed no decrease in mechanical hypersensitivity or cold allodynia following metformin treatment compared to vehicle treatment (**Fig 2.10A-D**).

At 42 days post-SNI, in the second prophylactic metformin treatment paradigm, mice were sacrificed and their spinal cords were stained with Iba1 and IB4 as in the reversal experiment. We used the 7-day treatment starting at the time of surgical injury paradigm for this experiment because the behavioral effect was more robust. Metformin treatment caused no decrease in the number of Iba-1 cells in the dorsal horn compared to vehicle treatment (**Fig 2.11A-E**). Moreover, the loss of IB4 staining in the dorsal horn observed in the vehicle treated male mice was still not observed in any of the female mice, consistent with our observations in the reversal treatment paradigm.

Treatment of isolated male and female DRG neurons with metformin induces AMPK signaling.

DRGs were removed from naïve male and female mice, cultured for 7 days on poly-D lysine coated coverslips and treated with 20 mM metformin dissolved in DMEM or vehicle for 1 hr. Following treatment, immunocytochemistry was performed on the cells as previously described to examine p-ACC and peripherin staining. For male and female DRG neurons, we observed a significant increase in p-ACC intensity (**Fig 2.12A-F**).

Treatment of isolated male and female CNS microglia with metformin induces AMPK signaling.

Microglia were isolated as described in the methods section for the brains and spinal cords of 4-week-old naïve male and female mice. These cells were cultured on poly-D lysine coated coverslips for 3 days and treated with 20 mM metformin dissolved in DMEM or vehicle for 1 hr. Immediately following treatment, immunocytochemistry was performed on the cells to examine p-ACC and Iba1 staining. As with the neuron culture, we observed a significant increase in p-ACC intensity following metformin treatment in microglia for both male and female mice (**Fig 2.13A-F**).

Discussion

Our key result is that metformin has a differential effect on neuropathic pain and microglial activation in the spinal cord in male versus female mice. In male mice, metformin is able to both reverse and prevent the full expression of neuropathic pain and this is negatively correlated with microglial activation in the spinal cord. In female mice we did not observe any effect of metformin on neuropathic pain and metformin also failed to reverse microglial activation. These findings are consistent with a growing literature suggesting that microglia play a more important role in promoting chronic neuropathic pain in male than in female rodents (Sorge, Mapplebeck et al. 2015, Taves, Berta et al. 2016). Whether or not similar sex differences will be found in humans is an open question, however, there is now strong evidence linking neuro-inflammation to

neuropathic pain in patients (Loggia, Chonde et al. 2015, Albrecht, Granziera et al. 2016, Albrecht, Ahmed et al. 2018).

A critical question arising from our work is why metformin lacked effects in neuropathic pain in female mice. Metformin is obviously effective for type II diabetes treatment in male and female humans. This indicates that metformin is likely able to engage AMPK in many tissues in males and females. However, metformin is a very water-soluble drug and cannot readily cross cell membranes without specific transporters, in particular the organic cation transporter OCT2 (Kimura N 2005). OCT2 shows sexually dimorphic expression in many tissues, in many species, with higher expression in males (Urakami, Nakamura et al. 1999, Alnouti, Petrick et al. 2006, Asaka, Terada et al. 2006, Groves, Suhre et al. 2006). We are unaware of any studies showing dimorphisms in OCT2 expression in DRG or spinal cord. However, OCT2 expression is regulated by androgen receptors (Asaka, Terada et al. 2006) and testosterone determines microglial contributions to neuropathic pain in mice (Sorge, Mapplebeck et al. 2015). Metformin is able to prevent chemotherapy-induced neuropathic pain in female mice (Mao-Ying, Kavelaars et al. 2014). However, chemotherapy neuropathic pain does not activate microglia but rather stimulates dorsal horn astrocytes (Zhang, Yoon et al. 2012, Yoon, Robinson et al. 2013, Makker, Duffy et al. 2017). Based on all of these factors, we propose that the most parsimonious explanation for our findings is a difference in pharmacokinetics for metformin between male and female mice. Metformin's ability to increase AMPK activity in male and female neurons and microglia in vitro further bolsters this hypothesis. Since androgen receptors drive OCT2 expression (Asaka,

Terada et al. 2006, Groves, Suhre et al. 2006), metformin may be incapable of activating AMPK in female microglia. Another possibility is that AMPK activation in microglia inhibits androgen-driven processes that promote neuropathic pain in males but AMPK activation in female microglia is incapable of acting on pathways in these cells that may promote neuropathic pain in females.

Loss of IB4 staining in the dorsal horn following peripheral nerve injury has been characterized previous in rats and mice (Bailey and Ribeiro-da-Silva 2006, Casals-Díaz, Vivó et al. 2009, Lorenzo, Magnussen et al. 2014). To the best of our knowledge, our work with metformin is the first report of a pharmacological reversal of this effect in the SNI model in mice. Both preemptive and reversal treatment was capable of reversing this loss of IB4 staining. The effect was accompanied by a decrease in spinal microglial activation in male mice. Interestingly, this effect did not emerge at all in female mice, even though there was robust activation of microglia in the spinal dorsal horn in these mice. The mechanism underlying the loss of IB4 staining in the dorsal horn of rodents after peripheral nerve injury are not known, but they apparently do not occur in female mice. We also observed a sustained mechanical hypersensitivity in female mice with sham SNI surgery that was not present in male mice. These are part of a growing abundance of major sexual dimorphisms in neuropathic and chronic pain mechanisms between male and female mice (Mogil and Bailey 2010, Sorge, Mapplebeck et al. 2015, Taves, Berta et al. 2016, Lopes, Malek et al. 2017, Megat, Shiers et al. 2018).

In conclusion, we have demonstrated that metformin has a disease modifying effect on male mice which includes a decrease in microglial activation in the dorsal horn of the

spinal cord when given to reverse or to prevent neuropathic pain. This effect is remarkably long lasting as it persists for weeks after cessation of metformin treatment. Metformin does not appear to have any observable effects on neuropathic pain or microglial activation in female mice. Our findings contribute to a growing literature suggesting that metformin can be repurposed for the treatment of chronic pain (Melemedjian, Khoutorsky et al. 2013, Russe, Moser et al. 2013, Taylor, Westveld et al. 2013, Mao-Ying, Kavelaars et al. 2014, Ma, Yu et al. 2015, Burton, Tillu et al. 2017, Ling, Li et al. 2017, Wang, Kobayashi et al. 2017, Ge, Wang et al. 2018) but suggest that the drug may only be effective in certain populations, when specific pain promoting mechanisms are engaged.

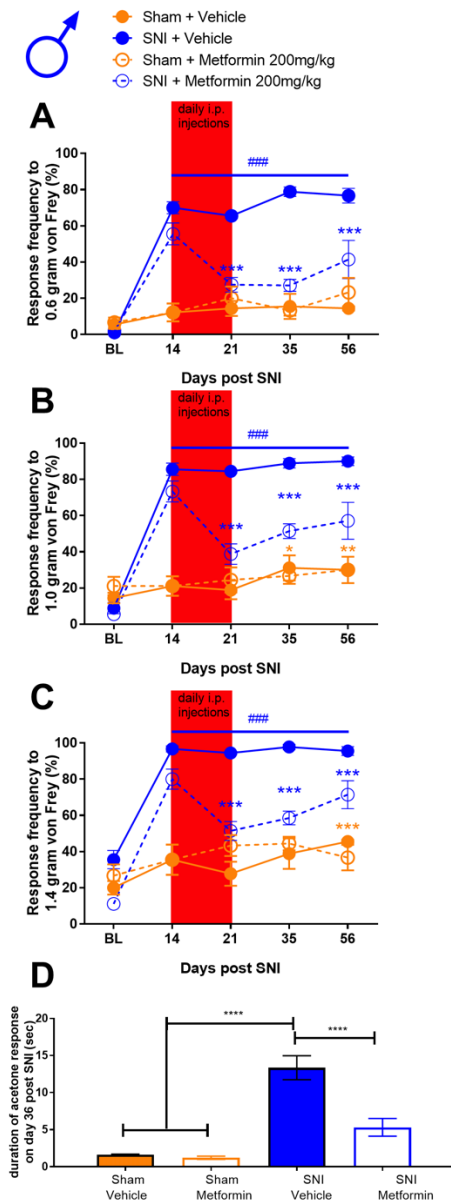


Figure 2.1: Metformin treatment reverses SNI-induced mechanical and cold hypersensitivity in male mice. A-C. SNI surgery caused mechanical hypersensitivity in male mice as measured using the withdrawal frequency test. After treatment with Metformin, the response frequency was decreased for all filament weights. D. Cold hypersensitivity was induced by SNI and the effect was reduced after metformin administration. * $p < 0.05$; ** $p < 0.01$; *** $p < 0.001$; **** $p < 0.0001$; ### $p < 0.001$ versus BL; N= 9 for all groups.

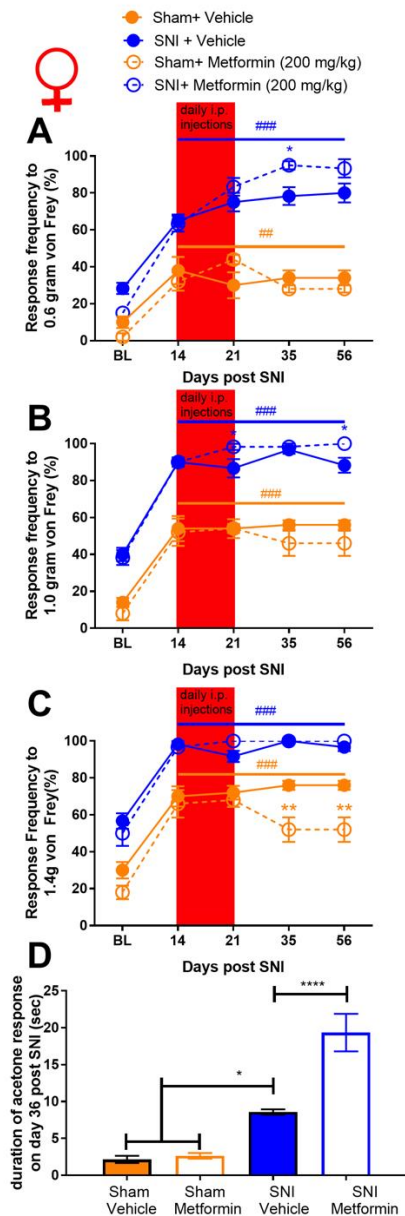


Figure 2.2: Metformin treatment does not influence SNI-induced mechanical or cold hypersensitivity in female mice. A-C. In female mice metformin failed to resolve mechanical hypersensitivity. Surgery (sham or SNI) induced a statistically significant difference from baseline for both groups $###p < .0001$. D. A statistically significant increase in cold hypersensitivity was observed in the female SNI and the SNI + metformin group when compared to the vehicle group. $*p < 0.05$; $**p < 0.01$; $***p < 0.001$; $****p < 0.0001$; $N = 6$ per group.

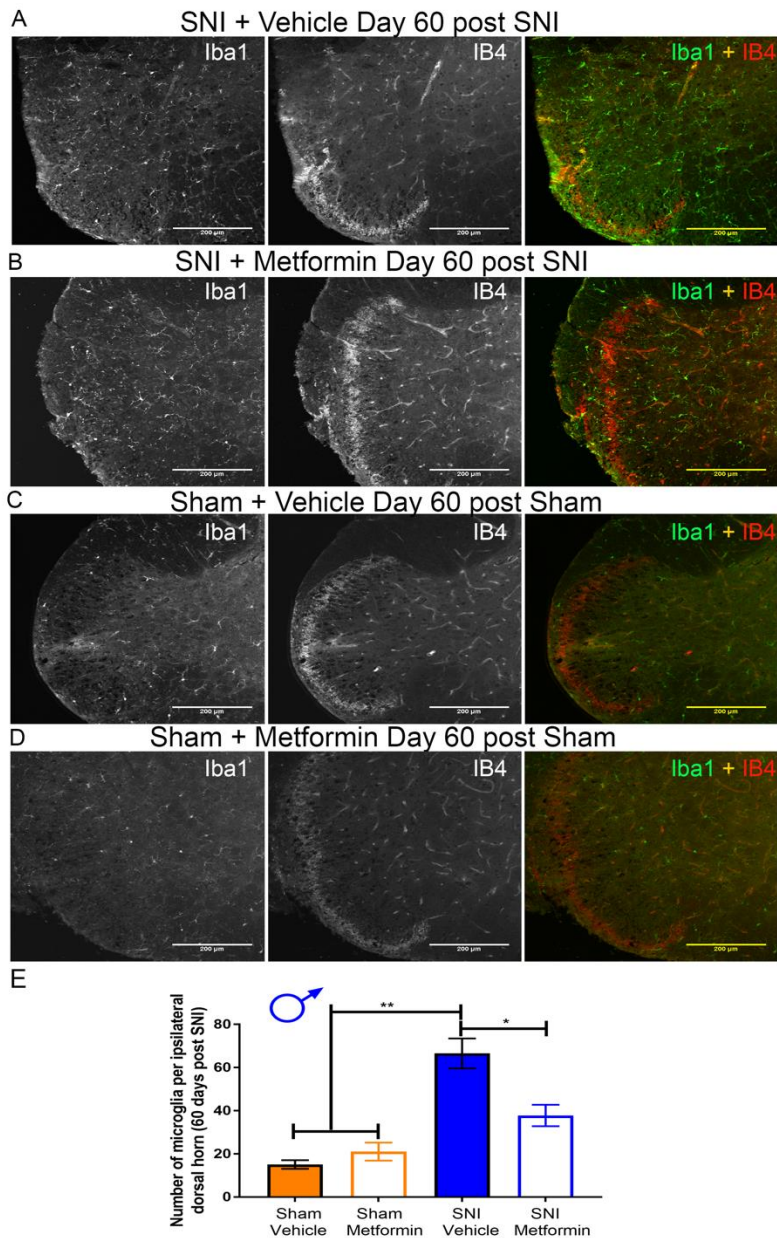


Figure 2.3: Metformin reverses microglial activation in SNI male mice. A-D. Representative immunohistochemistry images of the dorsal horn of male lumbar spinal cord at 20X magnification. Quantification of images shown in E. Metformin decreased SNI-induced microglia activation. SNI caused a loss of IB4 staining in the dorsal horn (A) that was reversed by metformin treatment (B) * $p < 0.05$; ** $p < 0.01$; N= 5 per group.

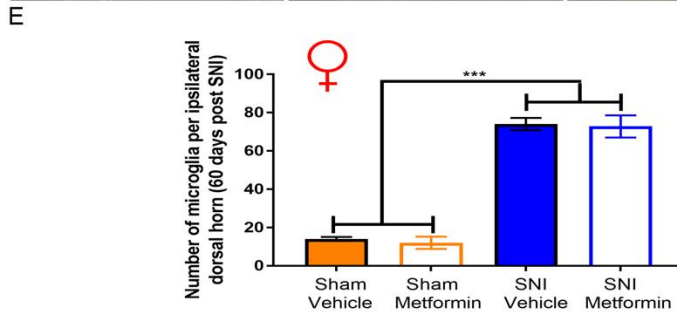
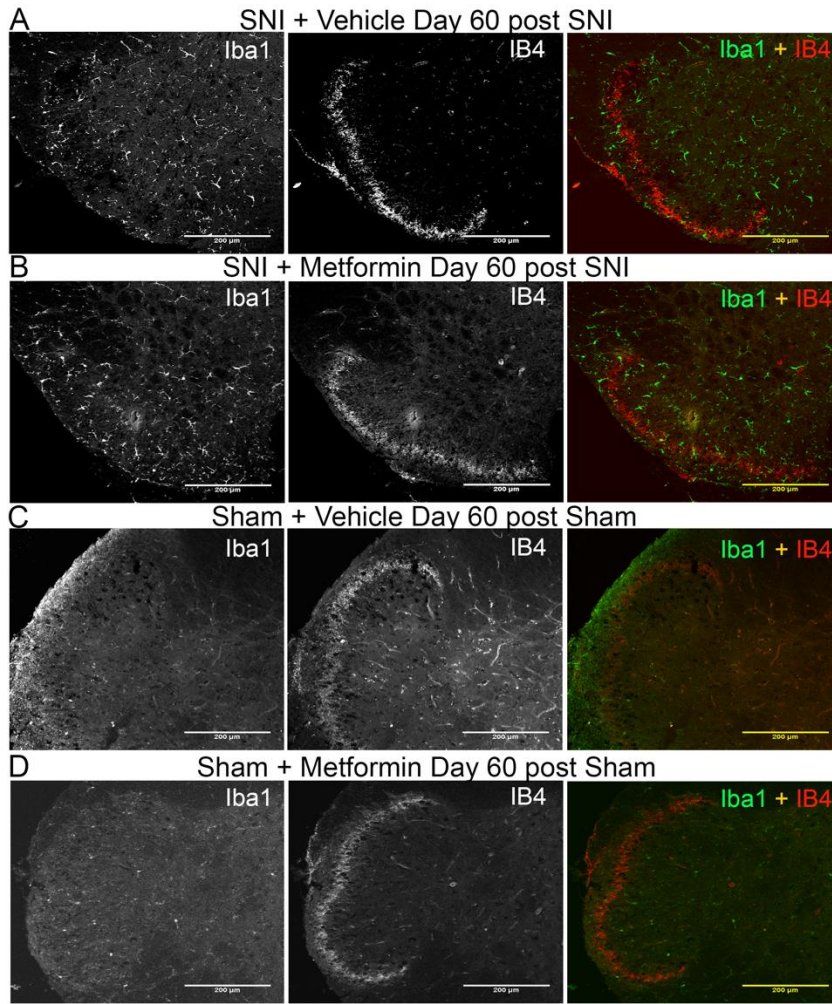


Figure 2.4: Metformin does not reverse microglial activation in SNI female mice. A-D. Representative immunohistochemistry images of the dorsal horn of female lumbar spinal cord at 20X magnification. Quantification of images shown in E. SNI robustly stimulated microglial activation in female SNI mice, but metformin had no effect. A loss of IB4 staining was not observed in female SNI mice (A-B). *** $p < 0.001$; $N = 5$ per group.

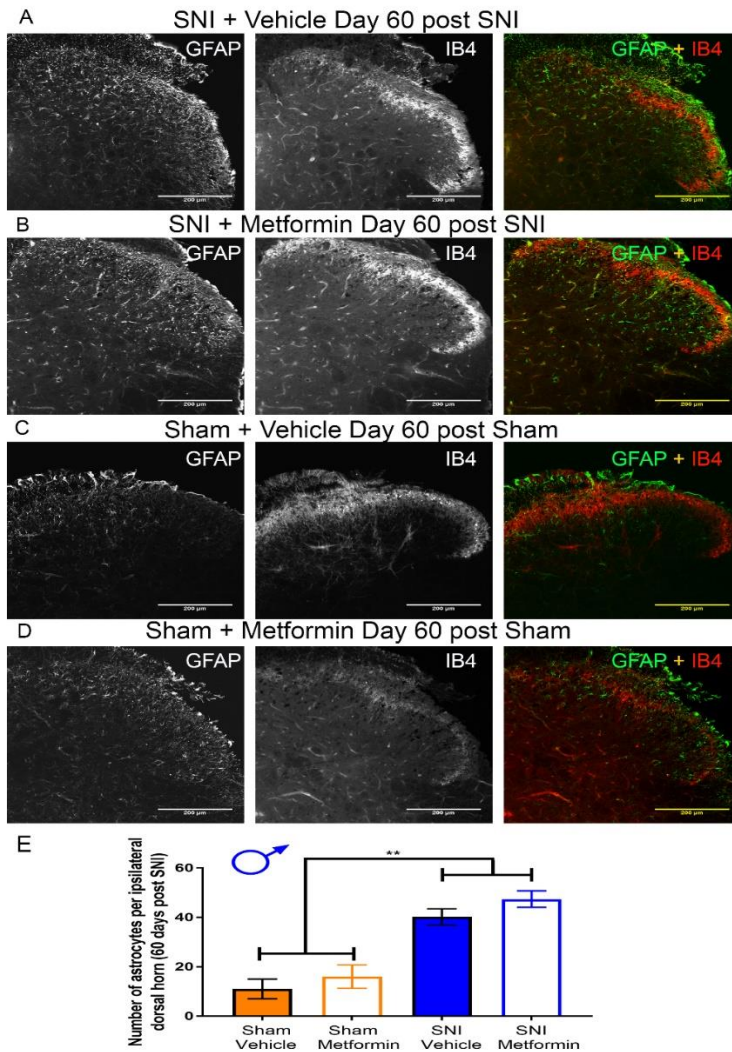


Figure 2.5: Metformin does not reverse astrocyte proliferation in SNI male mice. A-D. Representative immunohistochemistry images of the dorsal horn of male lumbar spinal cord at 20X magnification. Quantification of images shown in E. SNI robustly stimulated astrocyte proliferation in male mice, but metformin had no effect. *** $p < 0.01$; $N = 5$ per group.

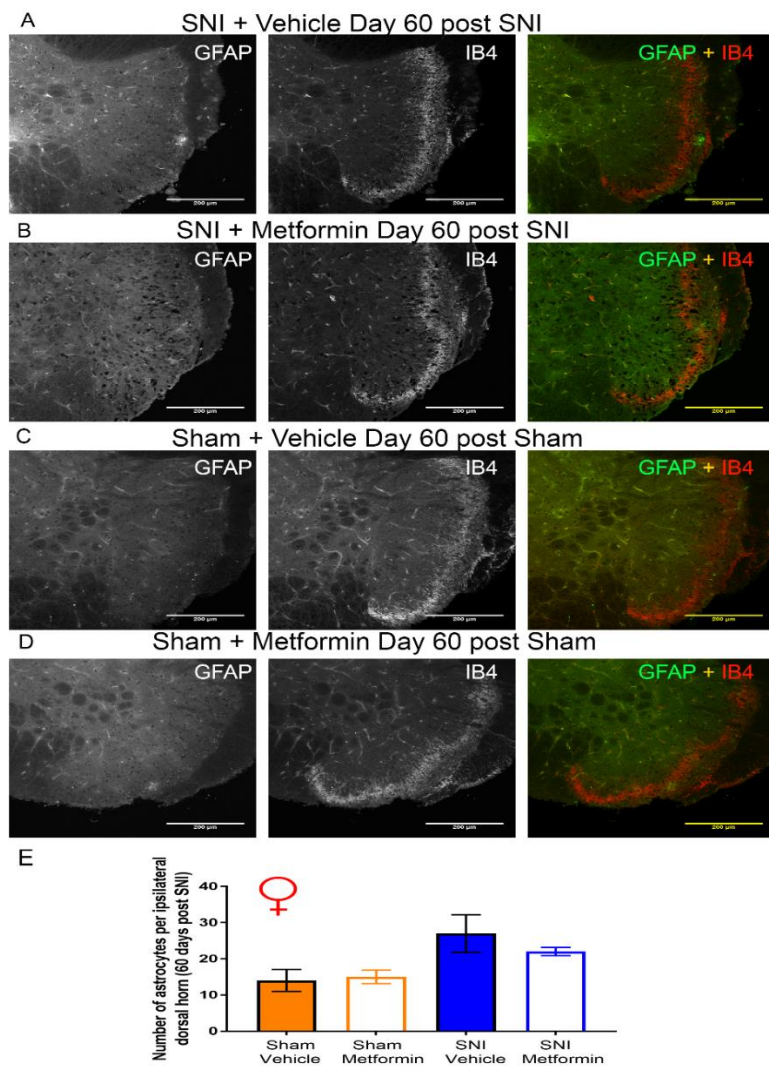


Figure 2.6: SNI did not result in an increase in astrocytes in the spinal dorsal horn of female mice. A-D. Representative immunohistochemistry images of the dorsal horn of female lumbar spinal cord at 20X magnification. Quantification of images shown in E. SNI did not cause an increase in the number of astrocytes seen in the dorsal horn of female mice. N= 5 per group.

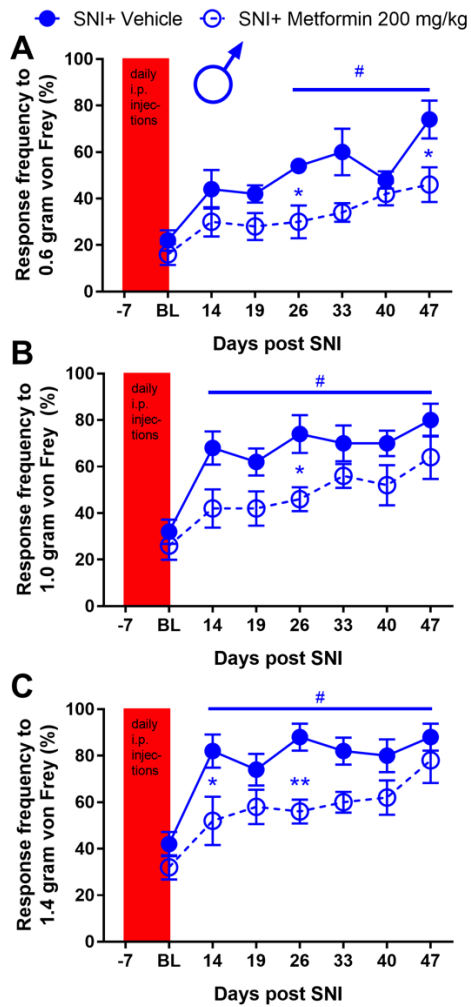


Figure 2.7: Preemptive treatment with metformin for 7 days prior to SNI inhibits neuropathic pain in male mice. Male mice were given metformin for 7 days prior to SNI. Mechanical hypersensitivity was inhibited at indicated time points after SNI. * $p < 0.05$; ** $p < 0.01$; # $p < 0.05$ versus BL. N= 6.

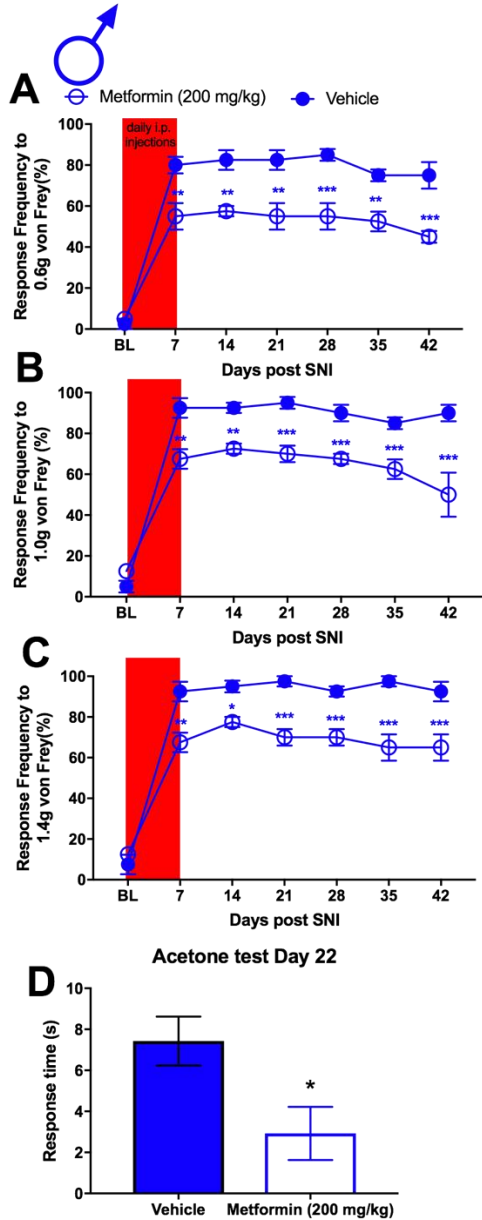


Figure 2.8: Treatment with metformin for the first 7 days after SNI inhibits neuropathic pain in male mice. Male mice were given metformin for 7 days starting at the day of SNI surgery. Mechanical hypersensitivity was inhibited at the indicated time points after SNI. D. Metformin also decreased in cold hypersensitivity after SNI. * $p < 0.05$; ** $p < 0.01$; *** $p < 0.001$; **** $p < 0.0001$; $N = 6$ per group.

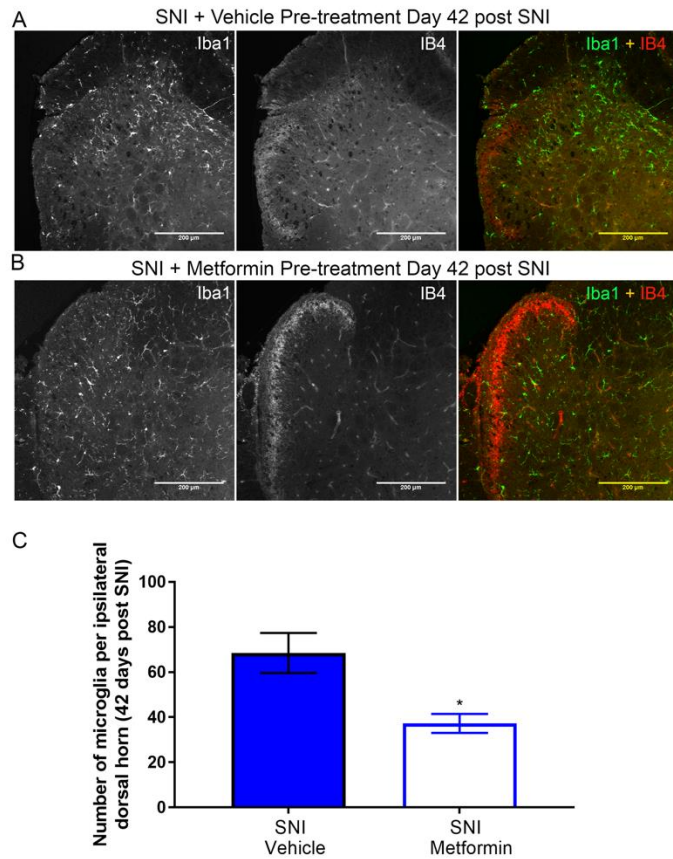


Figure 2.9: Early treatment with metformin blocks SNI-induced microglial activation in male mice. A-B. Representative immunohistochemistry images of the dorsal horn of male lumbar spinal cord at 20X magnification. Quantification of images shown in C. Metformin decreased SNI-induced microglia activation. SNI caused a loss of IB4 staining in the dorsal horn (A) that was reversed by metformin treatment for the first 7 days after surgery (B). * $p < 0.05$; $N = 5$ per group.

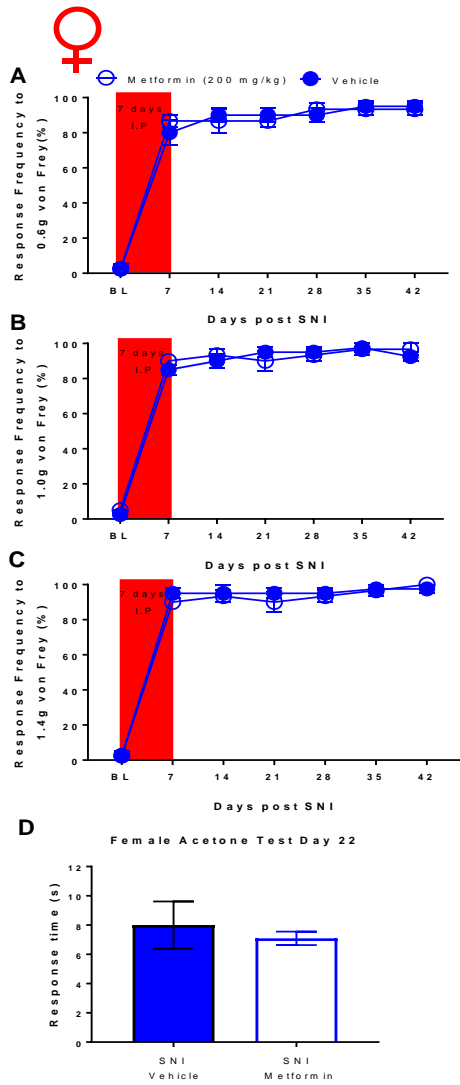


Figure 2.10: Treatment with metformin for the first 7 days after SNI failed to inhibit neuropathic pain in female mice. A-C. Female mice were given metformin for 7 days starting at the day of SNI surgery. Mechanical hypersensitivity was not inhibited at the indicated time points after SNI. D. Metformin also did not decrease cold hypersensitivity after SNI. N= 4 per group.

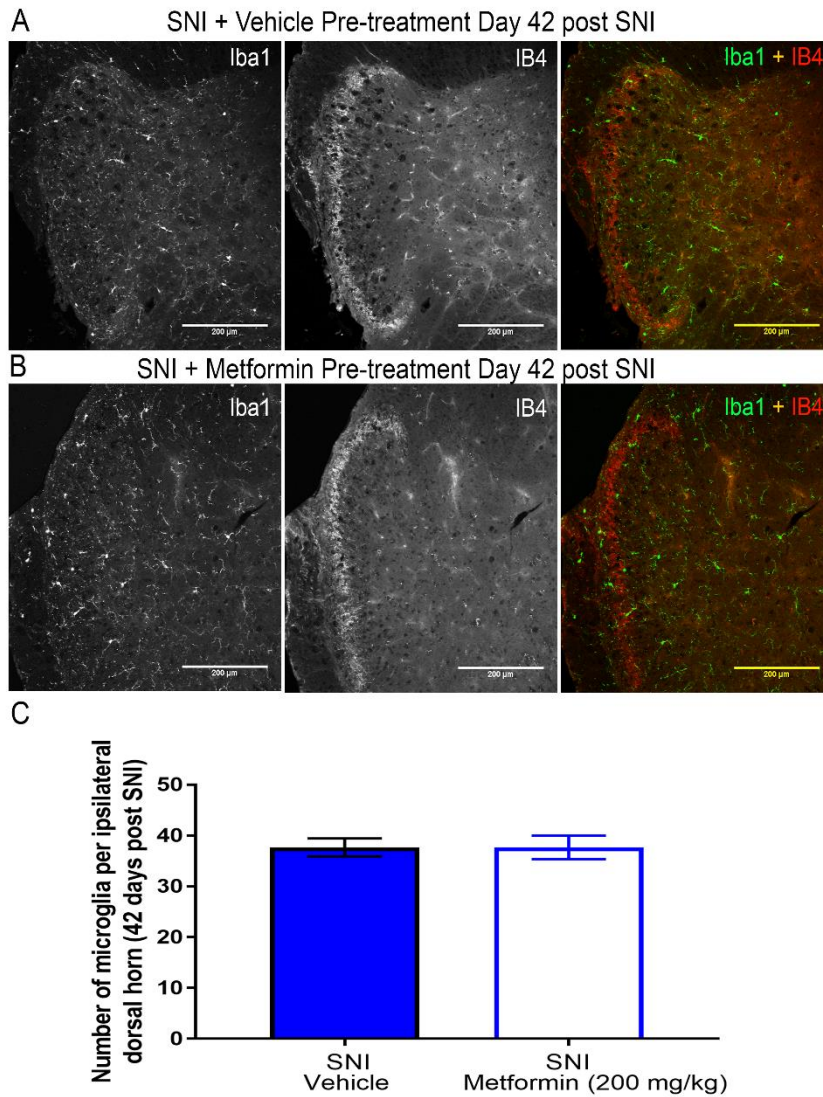


Figure 2.11: Early treatment with metformin does not block SNI-induced microglial activation in female mice. A-B. Representative immunohistochemistry images of the dorsal horn of female lumbar spinal cord. Quantification of images shown in C. Metformin did not decrease SNI-induced microglia activation. Again, SNI did not cause a loss in IB4 staining in female mice that was seen in males following SNI. N= 6 per group.

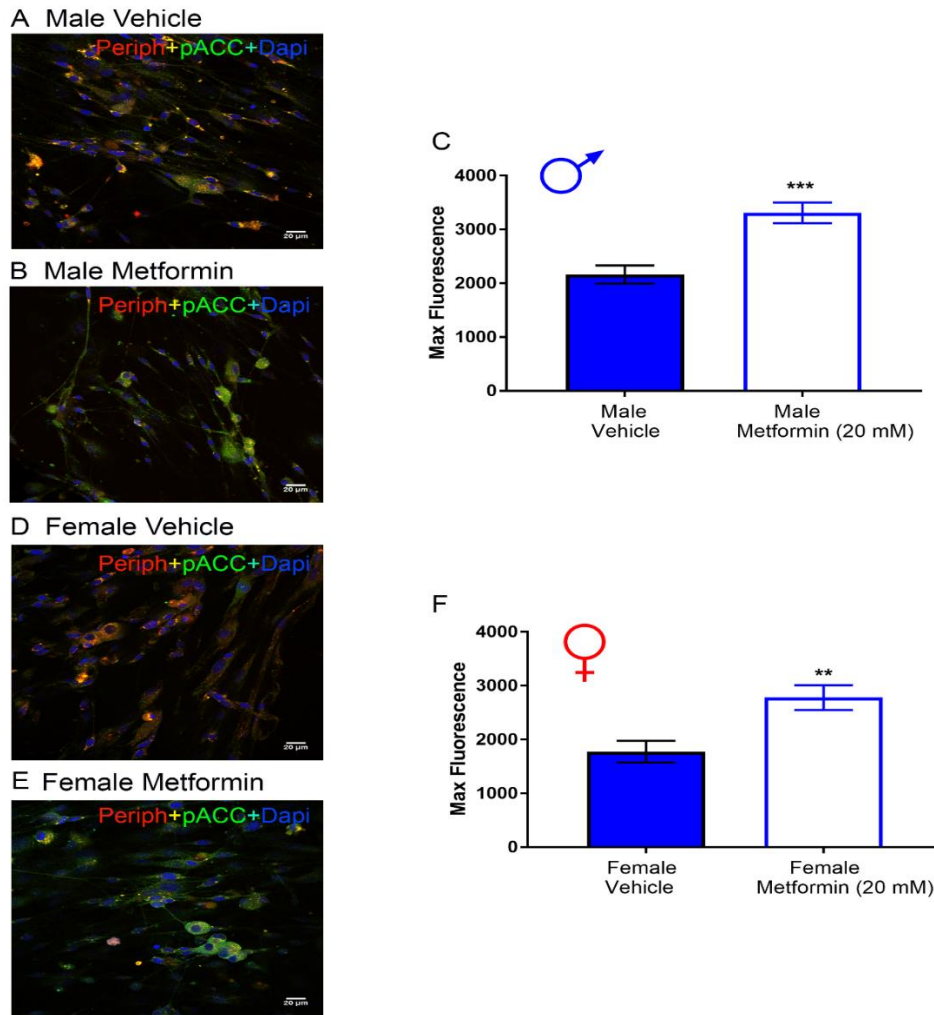


Figure 2.12: Metformin induces AMPK activity in male and female DRG neurons *in vitro*. Male and female neuron cultures were treated with metformin (20 mM) for 1 hr. A-B (male), D-E (female). Representative immunohistochemistry images of the DRG neurons at 40X magnification. Quantification of images shown in C (male) and F (female). Metformin increased p-ACC intensity in male and female neuron cultures. Only neurons that were positive for peripherin staining were analyzed. Maximum fluorescence refers to the maximum fluorescence intensity per neuron analyzed. ** $p < 0.01$; *** $p < 0.001$. N= 20 images analyzed per group.

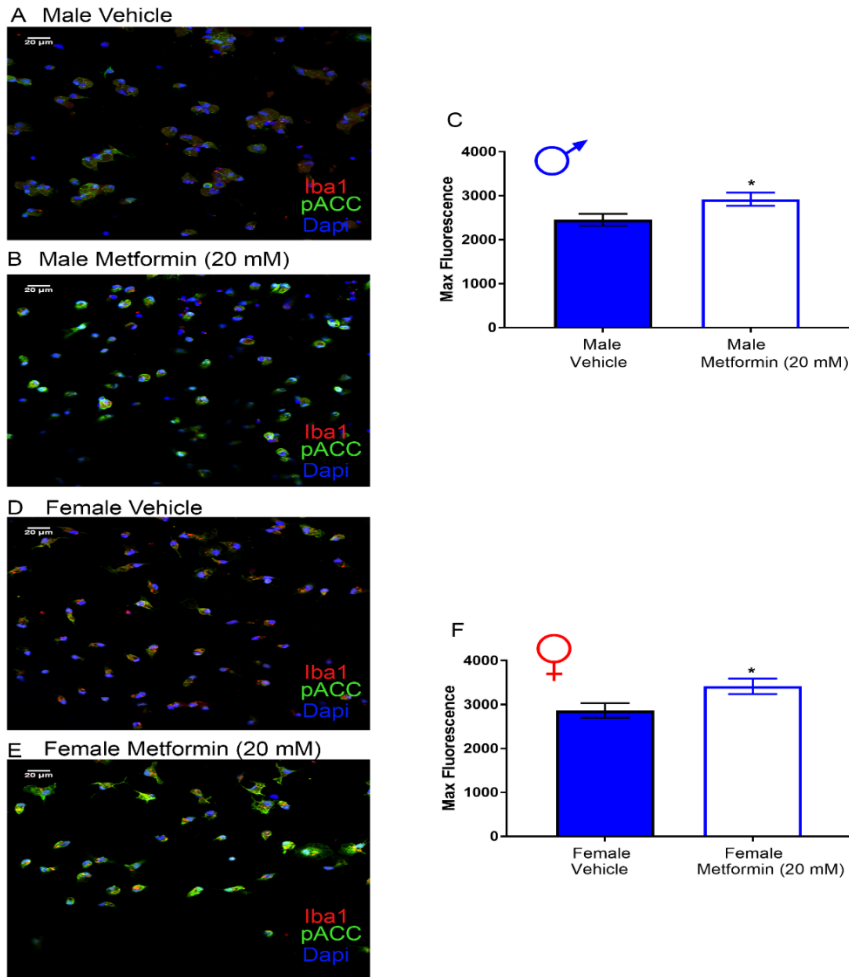


Figure 2.13: Metformin induces AMPK activity in male and female microglia *in vitro*. Male and female microglia cultures were treated with metformin (20 mM) for 1 hr. A-B (male), D-E (female). Representative immunohistochemistry images of the DRG neurons at 40X magnification. Quantification of images shown in C and F. Metformin increased p-ACC intensity in male and female microglia cultures. Only microglia that were positive for Iba1 staining were analyzed. Maximum fluorescence refers to the maximum fluorescence intensity per microglial cell analyzed. * $p < 0.05$. N= 20 images analyzed per group.

T

Table 2.1: Statistical tests and values

Test (Factor)	F (df1, df2) interaction F (df1, df2) time F (df1, df2) Drug treatment	P-Value	Adjusted p-value (Post-hoc comparison): BL, 14 days, 21 days, 35 days and 56 days
Two-way ANOVA (Fig 1A)	F (12, 155) = 10.46 F (4, 155) = 38.76 F (3, 155) = 103.7	P _l <0.0001 P _t <0.0001 P _d <0.0001	SNI + Met vs. SNI + Veh: 0.9982, 0.1167, <0.0001, <0.0001, <0.0001 SNI + Met vs. Sham + Met: 0.9009, <0.0001, 0.6721, 0.1907, 0.0463 SNI + Met vs. Sham + Veh: 0.9548, <0.0001, 0.2056, 0.3366, 0.0008 SNI + Veh vs. Sham + Met: 0.8243, <0.0001, <0.0001, <0.0001, <0.0001 SNI + Veh vs. Sham + Veh: 0.9009, <0.0001, <0.0001, <0.0001, <0.0001 Sham + Met vs. Sham + Veh: 0.9982, >0.9999, 0.8243, 0.9859, 0.5141
Two-way ANOVA (Fig 1B)	F (12, 155) = 11.74 F (4, 155) = 44.64 F (3, 155) = 105.2	P _l <0.0001 P _t <0.0001 P _d <0.0001	SNI + Met vs. SNI + Veh: >0.9999, 0.9631, <0.0001, 0.0002, 0.0023 SNI + Met vs. Sham + Met: 0.7535, <0.0001, 0.8882, 0.0974, 0.0374 SNI + Met vs. Sham + Veh: 0.9991, <0.0001, 0.3610, 0.3869, 0.0374 SNI + Veh vs. Sham + Met: 0.9631, <0.0001, <0.0001, <0.0001, <0.0001 SNI + Veh vs. Sham + Veh: >0.9999, <0.0001, <0.0001, <0.0001, <0.0001 Sham + Met vs. Sham + Veh: >0.9999, >0.9999, >0.9999, >0.9999
Two-way ANOVA (Fig 1C)	F (12, 154) = 5.76 F (4, 154) = 37.68 F (3, 154) = 90.99	P _l <0.0001 P _t <0.0001 P _d <0.0001	SNI + Met vs. SNI + Veh: 0.1271, 0.7751, <0.0001, 0.0004, 0.2327 SNI + Met vs. Sham + Met: 0.8594, <0.0001, 0.9999, 0.9651, 0.0037 SNI + Met vs. Sham + Veh: 0.9997, <0.0001, 0.2647, 0.6104, 0.1382 SNI + Veh vs. Sham + Met: 0.9997, <0.0001, <0.0001, <0.0001, <0.0001

Table 2.1: Statistical tests and values

			SNI + Veh vs. Sham + Veh: 0.8594, <0.0001, <0.0001, <0.0001, <0.0001 Sham + Met vs. Sham + Veh: >0.9999, >0.9999, 0.8594, >0.9999, 0.9997
One-way ANOVA (Fig 1D)	F (3, 30) = 33.78	P<0.0001	SNI+ Met vs. SNI+ Veh: <0.0001 SNI+ Met vs. Sham+ Met: 0.0418 SNI+ Met vs. Sham+ Veh: 0.0749 SNI+ Veh vs. Sham+ Met: <0.0001 SNI+ Veh vs. Sham+ Veh: <0.0001 Sham+ Met vs. Sham+ Veh: 0.9919
Two-way ANOVA (Fig 2A)	F (12, 90) = 7.708 F (4, 90) = 83.29 F (3, 90) = 146.3	P _l <0.0001 P _t <0.0001 P _d <0.0001	SNI+ Met vs. SNI + Veh: 0.4916, >0.9999, 0.9923, 0.1291, 0.4916 SNI+ Met vs. Sham+ Met: 0.6379, <0.0001, <0.0001, <0.0001, <0.0001 SNI+ Met vs. Sham+ Veh: >0.9999, 0.0018, <0.0001, <0.0001, <0.0001 SNI + Veh vs. Sham+ Met: 0.0010, <0.0001, <0.0001, <0.0001, <0.0001 SNI + Veh vs. Sham+ Veh: 0.0867, 0.0006, <0.0001, <0.0001, <0.0001 Sham+ Met vs. Sham+ Veh: 0.9990, >0.9999, 0.5775, >0.9999, >0.9999
Two-way ANOVA (Fig 2B)	F (12, 90) = 1.657 F (4, 90) = 113.6 F (3, 90) = 157.2	P _l 0.0902 P _t <0.0001 P _d <0.0001	SNI+ Met vs. SNI + Veh: >0.9999, >0.9999, 0.6447, >0.9999, 0.6447 SNI+ Met vs. Sham+ Met: <0.0001, <0.0001, <0.0001, <0.0001, <0.0001 SNI+ Met vs. Sham+ Veh: 0.0014, <0.0001, <0.0001, <0.0001, <0.0001 SNI + Veh vs. Sham+ Met: <0.0001, <0.0001, <0.0001, <0.0001, <0.0001 SNI + Veh vs. Sham+ Veh: 0.0005, <0.0001, <0.0001, <0.0001, <0.0001 Sham+ Met vs. Sham+ Veh: >0.9999, >0.9999, >0.9999, 0.9505, 0.9505
Two-way ANOVA	F (12, 90) = 1.806 F (4, 90) = 99.05 F (3, 90) = 114.5	P _l 0.0589 P _t <0.0001	SNI+ Met vs. SNI + Veh: 0.9992, >0.9999, 0.9769, >0.9999, >0.9999 SNI+ Met vs. Sham+ Met: <0.0001, <0.0001, <0.0001, <0.0001, <0.0001

Table 2.1: Statistical tests and values

(Fig 2C)		P_d <0.0001	SNI+ Met vs. Sham+ Veh: 0.0149, 0.0002, <0.0001, 0.0011, 0.0011 SNI + Veh vs. Sham+ Met: <0.0001, <0.0001, 0.0014, <0.0001, <0.0001 SNI + Veh vs. Sham+ Veh: 0.0002, <0.0001, 0.0182, 0.0011, 0.0099 Sham+ Met vs. Sham+ Veh: 0.7140, >0.9999, >0.9999, 0.0023, 0.0023
One-way ANOVA (Fig 2D)	F (3, 18) = 31.34	$P < 0.0001$	SNI + Met vs. SNI+ Veh: 0.0002 SNI + Met vs. Sham+ Met: <0.0001 SNI + Met vs. Sham+ Veh: <0.0001 SNI+ Veh vs. Sham+ Met: 0.0433 SNI+ Veh vs. Sham+ Veh: 0.0267 Sham+ Met vs. Sham+ Veh: 0.9957
One-way ANOVA (Fig 3E)	F (3, 9) = 15.69	$P = 0.0006$	SNI+ Met vs. SNI+ Veh: 0.0160 SNI+ Met vs. Sham + Met: 0.2254 SNI+ Met vs. Sham+ Veh: 0.1247 SNI+ Veh vs. Sham + Veh: 0.0014 SNI+ Veh vs. Sham+ Met: 0.0014 Sham + Veh vs. Sham+ Met: 0.9204
One-way ANOVA (Fig 4E)	F (3, 12) = 87.54	$P < 0.0001$	SNI+ Met vs. SNI+ Veh: 0.9950 SNI+ Met vs. Sham+ Met: <0.0001 SNI+ Met vs. Sham+ Veh: <0.0001 SNI+ Veh vs. Sham+ Met: <0.0001 SNI+ Veh vs. Sham+ Veh: <0.0001 Sham+ Met vs. Sham+ Veh: 0.9805
One-way ANOVA (Fig 5E)	F (3, 11) = 19.07	$P = 0.0001$	SNI+ Met vs. SNI+ Veh: 0.4476 SNI+ Met vs. Sham+ Met: 0.0006 SNI+ Met vs. Sham+ Veh: 0.8783 SNI+ Veh vs. Sham+ Met: 0.0043 SNI+ Veh vs. Sham+ Veh: 0.0030 Sham+ Met vs. Sham+ Veh: 0.0005
One-way ANOVA (Fig 6E)	F (3, 10) = 3.231	$P = 0.0693$	SNI+ Met vs. SNI+ Veh: 0.7526 SNI+ Met vs. Sham+ Met: 0.5263 SNI+ Met vs. Sham+ Veh: 0.4737 SNI+ Veh vs. Sham+ Met: 0.1040 SNI+ Veh vs. Sham+ Veh: 0.1027 Sham+ Met vs. Sham+ Veh: 0.9970

Table 2.1: Statistical tests and values

Two-way ANOVA VA (Fig 7A)	F (6, 56) = 1.127 F (6, 56) = 8.379 F (1, 56) = 26.33	$P_I = 0.3587$ $P_t < 0.0001$ $P_d < 0.0001$	SNI+ Met vs SNI+ Veh: 0.9914, 0.5675, 0.5675, 0.0531, 0.0285, 0.9914, 0.0148
Two-way ANOVA VA (Fig 7B)	F (6, 56) = 0.5617 F (6, 56) = 7.403 F (1, 56) = 23.8	$P_I = 0.7589$ $P_t < 0.0001$ $P_d < 0.0001$	SNI+ Met vs SNI+ Veh: 0.9961, 0.0761, 0.2940, 0.0451, 0.7135, 0.4200, 0.5655
Two-way ANOVA VA (Fig 7C)	F (6, 56) = 0.8278 F (6, 56) = 8.595 F (1, 56) = 28.91	$P_I = 0.5534$ $P_t < 0.0001$ $P_d < 0.0001$	SNI+ Met vs SNI+ Veh: 0.9233, 0.0215, 0.5389, 0.0118, 0.1757, 0.3928, 0.9233
Two-way ANOVA VA (Fig 8A)	F (4, 30) = 4.082 F (4, 30) = 78.85 F (1, 30) = 50.88	$P = 0.0093$ $P < 0.0001$ $P < 0.0001$	SNI+ Met vs SNI+ Veh: >0.9999, 0.0033, 0.0033, 0.0012, 0.0004
Two-way ANOVA VA (Fig 8B)	F (4, 30) = 7.94 F (4, 30) = 172.9 F (1, 30) = 59.79	$P = 0.0002$ $P < 0.0001$ $P < 0.0001$	SNI+ Met vs SNI+ Veh: 0.6879, <0.0001, 0.0016, <0.0001, 0.0004
Two-way ANOVA VA (Fig 8C)	F (4, 30) = 6.346 F (4, 30) = 157.5 F (1, 30) = 56.54	$P = 0.0008$ $P < 0.0001$ $P < 0.0001$	SNI+ Met vs SNI+ Veh: >0.9999, 0.0002, 0.0106, <0.0001, 0.0008

Table 2.1: Statistical tests and values

Unpaired T-test (Fig 8D)	F, DF _n , Df _d = 1.18, 3, 3	P= 0.0430	SNI+ Met vs SNI+ Veh: 0.0430
Unpaired T-test (Fig 9C)	F, DF _n , Df _d = 4.41, 3, 3	P= 0.0192	SNI+ Met vs SNI+ Veh: 0.0192
Two-way ANOVA (Fig 10A)	F (6, 36) = 0.3987 F (6, 36) = 144.8 F (1, 36) = 2.513e-013	P=0.874 9 P<0.000 1 P>0.999 9	SNI + Met vs. SNI + Veh: >0.9999, >0.9999, >0.9999, >0.9999, >0.9999, >0.9999, >0.9999.
Two-way ANOVA (Fig 10B)	F (6, 36) = 0.641 F (6, 36) = 249 F (1, 36) = 0.3919	P=0.696 7 P<0.000 1 P=0.535 2	SNI + Met vs. SNI + Veh: >0.9999, >0.9999, >0.9999, >0.9999, >0.9999, >0.9999, >0.9999.
Two-way ANOVA (Fig 10C)	F (6, 36) = 0.3442 F (6, 36) = 264.7 F (1, 36) = 0.9423	P=0.908 6 P<0.000 1 P=0.338 2	SNI + Met vs. SNI + Veh: >0.9999, >0.9999, >0.9999, >0.9999, >0.9999, >0.9999, >0.9999.
Unpaired T-test (Fig 10D)	F, DF _n , Df _d = 16.53, 3, 2	P= 0.1151	SNI+ Met vs. SNI+ Veh: 0.6617

Table 2.1: Statistical tests and values

Unpaired T-test (Fig 11C)	F, DF _n , Df _d = 1.729, 5, 5	P> 0.9999	SNI+ Met vs. SNI+ Veh: 0.5627
Unpaired T-test (Fig 12C)	F, DF _n , Df _d = 1.292, 19, 19	P <0.0001	Met vs. Veh: <0.0001
Unpaired T-test (Fig 12F)	F, DF _n , Df _d =1.309, 19, 19	P= 0.0022	Met vs. Veh: 0.0022
Unpaired T-test (Fig 13C)	F, DF _n , Df _d =1.241, 23, 23	P= 0.0250	Met vs. Veh: 0.0250
Unpaired T-test (Fig 13F)	F, DF _n , Df _d =1.127, 23, 23	P= 0.0281	Met vs. Veh: 0.0281

CHAPTER 3

INDIRECT AMPK ACTIVATORS PREVENT INCISION-INDUCED HYPERALGESIA AND BLOCK HYPERALGESIC PRIMING WHILE POSITIVE ALLOSTERIC MODULATORS ONLY BLOCK PRIMING IN MICE

Kufreobong E Inyang¹, Michael D Burton¹, Thomas Szabo-Pardi¹, Emma Wentworth¹,
Timothy A. McDougal¹, Eric D Ramirez¹, Grishma Pradhan¹, Gregory Dussor¹,
Theodore J Price^{1,*}

¹School of Behavioral and Brain Sciences,

The University of Texas at Dallas

800 W Campbell Rd

Richardson TX 75080

Abstract

AMPK is a multifunctional kinase that negatively regulates mechanistic target of rapamycin (mTOR) and mitogen activated protein kinase (MAPK) signaling, two signaling pathways that are linked to pain promotion after injury, such as surgical incision. AMPK can be activated directly using positive allosteric modulators as well as indirectly through the upregulation of upstream kinases such as liver kinase B1 (LKB1) which is a mechanism of action of metformin. Metformin is a commonly prescribed type II diabetes drug that could potentially be repurposed as an analgesic due to its ability to activate AMP activated protein kinase (AMPK). However, metformin's anti-hyperalgesic effects have been shown to be specific to male mice in the spared nerve injury (Myers, Guan et al. 2017) model, raising questions about how metformin regulates pain sensitivity. We conducted experiments to determine if the sex dependent anti-nociceptive effects of metformin were specific to this AMPK activator. To do this, we used metformin as well as other structurally distinct AMPK activators, narciclasine (NCLS), ZLN 024 and MK 8722, to treat incision-induced mechanic hypersensitivity and hyperalgesic priming in male and female mice. We found that metformin was the only AMPK activator to have sex specific effects. We also found that indirect AMPK activators metformin and NCLS were able to reduce mechanical hypersensitivity and block hyperalgesic priming, direct AMPK activators, ZLN 024 and MK 8722 only blocked priming. Direct and indirect AMPK activators stimulated AMPK in dorsal root ganglion (DRG) neuron cultures to a similar degree. However, incision decreased phosphorylated AMPK (p-AMPK) in DRG. Because AMPK phosphorylation is required

for kinase activity, we interpret our findings as evidence that indirect AMPK activators are more effective for treating pain hypersensitivity after incision because they are able to drive increased p-AMPK through upstream kinases like LKB1. Conversely, direct allosteric modulators of AMPK have decreased efficacy due to this injury-induced decrease in p-AMPK. These findings have important implications for the development of AMPK-targeting therapeutics for pain treatment.

Introduction

Chronic pain is a rapidly growing international health issue that contributes substantially to morbidity, mortality, disability, demands on health care systems, and economic burdens for societies (Institute of Medicine Committee on Advancing Pain Research and Education 2011). New classes of analgesics are needed to combat this growing problem (Finnerup NB 2015). One of the most common and significant forms of chronic pain is chronic post-surgical pain (Haroutiunian S 2013) which causes major functional impairment in 5-10% of surgery patients (Kehlet H 2006). Post-surgical pain medicines that can provide pain relief acutely and also diminish the probability of developing chronic pain would improve health care (Price TJ 2018). Adenosine monophosphate-activated protein kinase (AMPK) is a cellular fuel-sensing enzyme present in most cells across species (Hardie 2007). This kinase detects changes in the AMP/ATP ratio to regulate anabolic processes when cellular energy status is low (Kahn BB 2005). Several studies have shown that AMPK plays a key role in nociceptive sensitization (Song H 2015, Bullón P 2016). AMPK activation causes a decrease in mTOR and MAPK signaling leading to many cellular effects including a suppression of protein synthesis mediated by activation of mTOR and MAPK pathways (Hardie 2007). In animal models of incisional and nerve injury pain, MAPK and mTOR signaling pathways are turned on in dorsal root ganglion (DRG) neurons, including nociceptors, and these signaling events are a causative factor in increased nociceptor excitability and behavioral nociceptive hypersensitivity (Sato and Ohshima 2000, Banik, Subieta et al. 2005). Many groups have shown that AMPK activators can be effective in attenuating this cellular hyperexcitability

and behavioral hypersensitivity (Tillu DV 2012, Mejjia, Asiedu et al. 2016). We have also shown that AMPK activators prevent the development of hyperalgesic priming, a preclinical model mimicking aspects of the transition from acute to chronic pain.

Metformin is a very commonly prescribed drug for type II diabetes that activates AMPK indirectly in a liver kinase B1 (LKB1) dependent fashion (Shaw RJ 2005). While the exact mechanism of the drug remains an area of active inquiry, metformin is safe and could potentially be repurposed as a pain-relieving drug (Rena, Hardie et al. 2017, Wu, Wang et al. 2018). We have previously shown that metformin is effective in reversing SNI-induced neuropathic pain (Melemedjian OK 2011) as well as reducing mechanical hypersensitivity following surgical incision without reducing the rate of wound healing (Burton, Tillu et al. 2017). Interestingly, the anti-hyperalgesic effects of metformin seem to occur specifically in male mice (Inyang, Szabo-Pardi et al. 2018).

Various other AMPK activators have emerged in recent years and could be better potential analgesics than metformin (Cao, Huang et al. 2018, Qin, Qiao et al. 2018). It is also unknown whether these drugs could show sex-specific effects. Narciclasine is a natural compound from the plant *Amaryllidaceae* (Dumont, Ingrassia et al. 2007) and indirectly activates AMPK (Julien SG 2017) through a mechanism that may involve cAMP (Zhang, Zhou et al. 2009). Narciclasine and related compounds are also known to have anti-inflammatory effects (Yui, Mikami et al. 2001, Lubahn, Schaller et al. 2012). While indirect AMPK activators stimulate upstream kinases that phosphorylate AMPK, another way to activate AMPK is via direct positive allosteric mechanisms. Several positive allosteric modulators of AMPK, including ZLN024 (Zhang, Xu et al. 2013) and MK8722

(Feng, Biftu et al. 2018, Weihrauch and Handschin 2018), have recently been described and have favorable pharmacokinetics for *in vivo* dosing.

The goal of the experiments described here was to establish whether the sex-specificity seen with metformin treatment following spared nerve injury (Myers, Guan et al. 2017) was also found in the incisional pain model. We also sought to determine whether other AMPK activators can be effective in alleviating incision-induced nociceptive hypersensitivity and hyperalgesic priming in male and/or female mice. Our experiments demonstrate that metformin is effective in reducing hypersensitivity following incision as well as hyperalgesic priming in male but not female mice. On the other hand, narciclasine reduced acute pain caused by incision and blocked development of hyperalgesic priming in male and female mice. Direct AMPK allosteric modulators ZLN024 and MK8722 both only attenuated hyperalgesic priming but were effective in both sexes. We conclude that indirect AMPK activators have the best potential for future development as pain therapeutics.

Methods

Laboratory Animals

Animal procedures were approved by The University of Texas at Dallas Institutional Animal Care and Use Committee and were in accordance with National Institutes of Health Guidelines. All the experiments were performed on male or female ICR outbred mice obtained from Envigo at 4 weeks of age or bred at University of Texas at Dallas.

Mice were housed in the University of Texas at Dallas Animal Care Facility for at least one week prior to the start of behavior testing and surgery. Animals had *ad libitum* access to food and water and were on a 12 hr non-inverted light/dark cycle. Experimenters were blinded to treatment groups in behavioral experiments. Mice were randomized to treatment groups using a random number generator and in such a manner that multiple treatment groups were always found within any individual cage of animals. Male and female mice were housed separately in groups of 4 per cage.

Behavioral Testing

The plantar incision model was used to induce post-surgical pain in mice as described previously (Banik RK 2006). Mechanical sensitivity was assessed using stimulation of the hindpaw of the mouse with calibrated von Frey filaments from Stoelting. We used 0.6, 1.0 and 1.4-gram filaments and measured the response frequency to 10 consecutive stimulations of the hindpaw with each filament with stimulations spaced by at least 5 sec following 45 minutes of habituation to the testing boxes. The number of responses for each filament force was recorded. Following baseline testing, mice were treated systemically with an AMPK activator for 7 consecutive days. Immediately following day 3 of treatment, plantar incision surgery was performed by making a 5 mm longitudinal incision with a number 11 scalpel blade in the skin of the left hindpaw and the underlying muscle tissue 2 mm below the heel. The wound was closed using a 5-mm silk suture followed by a 200 μ L subcutaneous injection of gentamicin (Sigma-Aldrich, 5 mg/mL). For the sham surgery, mice were put under isoflurane for 5 minutes followed by subcutaneous gentamicin. Mice were tested for mechanical hypersensitivity periodically until response

frequency returned to baseline levels. Following the return to baseline, hyperalgesic priming was tested by giving each animal an intraplantar injection of prostaglandin E₂ (PGE₂) (100 ng/ 25 µL). Response frequency following PGE₂ was tested 3 and 24 hrs post-injection. The different AMPK activators used in this experiment were metformin i.p. (LKT Laboratories, 200 mg/kg), ZLN-024 hydrochloride i.p. (Tocris, 30 mg/kg) (Zhang, Xu et al. 2013), narciclasine p.o. (Santa Cruz Biotech, 3 mg/kg) (Julien SG 2017) and MK-8722 p.o. (a kind of gift from Merck, 30 mg/kg) (Feng, Biftu et al. 2018). Metformin and ZLN were dissolved in 0.9% saline and narciclasine was made in (2-Hydroxypropyl)-β-cyclodextrin (Sigma Aldrich). MK-8722 was administered in 0.25% methyl cellulose (MC), 5% Tween-80, and 0.02% sodium dodecyl sulfate (SDS)(Feng, Biftu et al. 2018).

Rotorod testing was done using a series 8 rotorod device from IITC Life Science. Mice were placed on the rotorod with the setting of 4 rotations per minute to start with an increase to 40 rotations per minute over the course of 108 seconds. The latency to fall was measured with the device. Testing was done before drug treatment and again on the last day of drug treatment.

Metformin Pharmacokinetics

This study was done at Sai Life Science Limited at Hinjewadi, India. Eighteen ICR mice weighing between 20 and 25 g were used, 9 male, and 9 female. Blood samples of approximately 60 µL were collected under light isoflurane anesthesia from sets of 3 male and female mice at 0.5, 1 and 4 hrs after dosing. Plasma was harvested by centrifugation of blood and stored at -70 C until analysis. After blood collection, brain samples were

isolated at each time point from the same animals. Brain was dipped 3 times in ice-cold phosphate buffered saline, blotted dry and weighed. Brain samples were homogenized using ice-cold phosphate buffered saline with twice the volume of brain weight and then stored at -70 until analysis. Plasma and brain samples were quantified by fit-for-purpose LC-MS/MS methods. Data are shown as ng/mL in plasma and ng/g brain weight.

Neuron Culture

DRGs were extracted aseptically from 4-week old male ICR mice in Hank's Buffered Salt Solution (HBSS, Invitrogen) on ice. The DRGs were dissociated enzymatically at 37 °C; first with collagenase A (1 mg/ml, Roche) for 25 min, then collagenase D (1 mg/ml, Roche) that included papain (30 µg/ml, Roche) for 20 min. Afterward, a trypsin inhibitor (1 mg/ml, Roche) that contained bovine serum albumin (BSA, Fisher, 1 mg/ml) was applied and the ganglia were mixed to allow for further dissociation with a polished Pasteur pipette. The tissue was then filtered through 70-µm nylon cell strainer (Falcon) and re-suspended in DMEM F-12 GlutaMax media (Invitrogen) that contained 10% fetal bovine serum (FBS, Hyclone) and 1× penicillin streptomycin (Pen-Strep). The media also contained NGF (10 ng/ml, Millipore) and 5-fluoro-2'-deoxyuridine + uridine (FRDU-U, 3.0 µg/ml + 7.0 µg/ml, Sigma) to reduce proliferation of glia and fibroblasts. Neurons were cultured for 7 days on 12-mm glass coverslips (#1 thickness, Chemglass) in a 24-well tissue culture plate (Falcon) coated with poly-d-lysine (Sigma) at 37 °C with 95% air and 5% CO₂. On the day of the experiment, drugs were diluted into DMEM F-12 plus GlutaMax media and added directly onto the neurons at concentrations indicated in the results for 1 hr. All

DRGs from 1 mouse were used to generate approximately 4 coverslips of primary cells. Coverslips from multiple independent animals were used in each experiment.

Immunocytochemistry (ICC) and digital image analysis

Following AMPK activator treatment, the cells were washed with phosphate buffered saline (PBS) and fixed with 10% formalin in phosphate buffered saline (PBS) for 30 minutes. Cells were blocked with 10% normal goat serum and labelled with Anti-peripherin, mouse monoclonal (Sigma, 1:500) and phospho-ACC (Ser 79) (p-ACC, 1:1000; Cell Signaling Technologies catalog # 3661) overnight at 4° C. Next, cells were washed and incubated with fluoro-chrome-conjugated secondary antibodies (Alexa Fluor, anti-rabbit 488 and anti-mouse 568, invitrogen) and counterstained with a DNA stain, 4',6-diamidino-2-phenylindole (DAPI) (Invitrogen) and mounted with Prolong Gold (Invitrogen). Images were taken on an Olympus Fluoview FV1200 laser scanning confocal microscope and analyzed using the co-localization tool within Olympus' FV software. The intensity of each channel was adjusted so that only areas that contained a strong signal of 488 nm and 405 nm were visible. This adjusted imaged contained distinct puncta that could then be counted and analyzed using Graphpad Prism. Results were reported as the average percent area of p-ACC signal in neurons labelled with peripherin for all representative pictures.

Western blotting

Male mice were anesthetized with isoflurane and spinal cords and DRGs innervating the hindpaw (L3 – L5) were removed. Fresh tissues were placed in ice cold lysis buffer (50

mM Tris pH 7.4, 150 mM NaCl, 1 mM EDTA pH 8.0, and 1% Triton X-100) containing protease and phosphatase inhibitors cocktails (Sigma–Aldrich) and homogenized using beaded homogenization tubes (Bertin Corp). Samples were centrifuged at 14,000 rpm for 15 min at 4°C and the supernatant containing protein extracts was collected. Protein concentrations were assessed using the Pierce BCA protein assay kit (ThermoFisher Scientific) as directed. A total of 10 µg of protein was mixed with Laemmli sample buffer (Bio-Rad) and 2-mercaptoethanol and was heated at 95°C for 5 min. Samples were loaded into each well of a 10% SDS–PAGE gel along with 15 µL of Precision plus protein kaleidoscope prestained protein standards (Bio-Rad). Proteins were transferred to a 0.45 PVDF membrane (Millipore, Billierca, MA, United States) at 100 V for 1 h. Membranes were blocked using 5% non-fat dry milk in 1× Tris Buffer Saline-Tween (TTBS) for 2 hrs prior to primary antibody incubation. Primary antibodies used for this experiment were pAMPKα (Thr 172) (1:1000, Cell Signaling catalog # 2535) and total AMPKα (1:1000, Cell Signaling, catalog # 2532). Bands were visualized using a Bio-Rad ChemiDoc Touch. Analysis was performed using Image Lab version 6.0.

Statistics

Data are shown as mean +/- standard error of the mean (SEM) and the number of animals or samples used in each analysis are given in figure legends. GraphPad Prism 7 was used to analyze data and to do curve fitting and other statistical tests are given in figure legends. Two-way ANOVAs were used to analyze von Frey data. Post-hoc tests used were the Bonferroni multiple comparisons test. Significance level was set at $\alpha < 0.05$. Details on test statistics are given in Table 3.1.

Results

Metformin decreases incision-induced mechanical hypersensitivity and blocked hyperalgesic priming in male but not female mice.

To assess the effects of metformin on incision-evoked mechanical hypersensitivity in male mice, we first obtained baseline responses for von Frey filament strengths of 0.6, 1.0 and 1.4 grams. Following baseline, mice were allocated into metformin (200 mg/kg) and vehicle (0.9% saline) i.p. treatment groups for 7 days. On day 3 of treatment, plantar incision surgery was performed on all of the mice. These mice were tested periodically over the next 2 weeks until they returned to baseline. Once the mice returned to baseline level sensitivity, animals received 100 ng PGE₂ into the affected hindpaw to assess hyperalgesic priming. These mice were tested 3 and 24 hrs post-injection. In male mice, metformin reduced acute mechanical hypersensitivity following plantar incision. Metformin also prevented the development of hyperalgesic priming (**Fig 3.1A-C**). These findings are consistent with our previously published data using the up-down von Frey testing method (Burton, Tillu et al. 2017). A separate group of sham surgery male mice were allocated into metformin and vehicle treatment groups and baselined for von Frey and rotarod testing to assess possible effects on motor behavior. These mice were treated for 7 days and given a sham surgery on day 3. The mice were tested periodically for von Frey responses and no differences were observed based on treatment (**Figure 3.11A-C**). Following the last day of drug treatment, these mice were tested on the rotarod again to assess the effects of metformin on motor behavior. Metformin had no effect on locomotive behavior in male mice (**Figure 3.11D**).

To test whether similar effects would be observed in female mice, we obtained baseline mechanical sensitivity measurements and randomized them into metformin and vehicle treatment groups under similar conditions as with males. On day 3 of treatment, plantar incision surgery was performed on these mice. Mechanical hypersensitivity was tested 1, 2, 4, 7, 10- and 14-days post-surgery. Once the mice returned to baseline level sensitivity, animals received 100 ng PGE₂ into the affected hindpaw. Unlike with male mice, metformin had no effect on the acute hypersensitivity caused by incision. Metformin also failed to block hyperalgesic priming in female mice (**Fig 3.1D-F**). These findings are consistent with our observations in female SNI mice where metformin only relieved mechanical hypersensitivity in male mice. While a pronounced difference in mechanical hypersensitivity was seen between male and female metformin treated mice after plantar incision, we did not observe any sex difference in the duration or magnitude of mechanical hypersensitivity in vehicle treated mice (**Fig 3.2**). To test the possibility that lower doses of metformin could be effective in female mice in the plantar incision test we did treatments with 100 and 50 mg/kg metformin. These doses also failed to impact acute mechanical hypersensitivity or to block hyperalgesic priming in female mice (**Figure 3.12**).

We next sought to determine whether this sex difference with metformin could be explained by pharmacokinetics. Nine male and 9 female ICR mice were given a single i.p. dose of 200 mg/kg metformin. A third of the mice were euthanized 30 min post-injection, another third 1 hr post-injection and the remaining 4 hrs post-injection with brain and plasma being taken at each time point. Metformin was measured in the brain and plasma of each animal and compared for each timepoint and across sexes. Surprisingly,

we found that plasma levels of metformin were higher in female mice at 0.5 and 1 hr post i.p. injection (**Figure 3.13A**). Brain levels were higher in female mice at all time points (**Figure 3.13B**). Brain to blood ratios did not differ between sexes (**Figure 3.13C**). Differences in pharmacokinetics for plasma or blood levels of metformin do not explain sex differences in efficacy seen in the incisional model.

Narciclasine decreased incision-induced mechanical hypersensitivity and blocked priming in male and female mice.

We then tested whether a structurally distinct AMPK activator would show similar sex-specific effects. We obtained baseline mechanical sensitivity measurements from male mice then sorted them into narciclasine (1, 3 or 6 mg/kg) and vehicle ((2-Hydroxypropyl)- β -cyclodextrin) p.o. groups. These mice were treated orally for 7 consecutive days and plantar incision surgery was performed on day 3 of treatment. These mice were tested for von Frey responses under the same time course as in the metformin experiments. Once the mice returned to baseline sensitivity, animals received PGE₂ into the hindpaw and were tested 3 and 24 hrs post-injection. In male mice, narciclasine reduced mechanical hypersensitivity following plantar incision in a dose-dependent fashion. All narciclasine doses completely blocked development of hyperalgesic priming (**Fig 3.3A-C**). Because the 3 mg/kg dose showed full efficacy in male mice, we chose to continue our experiments in female mice using only this dose. The male experiment was repeated in its entirety in a group of female mice over the same time course. Once the females returned to baseline, they also received PGE₂ into the affected paw and were tested 3 and 24 hrs post-surgery. Similar to the experiment with males, narciclasine prevented

acute mechanical hypersensitivity in female mice and blocked development of hyperalgesic priming (**Fig 3.3D-F**). Therefore, indirect AMPK activators can be effective in reducing incision-evoked mechanical hypersensitivity and hyperalgesic priming in both male and female mice. A separate group of sham surgery male mice were allocated into narciclasine and vehicle treatment groups and baselined for von Frey and rotarod testing to assess possible effects on motor behavior. These mice were also treated for 7 days but given a sham surgery treatment on day 3. The mice were tested periodically for von Frey responses and no differences were observed based on treatment (**Figure 3.14A-C**). Narciclasine also had no effect on rotarod behaviors (**Figure 3.14D**).

While narciclasine has been shown to activate AMPK in other cell types, it has never been tested for AMPK activity in DRG neurons. To directly assess this, DRGs were cultured from naïve male mice and treated with vehicle, 100 nM, 1 μ M narciclasine for 1 hr. We observed a significant increase in p-ACC intensity with narciclasine treatment at 1 μ M demonstrating that narciclasine induces AMPK activation in DRG neurons (**Fig 3.4A-D**). This concentration is higher than previous demonstrations of AMPK activation with 20 nM narciclasine in skeletal muscle cells, but those experiments were done over 48 hr treatment and ours was done with a 1 hr treatment time. The discrepancy in concentration of narciclasine needed to activate AMPK may be cell type- or time course-dependent. We conclude from this biochemical study that narciclasine is a potent activator of AMPK in DRG neurons.

In addition to these *in vitro* findings, we used western blotting to confirm that narciclasine can activate AMPK in the DRG in males and females *in vivo*. Mice of both sexes were

given a single dose of NCLS (3 mg/kg) and DRGs and livers were taken 1 hr post-injection and homogenized for Western blotting. Primary antibodies used were p-AMPK and total-AMPK to assess the effects of narciclasine on AMPK signaling in these tissues. We observed a significant increase in p-AMPK/total-AMPK ratio in both the male and female DRGs with narciclasine treatment compared to vehicle (**Fig 3.5**). There was no difference in p-AMPK/total-AMPK ratio in male or female liver with narciclasine treatment, which is consistent with previously published data with this compound (Julien SG 2017).

Direct, allosteric AMPK activators reduce hyperalgesic priming in male and female mice without impacting acute incision-induced mechanical hypersensitivity.

Metformin and narciclasine activate AMPK via upstream signaling mechanisms. ZLN024 and MK8722 are structurally distinct AMPK activators that bind directly to the kinase to allosterically increase kinase activity, albeit via distinct mechanisms. We used these compounds because they have thoroughly described pharmacokinetics. After establishing baseline mechanical sensitivity measurements from male mice, we then assigned them to ZLN-024 (30 mg/kg) and vehicle (0.9% saline) i.p. treatment groups. These mice received i.p. ZLN-024 for 7 consecutive days and plantar incision surgery was performed on day 3 of treatment. Once the mice returned to baseline sensitivity, animals received PGE₂ into the hindpaw and tested 3 and 24 hrs post-injection. In male mice, ZLN-024 did not significantly decrease mechanical hypersensitivity following plantar incision surgery, but 7-day treatment did block hyperalgesic priming (**Fig 3.6A-C**). For the female cohorts, ZLN-024 also had no effect on the initial surgery-induced mechanical hypersensitivity but did block hyperalgesic priming following PGE₂ just as with

the male cohort (**Fig 3.6D-F**). Using the same paradigm for testing in male mice, MK8722 did not significantly decrease mechanical hypersensitivity following plantar incision surgery, except a small effect at day 7 after incision. However, 7-day treatment did block hyperalgesic priming (**Fig 3.7A-C**). In the female cohorts, MK8722 again had no effect on the initial incision-induced mechanical hypersensitivity but also blocked hyperalgesic priming following PGE₂ just as with the male cohort (**Fig 3.7D-F**). These experiments demonstrate that direct activators of AMPK have a strong effect on hyperalgesic priming, but do not influence pain hypersensitivity caused by acute incision. A separate group of male mice were allocated into MK8722 and vehicle treatment groups and baselined for von Frey and the rotarod. These mice were treated for 7 days and given a sham surgery on day 3. The mice were tested in the von Frey test throughout this time and, following treatment, they were tested on the rotarod again to assess the effects of MK8722 on locomotive behavior. As with metformin and narciclasine on sham mice, MK8722 had no effect on von Frey or locomotive behavior in male mice (**Figure 3.15A-D**).

We have previously given 2 local injections of AMPK activators (one at the time of incision and another 24 hrs later) to demonstrate that local activation of AMPK can attenuate incision-evoked mechanical hypersensitivity (Tillu DV 2012, Burton, Tillu et al. 2017). We assessed whether MK8722 (10 µg dose per injection) would have an effect on incision-evoked pain. We found that in both males (**Fig 3.8A-C**) and females (**Fig 3.8D-F**) MK8722 had no effect on acute mechanical hypersensitivity but local treatment with this direct AMPK activator did attenuate hyperalgesic priming (**Fig 3.8A-F**). This effect is consistent with the systemic dosing experiment with MK8722 but is in contrast to our previous

findings with local injection of indirect AMPK activators (e.g. resveratrol) that blocked acute mechanical hypersensitivity and hyperalgesic priming (Tillu DV 2012, Burton, Tillu et al. 2017).

Like narciclasine, MK8722 activates AMPK in many cell types but has not previously been tested on DRG neurons. DRGs were cultured from naïve male mice and treated with vehicle, 100 nM or 10 μ M MK8722 for 1 h. We observed a significant increase in p-ACC intensity with MK8722 treatment at 100 nM and 10 μ M demonstrating that MK8722 induces AMPK activation neurons (**Fig 3.9A-D**). Quantification was done by measuring the maximum fluorescence (**Fig 3.9D**). Based on this result we conducted a full concentration response curve for MK8722 and obtained an approximate EC₅₀ of 900 nM (95% confidence interval 253 nM – 2.62 μ M) for AMPK activation in DRG neurons (**Fig 3.9E**). This EC₅₀ for MK8722 is similar to observations in rat primary hepatocytes for AMPK activation (Myers, Guan et al. 2017).

Plantar incision decreases pAMPK in the DRG ipsilateral to incision injury.

Male mice went through the same behavioral battery described above and then plantar incision surgery was performed. Two hrs post-surgery, lumbar DRGs were taken on the ipsilateral and contralateral sides from these mice and homogenized for western blotting. Primary antibodies used were p-AMPK and total-AMPK to assess the effects of injury on AMPK signaling. We saw a significant decrease in p-AMPK/total-AMPK ratio in ipsilateral DRGs compared to contralateral DRGs (**Fig 3.10**). This finding is consistent with previously published data demonstrating that pain-inducing stimuli cause a decrease in

AMPK signaling in DRG (Atef, El-Sayed et al. 2018). Given that many direct AMPK activators require AMPK phosphorylation for their pharmacological activity, this potentially explains why those compounds are less efficacious for acute incisional pain.

Discussion

One of the key findings of this study is that while metformin's sex differential effect on neuropathic pain (Inyang, Szabo-Pardi et al. 2018) can also be observed in the incisional pain model, other AMPK activators did not have a sex-specific effect on pain in our experiments. Narciclasine, ZLN-024 and MK 8722 all had the same level of efficacy on hyperalgesic priming in male and female mice. Metformin had a robust initial anti-hyperalgesic effect and blocked hyperalgesic priming in male mice but showed no effect in female mice. These sex differences were not readily explained by pharmacokinetics of metformin. In fact, female mice had higher plasma and brain levels of metformin than did male mice. While we do not have an explanation for sex differences in metformin's efficacy in incisional or neuropathic pain models in mice, our work does illustrate that other AMPK activators can be effective in the incisional model in both sexes.

Another key finding of this study is our demonstration that indirect AMPK activators are more efficacious in the acute phase of mechanical hypersensitivity following incisional injury. While the positive allosteric modulators ZLN-024 and MK 8722 showed a robust ability to block hyperalgesic priming, these drugs did little to attenuate the initial mechanical hypersensitivity caused by incision pain. In contrast, pretreatment with narciclasine (in males and females) and metformin (in males) caused a large initial anti-

hyperalgesic effect and more rapid resolution of surgery-induced hypersensitivity in addition to blocking priming. Despite this behavioral difference, we did not see a difference *in vitro* in the ability of these compounds to activate AMPK. Both narciclasine as well as MK 8722 induced significant AMPK activation in DRG neurons culture with an EC₅₀ for MK 8722 that was consistent with values previously reported in the literature (Myers, Guan et al. 2017). It is unlikely that these differences occurred due to pharmacokinetic or pharmacodynamic issues in the DRG because we used these compounds at *in vivo* doses that have been thoroughly vetted previously for AMPK activation. In line with this, we show here that narciclasine activates AMPK in the DRG, but not liver, of male and female mice.

How, then, can the difference in acute effects of these different modes of AMPK activation be explained? One potential explanation for the behavioral difference we saw between the indirect AMPK activators and positive allosteric modulators is the decrease in pAMPK in the DRG caused by incision injury, and has been shown previously in diabetic neuropathic pain (Atef, El-Sayed et al. 2018). A decrease in DRG neuron levels of phosphorylated AMPK would theoretically substantially decrease the ability of allosteric modulators to activate AMPK. This is because these drugs are thought to rely on phosphorylated AMPK to be able to increase AMPK activity. If AMPK phosphorylation is decreased by a preceding injury, these drugs would achieve a smaller amount of enhanced AMPK activation unless upstream AMPK phosphorylation is increased via some other mechanism. On the other hand, indirect AMPK activators increase AMPK phosphorylation because they act via upstream kinases that then phosphorylate AMPK.

A limitation of this idea is that the existing data on MK8722 has not directly assessed whether AMPK phosphorylation is needed for AMPK activation with this compound but it is clearly a direct activator of the enzyme (Myers, Guan et al. 2017).

As previously mentioned, metformin activates AMPK indirectly through the upstream kinase LKB1 (Shaw RJ 2005). Narciclasine is thought to increase AMPK phosphorylation via a cAMP- and ADP/ATP ratio-dependent mechanism which may act similarly to resveratrol (Julien SG 2017). Importantly, resveratrol also inhibits acute incision-evoked pain and blocks the development of hyperalgesic priming (Burton, Tillu et al. 2017). Therefore, from the perspective of therapeutic development of AMPK activators for the treatment of post-surgical pain, our findings support a focus on potent indirect AMPK activators. Given that narciclasine is far more potent than metformin, this molecule may represent an excellent starting point for further refinement in this space.

Another question arising from our work is why direct allosteric modulators of AMPK are effective in blocking the development of hyperalgesic priming but not acute incision-evoked hypersensitivity. Previous studies have made it clear that hyperalgesic priming can be completely reversed without having any effect at all on the acute pain phase (Asiedu, Tillu et al. 2011, Price and Inyang 2015) as we have shown here with ZLN024 and MK8722. While we have not investigated this directly, we favor the hypothesis that these compounds block mTOR and MAPK-dependent protein synthesis sufficiently to attenuate gene expression of proteins that are needed for the development of hyperalgesic priming. This could include the synthesis of proteins like CREB that act as retrograde signaling factors from the site of injury to then regulate transcriptional

programs that are needed for the transition to a chronic pain state (Melemedjian 2014). Our findings would suggest that the inhibition of translation of these proteins requires less AMPK activation than the translation of proteins that are required for the acute sensitization of nociceptors. This hypothesis can be explored in future studies.

There are several shortcomings to our study that should be addressed in the future. First, while we have done a large number of pharmacological manipulations in this study, we have not used genetic approaches to directly determine whether AMPK is responsible for the effects we have observed. Second, narciclasine's pharmacology is potentially complex and may involve signaling pathways that are independent of AMPK. We cannot rule this out based on our current experiments. Another caveat is that we have relied on evoked testing for pain assessment and we have not used other methods like paw guarding or mouse grimace scale. Our future work will focus on non-evoked pain measures. Finally, whether the hyperalgesic priming paradigm truly models development of chronic post-surgical pain is controversial, however, we are not aware of a widely accepted model of chronic post-surgical pain.

In conclusion, direct and indirect AMPK activators block the transition of acute to chronic pain that is potentially modeled preclinically by the hyperalgesic priming paradigm, and they can do this in males and females. However, indirect AMPK activators have an acute anti-hyperalgesic effect that is not seen with direct positive allosteric modulators. Based on these findings, we conclude that indirect AMPK activators, like narciclasine, should be further pursued as a treatment option for post-surgical pain that could achieve analgesia and a blockade of development of chronic pain in both sexes. More work is needed to

ultimately determine the selectivity of narciclasine at AMPK but given the favorable pharmacological profile that has already been described for this compound, we propose that it has excellent potential as a starting point for further development.

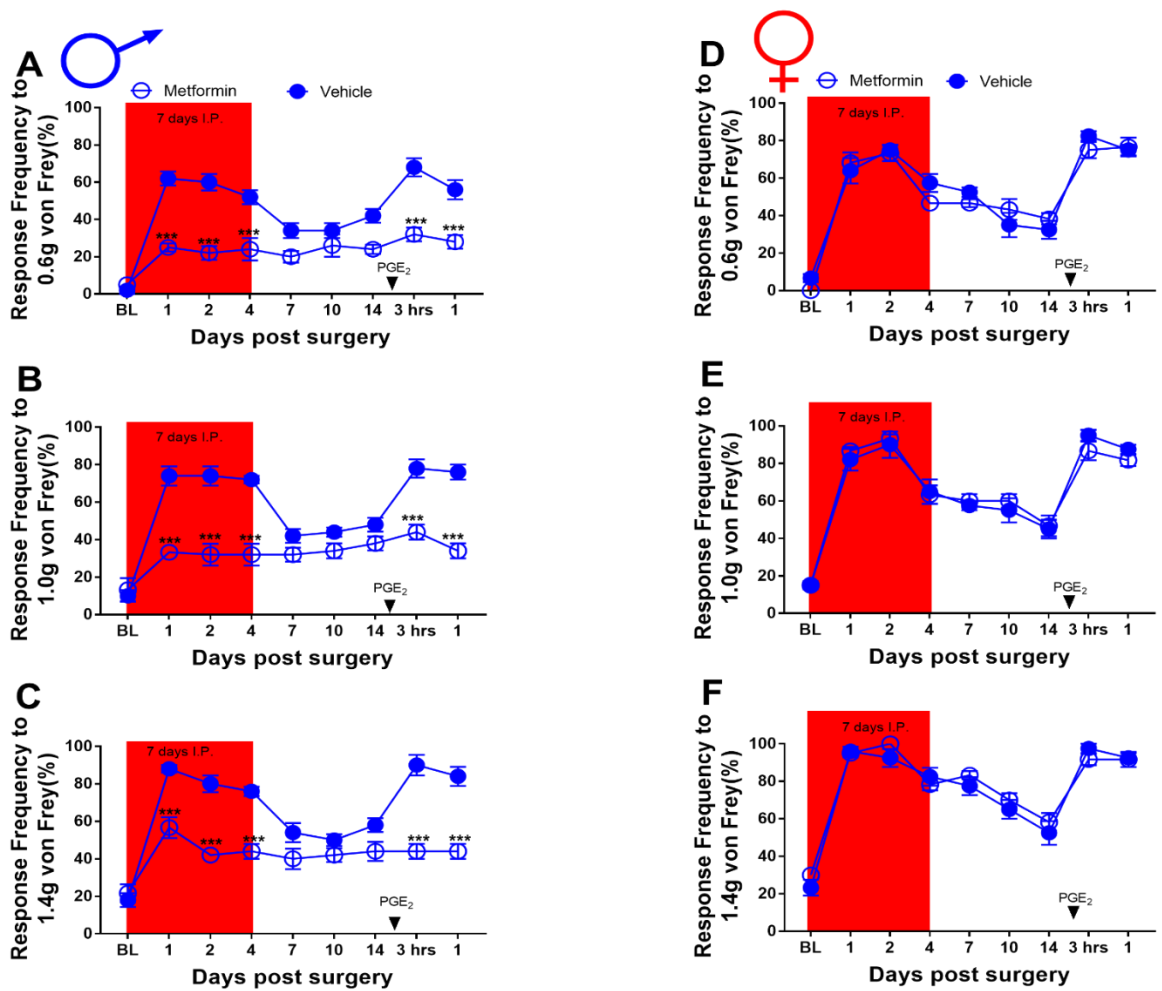


Figure 3.1: Metformin treatment attenuates incision-induced mechanical hypersensitivity and blocks hyperalgesic priming in male mice. A-C. Metformin treatment starting immediately after baseline measurements, which were done 3 days prior to plantar incision, decreased mechanical hypersensitivity following plantar incision surgery and prevented plantar incision-induced hyperalgesic priming precipitated by PGE₂ injection. D-F: In female mice, metformin treatment failed to decrease mechanical hypersensitivity compared to vehicle treated mice. Metformin also failed to prevent plantar incision-induced hyperalgesic priming precipitated by PGE₂ injection. ***p < 0.001; treatment effect; N= 6 for the metformin groups and N= 5 for the vehicle groups.

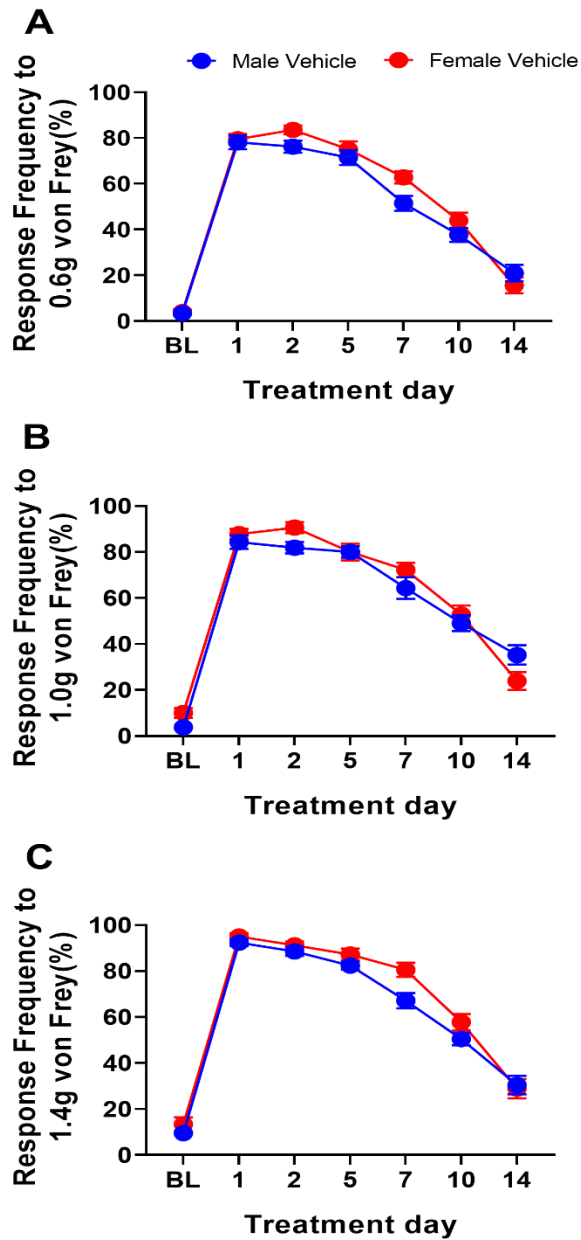


Figure 3.2: Male and female mice recover from plantar incision surgery at the same rate. A-C. Plantar incision surgery in male and female mice caused an increase in mechanical hypersensitivity that resolved at the same rate with no significant differences in mechanical hypersensitivity. N= 21 males and N= 18 females.

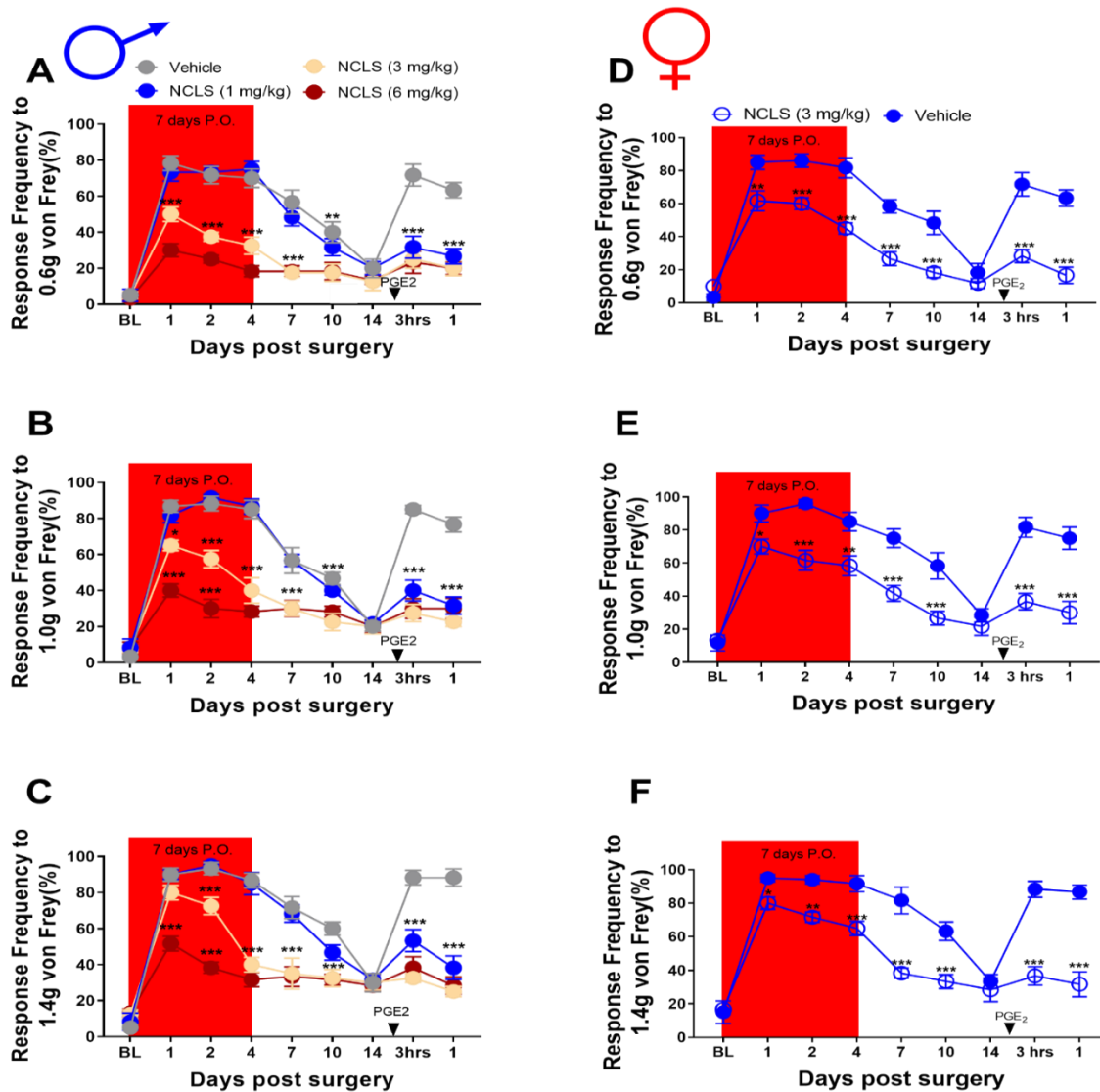


Figure 3.3: Narciclasine treatment attenuates surgery-induced mechanical hypersensitivity and blocks hyperalgesic priming in male and female mice. A-C. Narciclasine treatment starting immediately after baseline measurements dose-dependently decreased mechanical hypersensitivity following plantar incision surgery and prevented plantar incision-induced hyperalgesic priming precipitated by PGE₂ injection at all doses. **p* < 0.05; ***p* < 0.01; ****p* < 0.001; N= 4 for the NCLS groups and N= 3 for the vehicle group. D-F. Narciclasine treatment also decreased mechanical hypersensitivity following plantar incision surgery and prevented surgery-induced hyperalgesic priming precipitated by PGE₂ injection. **p* < 0.05; ***p* < 0.01; ****p* < 0.001; N= 6 for the NCLS group and N= 6 for the vehicle group.

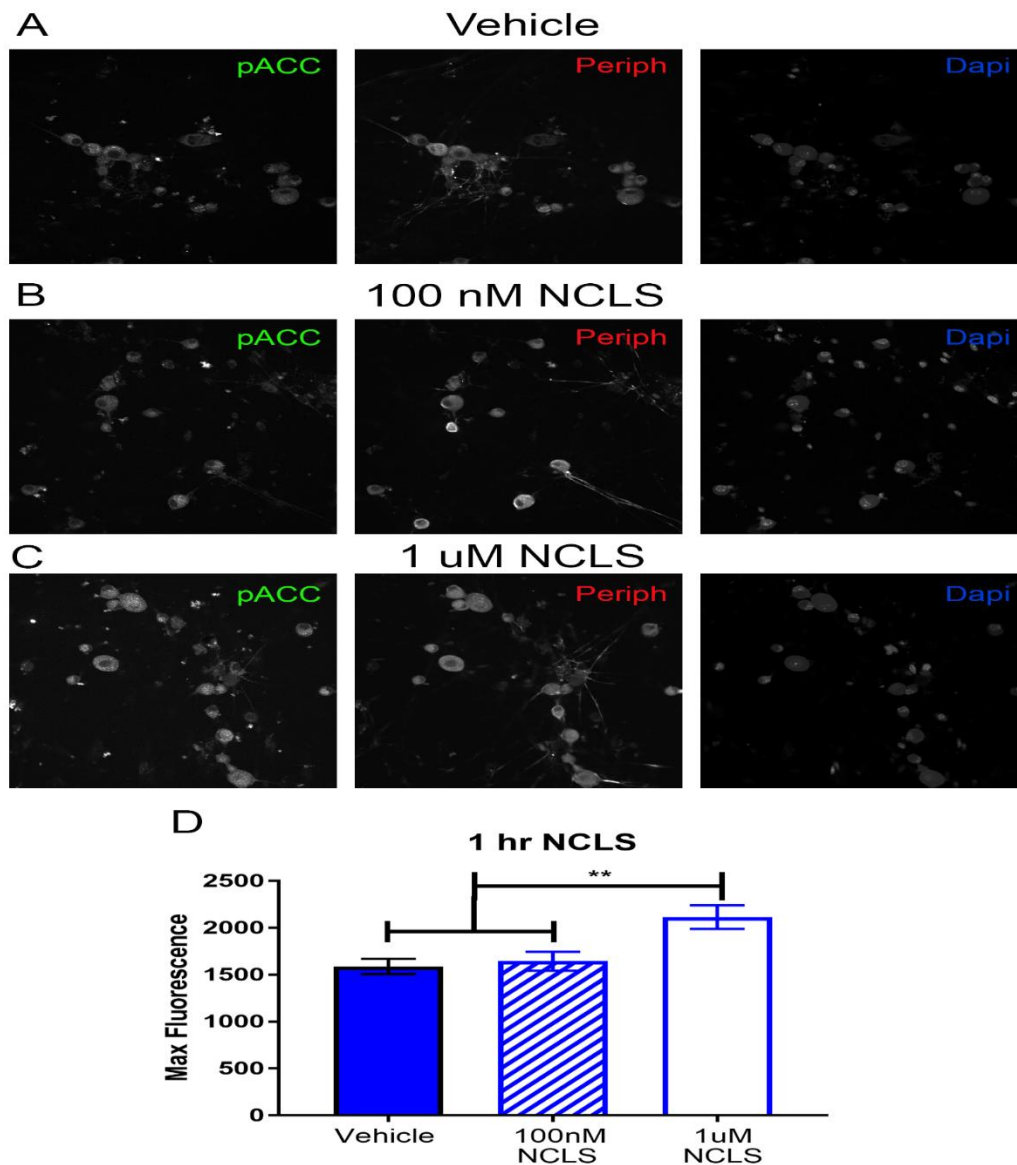


Figure 3.4: Narciclasine induces AMPK activity in male DRG neurons in vitro. Male neuron cultures were treated with vehicle A), 100 nM (B) or 1 μ M narciclasine (NCLS) (C) for 1 hr. Representative immunohistochemistry images of the DRG neurons at 40X magnification. Quantification of images shown in D. 1 μ M NCLS increased p-ACC intensity in neuron cultures. Only neurons that were positive for peripherin staining were analyzed. Maximum fluorescence refers to the maximum fluorescence intensity per neuron analyzed. ** $p < 0.01$. N= 39 images analyzed per group.

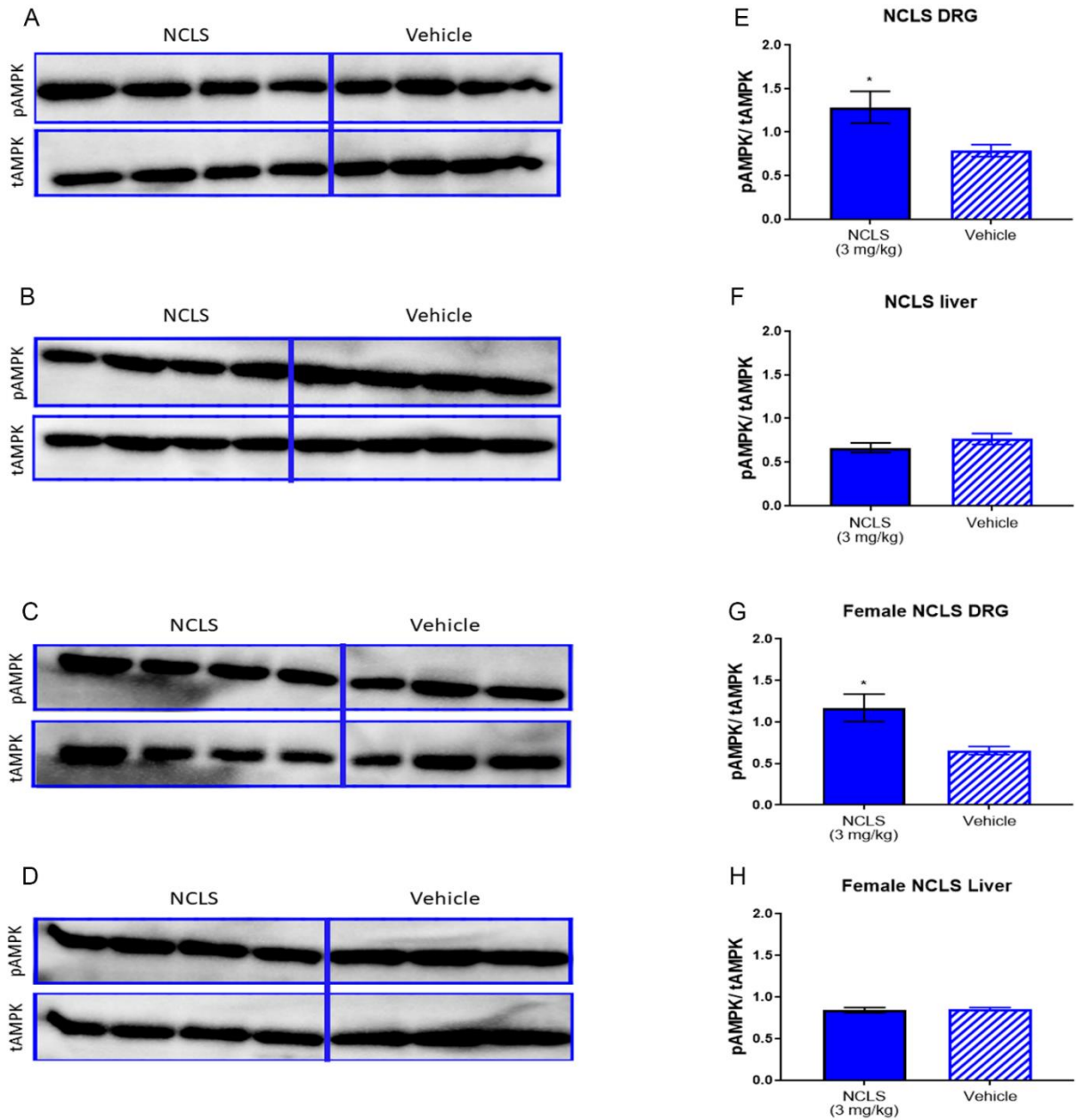


Figure 3.5: Narciclasine increases AMPK signaling in male and female DRGs. A single dose of NCLS (3 mg/kg) caused a significant increase in AMPK signaling in DRGs for male (A) and female (C) mice 1 hr post-injection while not effecting AMPK signaling in liver for male (B) or females (D). NCLS treatment increased the ratio of p-AMPK to total-AMPK in male (E) and females (G) DRGs but not in male (F) or female (H) liver. * $p < 0.05$; students t-test; N= 4 per condition in male mice; N= 4 for female NCLS treatment and N=3 for female vehicle.

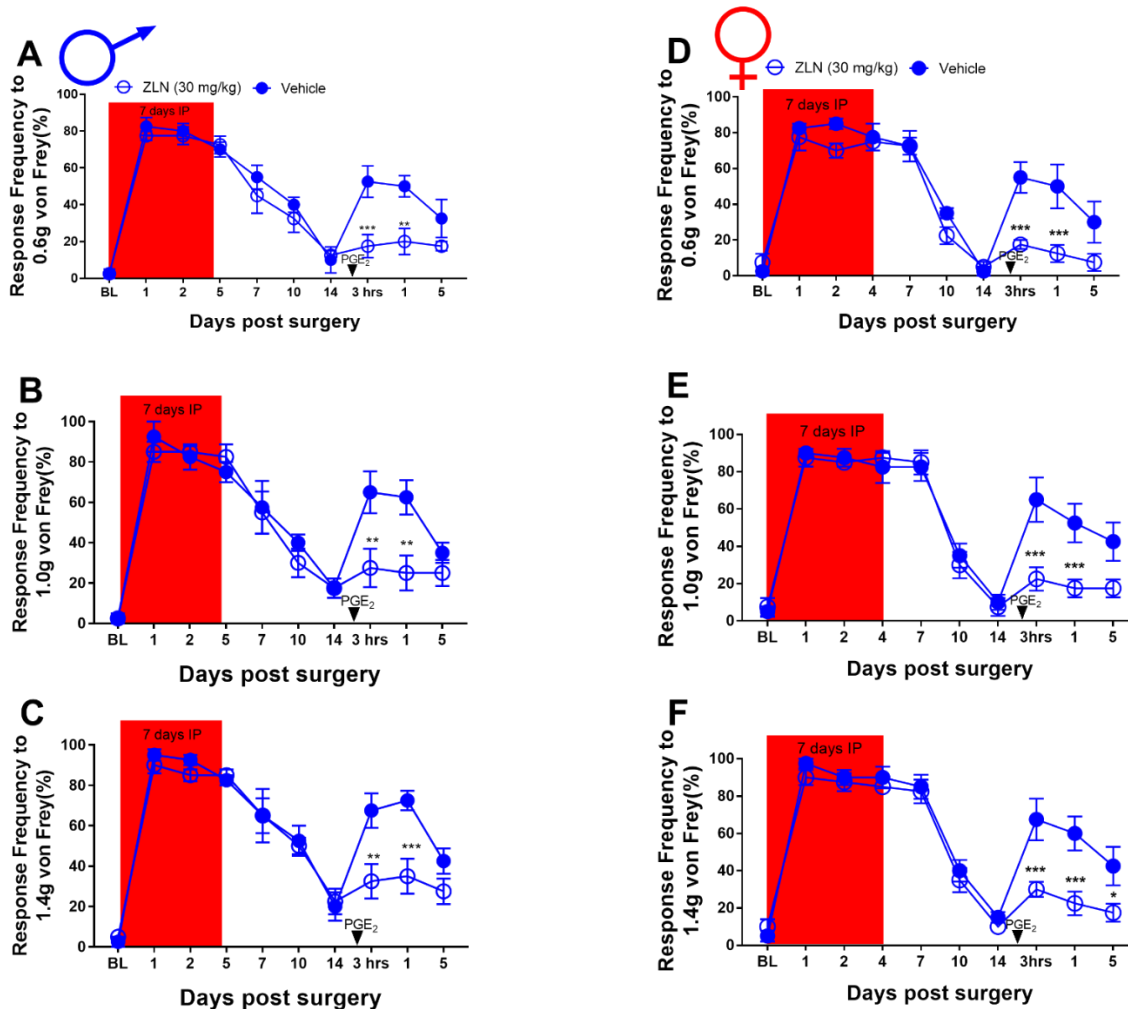


Figure 3.6: ZLN-024 treatment blocks hyperalgesic priming in male and female mice but had no effect on acute incision-induced mechanical hypersensitivity. A-F. While ZLN-024 treatment starting immediately after baseline measurements had no effect on initial mechanical hypersensitivity following plantar incision surgery, drug treatment was effective in prevention of plantar incision-induced hyperalgesic priming precipitated by PGE₂ injection in male (A-C) and female (D-F) mice. **p* < 0.05; ***p* < 0.01; ****p* < 0.001; *****p* < 0.0001; N= 6 for the ZLN-024 group and N= 6 for the vehicle group.

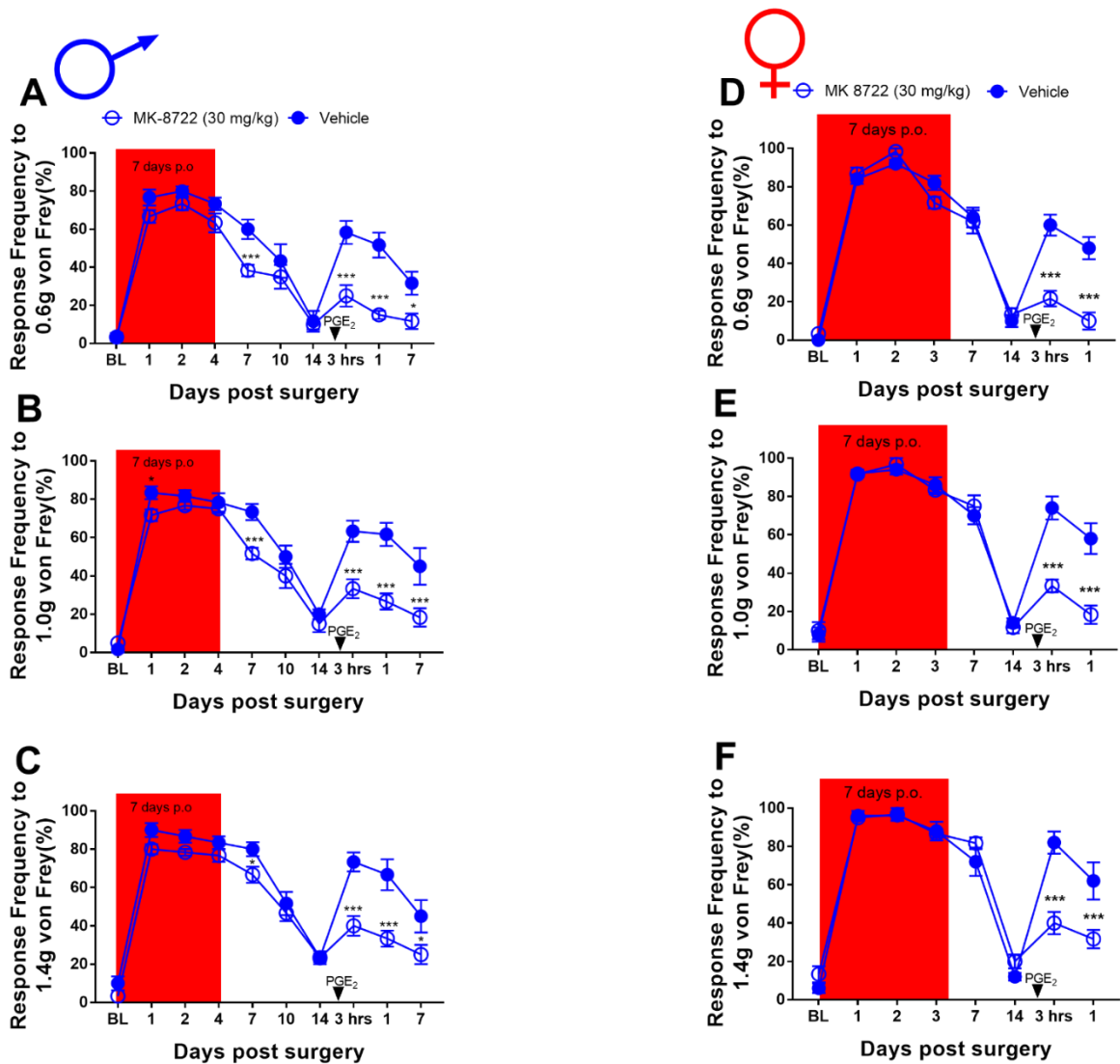


Figure 3.7: MK8722 treatment blocks hyperalgesic priming in male and female mice but had no effect on acute incision-induced mechanical hypersensitivity. A-F. While MK8722 treatment starting immediately after baseline measurements had no effect on initial mechanical hypersensitivity following plantar incision surgery, drug treatment was effective in prevention of plantar incision-induced hyperalgesic priming precipitated by PGE₂ injection in male (A-C) and female (D-F) mice. *p < 0.05; **p < 0.01; ***p < 0.001; ****p < 0.0001; N= 6 for the MK8722 group and N= 5 for the vehicle group.

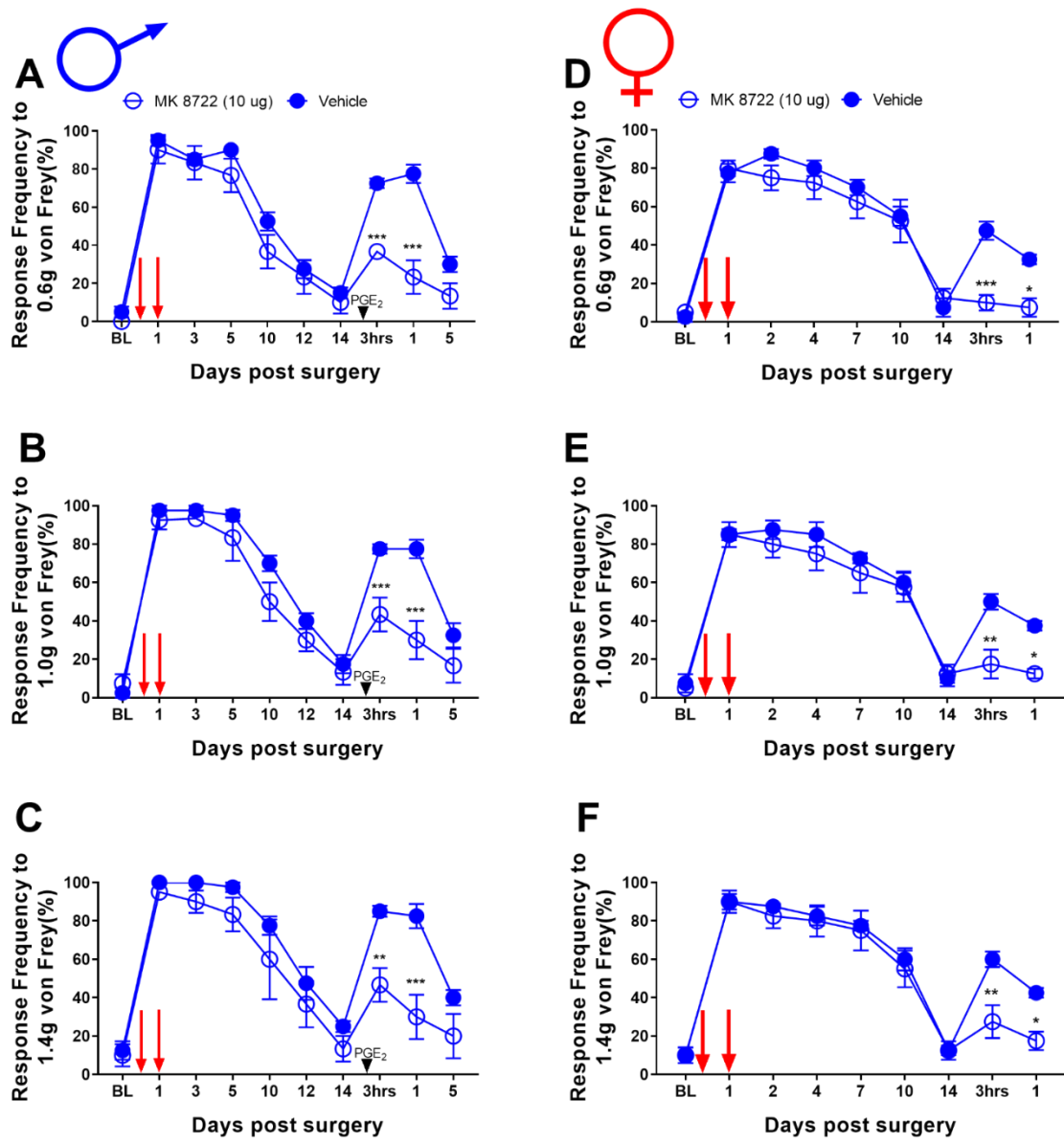


Figure 3.8: Local MK8722 treatment attenuates hyperalgesic priming in male and female mice but had no effect on acute incision-induced mechanical hypersensitivity. Local injection of MK8722 at the time of incision and again 24 hrs later (red arrows) had no effect on initial mechanical hypersensitivity following plantar incision surgery in males or females. However, drug treatment was effective in prevention of plantar incision-induced hyperalgesic priming precipitated by PGE₂ injection in male (A-C) and female (D-F) mice. *p < 0.05; **p < 0.01; ***p < 0.001; N= 4 for the MK8722 group and N= 4 for the vehicle group in both males and females.

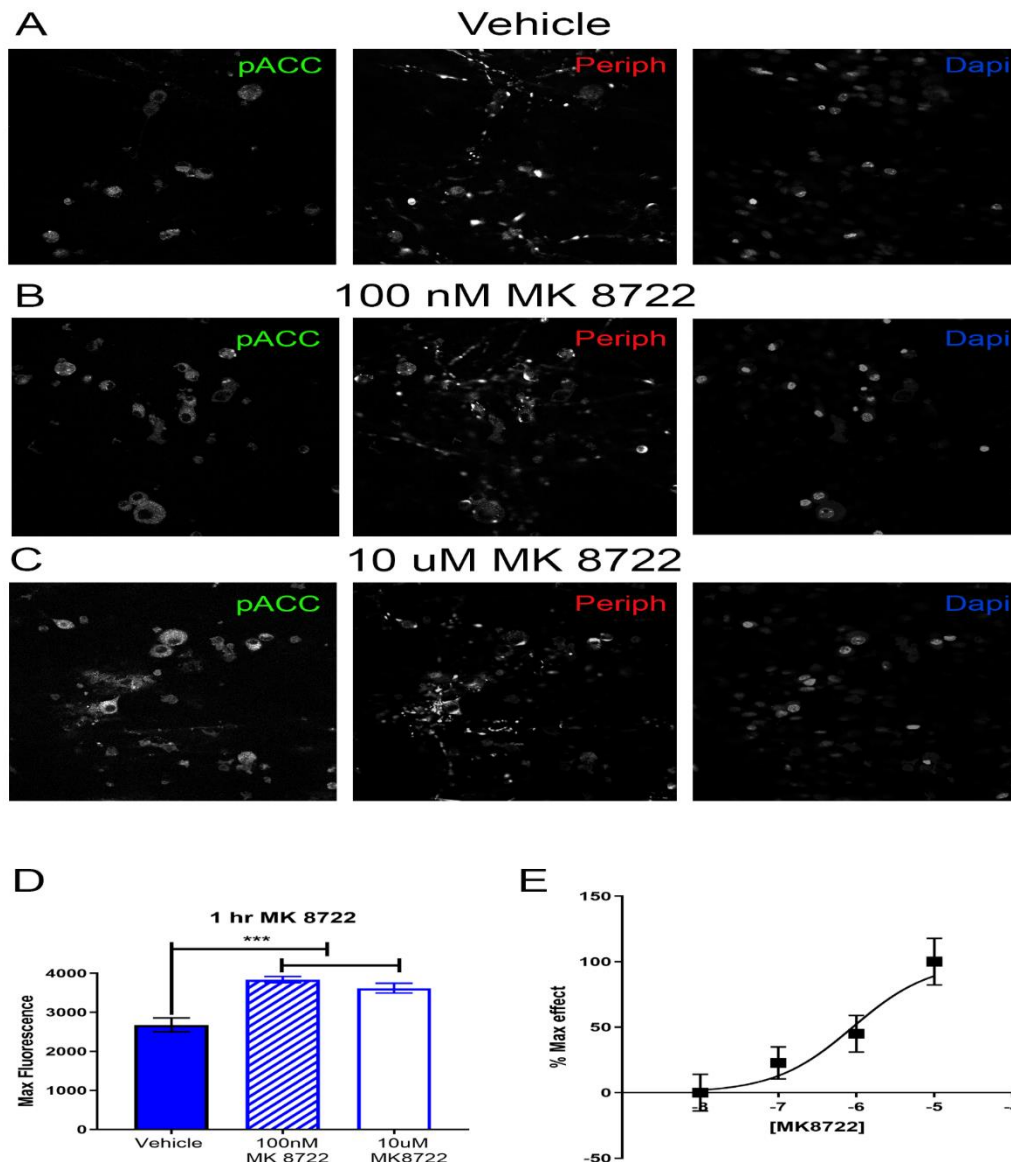


Figure 3.9: MK8722 induces AMPK activation in DRG neurons in vitro. Neuron cultures were treated with vehicle (A), 100 nM (B) or 10 μ M MK 8722 (C) for 1 hr. Representative immunohistochemistry images of the DRG neurons at 40X magnification. Quantification of images shown in D. 100 nM and 10 μ M NCLS increased p-ACC intensity in male neuron cultures. Only neurons that were positive for peripherin staining were analyzed. Maximum fluorescence refers to the maximum fluorescence intensity per neuron analyzed. ** $p < 0.01$; *** $p < 0.001$. N= 39 images analyzed per group. E) Shows a full concentration-response curve of MK8722 with an approximate EC50 of 900 nM (95% confidence interval 253 nM – 2.62 μ M).

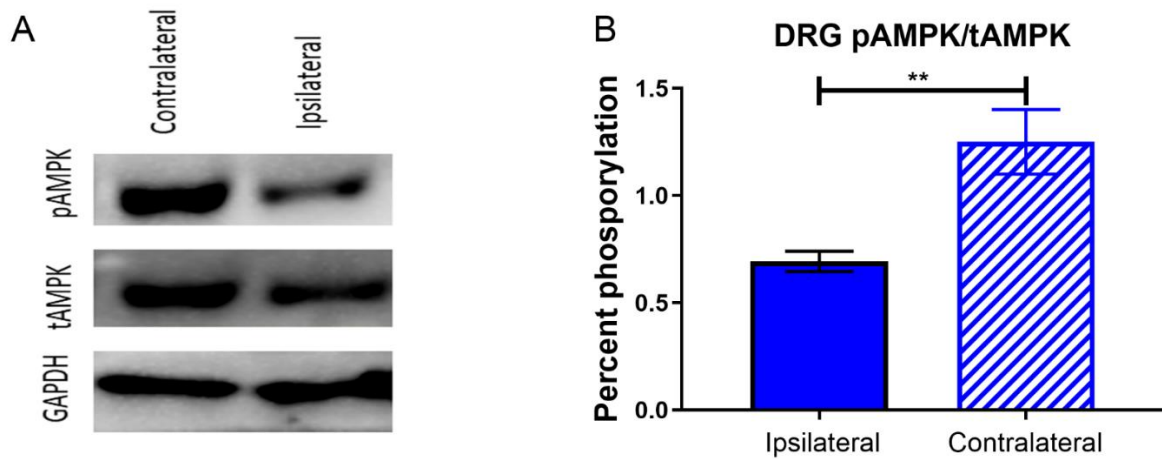


Figure 3.10: Incision decreases AMPK signaling in injured lumbar DRGs. A) Plantar incision caused a decrease in p-AMPK signaling in ipsilateral lumbar DRGs 2 hrs post-surgery measured by Western blot. B) Incision decreased the ratio between p-AMPK and total-AMPK in the ipsilateral DRGs compared to the side contralateral from the injury. ** $p < 0.01$; students t-test; N= 5 per condition in male mice.

Table 3.1: Statistical test values given by figure number and panel

Test (Factor)	F (df1, df2) interaction F (df1, df2) time F (df1, df2) Drug treatment	P-Value	Adjusted p-value (Post-hoc comparison): BL, day 1, 2, 4, 7, 10, 14, 3 hrs post PGE ₂ and 1-day post.
Two-Way ANOVA (Fig 1A)	F (8, 74) = 6.618 F (8, 74) = 23.66 F (1, 74) = 148.7	P _l <0.0001 P _t <0.0001 P _d <0.0001	Met vs. Veh: >0.9999, <0.0001, <0.0001, <0.0001, 0.1360, >0.9999, 0.0183, <0.0001, <0.0001.
Two-Way ANOVA (Fig 1B)	F (8, 74) = 8.596 F (8, 74) = 23.2 F (1, 74) = 148.8	P _l <0.0001 P _t <0.0001 P _d <0.0001	Met vs. Veh: >0.9999, <0.0001, <0.0001, <0.0001, >0.9999, >0.9999, >0.9999, <0.0001, <0.0001.
Two-Way ANOVA (Fig 1C)	F (8, 74) = 7.382 F (8, 74) = 25.7 F (1, 74) = 139.3	P _l <0.0001 P _t <0.0001 P _d <0.0001	Met vs. Veh: 0.9991, <0.0001, <0.0001, <0.0001, 0.2285, 0.8738, 0.2285, <0.0001, <0.0001.
Two-Way ANOVA (Fig 1D)	F (8, 75) = 1.276 F (8, 75) = 67.28 F (1, 75) = 0.4753	P _l = 0.2689 P _t <0.0001 P _d 0.4927	Met vs. Veh: >0.9999, >0.9999, >0.9999, 0.7060, >0.9999, >0.9999, >0.9999, >0.9999.
Two-Way ANOVA (Fig 1E)	F (8, 75) = 0.57 F (8, 75) = 67.12 F (1, 75) = 0.005207	P _l = 0.7993 P _t <0.0001 P _d = 0.9427	Met vs. Veh: >0.9999, >0.9999, >0.9999, >0.9999, >0.9999, >0.9999, >0.9999, >0.9999.
Two-Way ANOVA (Fig 1F)	F (8, 75) = 0.9607 F (8, 75) = 81.06 F (1, 75) = 1.491	P _l = 0.4731 P _t <0.0001 P _d = 0.2258	Met vs. Veh: >0.9999, >0.9999, >0.9999, >0.9999, >0.9999, >0.9999, >0.9999, >0.9999.
Two-Way ANOVA (Fig 2A)	F (6, 258) = 1.774 F (6, 258) = 222.8 F (1, 258) = 5.391	P _l =0.1048 P _t <0.0001 P _d =0.0210	Male vs. Female: >0.9999, >0.9999, 0.5376, >0.9999, 0.0396, 0.8705, >0.9999.

Table 3.1: Statistical test values given by figure number and panel

Two-Way ANOVA (Fig 2B)	F (6, 258) = 2.247 F (6, 258) = 179.9 F (1, 258) = 2.385	P _I =0.0394 P _t <0.0001 P _d =0.1238	Male vs. Female: >0.9999, >0.9999, 0.4347, >0.9999, 0.5820, >0.9999, 0.0945.
Two-Way ANOVA (Fig 2C)	F (6, 258) = 1.439 F (6, 258) = 266.0 F (1, 258) = 10.16	P _I =0.1998 P _t <0.0001 P _d =0.0016	Male vs. Female: >0.9999, >0.9999, >0.9999, >0.9999, 0.0048, 0.4378, >0.9999.
Two-Way ANOVA (Fig 3A)	F (24, 170) = 7.674 F (8, 170) = 64.91 F (3, 170) = 122.2	P _I <0.0001 P _t <0.0001 P _d <0.0001	Veh vs NCLS 1 mg/kg: >0.9999, 0.8367, 0.9924, 0.8367, 0.5040, 0.5040, 0.9999, <0.0001, <0.0001. Veh vs NCLS 3 mg/kg: >0.9999, 0.0002, <0.0001, <0.0001, <0.0001, 0.0051, 0.6757, <0.0001, <0.0001. Veh vs NCLS 6 mg/kg: 0.9924, <0.0001, <0.0001, <0.0001, <0.0001, 0.0021, 0.6800, <0.0001, <0.0001. NCLS 1 mg/kg vs NCLS 3 mg/kg: >0.9999, 0.0034, <0.0001, <0.0001, <0.0001, 0.1504, 0.6757, 0.7505, 0.7505. NCLS 1 mg/kg vs NCLS 6 mg/kg: 0.9924, <0.0001, <0.0001, <0.0001, <0.0001, 0.1187, 0.6800, 0.5040, 0.6800. NCLS 3 mg/kg vs NCLS 6 mg/kg: 0.9884, 0.0165, 0.2440, 0.1504, 0.9993, 0.9993, 0.9993, 0.9994, 0.9999.

Table 3.1: Statistical test values given by figure number and panel

<p>Two-Way ANOVA (Fig 3B)</p>	<p>F (24, 170) = 12.93 F (8, 170) = 105.7 F (3, 170) = 134.7</p>	<p>$P_l < 0.0001$ $P_t < 0.0001$ $P_d < 0.0001$</p>	<p>Veh vs NCLS 1 mg/kg: 0.8107, 0.8107, 0.9324, 0.9909, >0.9999, 0.6371, 0.9909, <0.0001, <0.0001. Veh vs NCLS 3 mg/kg: 0.8278, 0.0040, <0.0001, <0.0001, 0.0002, 0.0010, >0.9999, <0.0001, <0.0001. Veh vs NCLS 6 mg/kg: 0.8107, <0.0001, <0.0001, <0.0001, <0.0001, 0.0073, >0.9999, <0.0001, <0.0001. NCLS 1 mg/kg vs NCLS 3 mg/kg: 0.9982, 0.0433, <0.0001, <0.0001, 0.0002, 0.0303, 0.9935, 0.1968, 0.4656. NCLS 1 mg/kg vs NCLS 6 mg/kg: >0.9999, <0.0001, <0.0001, <0.0001, <0.0001, 0.1659, 0.9909, 0.2877, 0.9909. NCLS 3 mg/kg vs NCLS 6 mg/kg:</p>
<p>Two-Way ANOVA (Fig 3C)</p>	<p>F (24, 170) = 10.81 F (8, 170) = 97.49 F (3, 170) = 122.0</p>	<p>$P_l < 0.0001$ $P_t < 0.0001$ $P_d < 0.0001$</p>	<p>Veh vs NCLS 1 mg/kg: 0.9470, >0.9999, 0.9928, 0.9928, 0.9470, 0.1295, 0.9928, <0.0001, <0.0001. Veh vs NCLS 3 mg/kg: 0.4862, 0.4576, 0.0134, <0.0001, <0.0001, 0.0005, >0.9999, <0.0001, <0.0001 Veh vs NCLS 6 mg/kg: 0.5198, <0.0001, <0.0001, <0.0001,</p>

Table 3.1: Statistical test values given by figure number and panel

			<p><0.0001, <0.0001, 0.9928, <0.0001, <0.0001.</p> <p>NCLS 1 mg/kg vs NCLS 3 mg/kg: 0.8584, 0.4576, 0.0062, <0.0001, <0.0001, 0.1627, 0.9948, 0.134, 0.2071.</p> <p>NCLS 1 mg/kg vs NCLS 6 mg/kg: 0.8440, <0.0001, <0.0001, <0.0001, <0.0001, 0.0690, 0.9470, 0.0690, 0.3568.</p> <p>NCLS 3 mg/kg vs NCLS 6 mg/kg: 0.9986, 0.0003, <0.0001, 0.6116, 0.9948, 0.9993, 0.9928, 0.8265, 0.9612.</p>
Two-Way ANOVA (Fig 3D)	<p>F (8, 89) = 6.662</p> <p>F (8, 89) = 50.21</p> <p>F (1, 89) = 141.6</p>	<p>P_l <0.0001</p> <p>P_t <0.0001</p> <p>P_d <0.0001</p>	<p>NCLS vs. Veh: >0.9999, 0.0061, 0.0029, <0.0001, <0.0001, 0.0002, >0.9999, <0.0001, <0.0001.</p>
Two-Way ANOVA (Fig 3E)	<p>F (8, 89) = 4.359</p> <p>F (8, 89) = 36.59</p> <p>F (1, 89) = 109</p>	<p>P_l = 0.0002</p> <p>P_t <0.0001</p> <p>P_d <0.0001</p>	<p>NCLS vs. Veh: >0.9999, 0.0947, 0.0004, 0.0069, 0.0003, 0.0007, >0.9999, <0.0001, <0.0001.</p>
Two-Way ANOVA (Fig 3F)	<p>F (8, 89) = 7.836</p> <p>F (8, 89) = 44.78</p> <p>F (1, 89) = 134.4</p>	<p>P_l <0.0001</p> <p>P_t <0.0001</p> <p>P_d <0.0001</p>	<p>NCLS vs. Veh: >0.9999, 0.3303, 0.0305, 0.0026, <0.0001, 0.0005, >0.9999, <0.0001, <0.0001.</p>
One-Way ANOVA (Fig 4D)	<p>F (2, 114) = 7.639</p>	<p>P = 0.0008</p>	<p>Veh vs. 100 nM NCLS: 0.9253</p> <p>Veh vs. 1 uM NCLS: 0.0016</p> <p>100 nM NCLS vs 1 uM NCLS: 0.0053</p>
Unpaired T-test (Fig 5E)	<p>F, DF_n, Df_d = 6.914, 3, 3</p>	<p>P = 0.0437</p>	<p>P = 0.0437</p>

Table 3.1: Statistical test values given by figure number and panel

Unpaired T-test (Fig 5F)	F, DFn, Dfd= 1.222, 3, 3	P= 0.2735	P= 0.2735
Unpaired T-test (Fig 5G)	F, DFn, Dfd= 14.80, 3, 2	P= 0.0499	P=0.0499
Unpaired T-test (Fig 5H)	F, DFn, Dfd= 4.328, 3, 2	P= 0.7319	P= 0.7319
Two-Way ANOVA (Fig 6A)	F (9, 60) = 2.49 F (9, 60) = 42.65 F (1, 60) = 14.46	P _l = 0.0173 P _t <0.0001 P _d = 0.0003	ZLN vs. Veh: >0.9999, >0.9999, >0.9999, >0.9999, >0.9999, >0.9999, >0.9999, 0.0009, 0.0063.
Two-Way ANOVA (Fig 6B)	F (9, 60) = 2.453 F (9, 60) = 32.77 F (1, 60) = 8.914	P _l = 0.0189 P _t <0.0001 P _d = 0.0041	ZLN vs. Veh: >0.9999, >0.9999, >0.9999, >0.9999, >0.9999, >0.9999, >0.9999, 0.0043, 0.0043.
Two-Way ANOVA (Fig 6C)	F (9, 60) = 2.846 F (9, 60) = 42.42 F (1, 60) = 11.22	P _l = 0.0074 P _t <0.0001 P _d = 0.0014	ZLN vs. Veh: >0.9999, >0.9999, >0.9999, >0.9999, >0.9999, >0.9999, >0.9999, 0.0024, 0.0010.
Two-Way ANOVA (Fig 6D)	F (9, 60) = 3.333 F (9, 60) = 51.48 F (1, 60) = 21.31	P _l = 0.0023 P _t <0.0001 P _d <0.0001	ZLN vs. Veh: >0.9999, >0.9999, 0.8495, >0.9999, >0.9999, >0.9999, >0.9999, 0.0005, 0.0005, 0.1091.
Two-Way ANOVA (Fig 6E)	F (9, 60) = 3.513 F (9, 60) = 52.08 F (1, 60) = 13.23	P _l = 0.0015 P _t <0.0001 P _d = 0.0006	ZLN vs. Veh: >0.9999, >0.9999, >0.9999, >0.9999, >0.9999, >0.9999, >0.9999, 0.0002, 0.0030, 0.0811.
Two-Way ANOVA (Fig 6F)	F (9, 60) = 3.413 F (9, 60) = 62.96 F (1, 60) = 21.89	P _l = 0.0019 P _t <0.0001 P _d <0.0001	ZLN vs. Veh: >0.9999, >0.9999, >0.9999, >0.9999, >0.9999, >0.9999, >0.9999, 0.0003, 0.0003, 0.0371.
Two-Way ANOVA (Fig 7A)	F (9, 100) = 3.581 F (9, 100) = 57.52 F (1, 100) = 49.2	P _l = 0.0007 P _t <0.0001 P _d <0.0001	MK8722 vs. Veh: >0.9999, >0.9999, >0.9999, >0.9999, 0.0162, >0.9999, >0.9999, <0.0001, <0.0001.

Table 3.1: Statistical test values given by figure number and panel

Two-Way ANOVA (Fig 7B)	F (9, 100) = 4.004 F (9, 100) = 64.49 F (1, 100) = 50.13	$P_I =$ 0.0002 $P_t < 0.0001$ $P_d < 0.0001$	MK8722 vs. Veh: >0.9999, 0.7465, >0.9999, >0.9999, 0.0116, >0.9999, >0.9999, 0.0001, <0.0001.
Two-Way ANOVA (Fig 7C)	F (9, 100) = 3.339 F (9, 100) = 70.45 F (1, 100) = 46.18	$P_I =$ 0.0013 $P_t < 0.0001$ $P_d < 0.0001$	MK8722 vs. Veh: >0.9999, >0.9999, >0.9999, >0.9999, 0.3856, >0.9999, >0.9999, <0.0001, <0.0001.
Two-Way ANOVA (Fig 7D)	F (7, 72) = 11.69 F (7, 72) = 164.1 F (1, 72) = 22.71	$P_I < 0.0001$ $P_t < 0.0001$ $P_d < 0.0001$	MK8722 vs. Veh: >0.9999, >0.9999, >0.9999, >0.9999, 0.4924, >0.9999, >0.9999, <0.0001, <0.0001.
Two-Way ANOVA (Fig 7E)	F (7, 72) = 10.35 F (7, 72) = 134.7 F (1, 72) = 20.49	$P_I < 0.0001$ $P_t < 0.0001$ $P_d < 0.0001$	MK8722 vs. Veh: >0.9999, >0.9999, >0.9999, >0.9999, >0.9999, >0.9999, >0.9999, <0.0001, <0.0001.
Two-Way ANOVA (Fig 7F)	F (7, 72) = 9.025 F (7, 72) = 114.5 F (1, 72) = 7.297	$P_I < 0.0001$ $P_t < 0.0001$ $P_d = 0.0086$	MK8722 vs. Veh: >0.9999, >0.9999, >0.9999, >0.9999, >0.9999, >0.9999, >0.9999, <0.0001, 0.0198.
Two-Way ANOVA (Fig 8A)	F (9, 52) = 5.188 F (9, 52) = 78.17 F (1, 52) = 45.35	$P_I =$ <0.0001 $P_t < 0.0001$ $P_d < 0.0001$	MK8722 vs. Veh: >0.9999, >0.9999, >0.9999, 0.7988, 0.3869, >0.9999, >0.9999, 0.0001, 0.0001, 0.2989.
Two-Way ANOVA (Fig 8B)	F (9, 52) = 3.852 F (9, 52) = 70.42 F (1, 52) = 33.79	$P_I =$ 0.0009 $P_t < 0.0001$ $P_d < 0.0001$	MK8722 vs. Veh: >0.9999, >0.9999, >0.9999, >0.9999, 0.1740, >0.9999, >0.9999, 0.0011, <0.0001, 0.5721.

Table 3.1: Statistical test values given by figure number and panel

Two-Way ANOVA (Fig 8C)	F (9, 52) = 2.391 F (9, 52) = 40.35 F (1, 52) = 32.72	$P_l = 0.0238$ $P_t < 0.0001$ $P_d < 0.0001$	MK8722 vs. Veh: >0.9999, >0.9999, >0.9999, >0.9999, 0.9332, >0.9999, >0.9999, 0.0045, <0.0001, 0.5612.
Two-Way ANOVA (Fig 8D)	F (8, 54) = 3.284 F (8, 54) = 64.16 F (1, 54) = 12.52	$P_l = 0.0040$ $P_t < 0.0001$ $P_d = 0.0008$	MK8722 vs. Veh: >0.9999, >0.9999, >0.9999, >0.9999, >0.9999, >0.9999, >0.9999, 0.0001, <0.0001.
Two-Way ANOVA (Fig 8E)	F (8, 54) = 2.081 F (8, 54) = 59.97 F (1, 54) = 12.04	$P_l = 0.0538$ $P_t < 0.0001$ $P_d = 0.0010$	MK8722 vs. Veh: >0.9999, >0.9999, >0.9999, >0.9999, >0.9999, >0.9999, >0.9999, 0.0019, <0.0308.
Two-Way ANOVA (Fig 8F)	F (8, 54) = 2.154 F (8, 54) = 58.24 F (1, 54) = 8.670	$P_l = 0.0462$ $P_t < 0.0001$ $P_d = 0.0048$	MK8722 vs. Veh: >0.9999, >0.9999, >0.9999, >0.9999, >0.9999, >0.9999, >0.9999, 0.0020, 0.0322.
One-Way ANOVA (Fig 9D)	F (2, 116) = 21.68	$P < 0.0001$	Veh vs. 100 nM MK8722: <0.0001 Veh vs. 1 uM MK8722: <0.0001 100 nM MK8722 vs 1 uM MK8722: 0.4652
Unpaired T-test (Fig 10B)	F, DF _n , Df _d = 10.21, 4, 4	$P = 0.0077$	$P = 0.0077$
Two-Way ANOVA (Sup Fig 1A)	F (8, 54) = 0.3068 F (8, 54) = 0.7841 F (1, 54) = 2.455	$P_l = 0.9603$ $P_t = 0.6186$ $P_d = 0.1230$	Met vs. Veh: >0.9999, >0.9999, >0.9999, >0.9999, >0.9999, >0.9999, >0.9999, >0.9999, >0.9999.
Two-Way ANOVA (Sup Fig 1B)	F (8, 54) = 0.5263 F (8, 54) = 0.4474 F (1, 54) = 0.05263	$P_l = 0.8315$ $P_t = 0.8869$ $P_d = 0.8194$	Met vs. Veh: >0.9999, >0.9999, >0.9999, >0.9999, >0.9999, >0.9999, >0.9999, >0.9999, >0.9999.

Table 3.1: Statistical test values given by figure number and panel

Two-Way ANOVA (Sup Fig 1C)	F (8, 54) = 0.5270 F (8, 54) = 0.6486 F (1, 54) = 0.1622	P _I =0.8310 P _t =0.7334 P _d =0.6888	Met vs. Veh: >0.9999, 0.6798, >0.9999, >0.9999, >0.9999, >0.9999, >0.9999.
Two-Way ANOVA (Sup Fig 1D)	F (1, 12) = 3.812e ⁻⁰⁰⁵ F (1, 12) = 0.7154 F (1, 12) = 0.2885	P _I =0.9952 P _t =0.4142 P _d =0.6010	Met vs. Veh: >0.9999, >0.9999.
Two-Way ANOVA (Sup Fig 2A)	F (16, 81) = 0.6694 F (8, 81) = 137.6 F (2, 81) = 7.573	P _I =0.8154 P _t <0.0001 P _d =0.0010	Met 100 mg/kg vs Met 50 mg/kg: >0.9999, >0.9999, 0.8373, 0.2192, 0.4504, >0.9999, 0.4504, 0.0967, 0.2192. Met 100 mg/kg vs. Veh: >0.9999, 0.4504, 0.4504, 0.2192, 0.4504, >0.9999, 0.4504, >0.9999, 0.2192. Met 50 mg/kg vs. Veh: >0.9999, 0.8373, >0.9999, >0.9999, >0.9999, 0.8373, >0.9999, 0.4504, >0.9999.
Two-Way ANOVA (Sup Fig 2B)	F (16, 81) = 0.7423 F (8, 81) = 171.6 F (2, 81) = 15.97	P _I =0.7430 P _t <0.0001 P _d <0.0001	Met 100 mg/kg vs Met 50 mg/kg: >0.9999, 0.6755, 0.3212, 0.6755, 0.3212, 0.6755, 0.0500, 0.1650, 0.0500. Met 100 mg/kg vs Veh: >0.9999, 0.3212, 0.3212, 0.3212, 0.6755, 0.3212, 0.3212, 0.1650, 0.0500. Met 50 mg/kg vs Veh: >0.9999, >0.9999, >0.9999, >0.9999, >0.9999, >0.9999, >0.9999, >0.9999, >0.9999.
Two-Way ANOVA (Sup Fig 2C)	F (16, 81) = 0.8074 F (8, 81) = 189.0 F (2, 81) = 12.61	P _I =0.6733 P _t <0.0001 P _d <0.0001	Met 100 mg/kg vs Met 50 mg/kg: >0.9999, 0.3020, 0.6497, 0.3020, 0.1223,

Table 3.1: Statistical test values given by figure number and panel

			0.6497, >0.9999, 0.1223, 0.001. Met 100 mg/kg vs Veh: >0.9999, 0.3020, 0.3020, 0.3020, 0.6497, 0.6497, 0.3020, >0.9999, 0.1223. Met 50 mg/kg vs Veh: >0.9999, >0.9999, >0.9999, >0.9999, >0.9999, >0.9999, 0.6497, 0.3020.
Two-Way ANOVA (Sup Fig 3A)	F (2, 12) = 7.203 F (2, 12) = 23.76 F (1, 12) = 31.92	P _I =0.0088 P _t <0.0001 P _{sex} =0.0001	Male vs Female: 0.0006, 0.0033, 0.9949
Two-Way ANOVA (Sup Fig 3B)	F (2, 12) = 0.4276 F (2, 12) = 0.1726 F (1, 12) = 40.04	P _I =0.6616 P _t =0.8435 P _{sex} <0.0001	Male vs Female: 0.0158, 0.0242, 0.0026
Two-Way ANOVA (Sup Fig 3C)	F (2, 12) = 0.1444 F (2, 12) = 21.42 F (1, 12) = 0.002518	P _I =0.8670 P _t =0.0001 P _{sex} =0.9608	Male vs Female: 0.9998, 0.9744, 0.9776
Two-Way ANOVA (Sup Fig 4A)	F (8, 53) = 0.9597 F (8, 53) = 0.7186 F (1, 53) = 6.383	P _I =0.4770 P _t =0.6742 P _d =0.0145	NCLS vs. Veh: >0.9999, >0.9999, >0.9999, >0.9999, >0.9999, >0.9999, 0.1727, >0.9999.
Two-Way ANOVA (Sup Fig 4B)	F (8, 53) = 0.3195 F (8, 53) = 0.3211 F (1, 53) = 5.202	P _I =0.9552 P _t =0.9545 P _d =0.0266	NCLS vs Veh: >0.9999, >0.9999, >0.9999, >0.9999, >0.9999, >0.9999, >0.9999, >0.9999.
Two-Way ANOVA (Sup Fig 4C)	F (8, 53) = 0.3676 F (8, 53) = 1.653 F (1, 53) = 3.674	P _I =0.9330 P _t =0.1323 P _d =0.0607	NCLS vs. Veh: >0.9999, >0.9999, >0.9999, >0.9999, >0.9999, >0.9999, 0.4319, >0.9999.
Two-Way ANOVA (Sup Fig 4D)	F (1, 12) = 0.9088 F (1, 12) = 5.217 F (1, 12) = 0.05680	P _I =0.3592 P _t =0.0414 P _d =0.8156	NCLS vs Veh: >0.9999, 0.8318.
Two-Way ANOVA (Sup Fig 5A)	F (8, 54) = 0.1927 F (8, 54) = 0.2339 F (1, 54) = 4.651	P _I =0.9909 P _t =0.9828 P _d =0.0355	MK8722 vs. Veh: >0.9999, >0.9999, >0.9999, >0.9999, >0.9999, >0.9999,

Table 3.1: Statistical test values given by figure number and panel

			>0.9999, >0.9999, >0.9999.
Two-Way ANOVA (Sup Fig 5B)	F (8, 54) = 0.3277 F (8, 54) = 0.5752 F (1, 54) = 2.359	P _I =0.9518 P _t =0.7936 P _d =0.1304	MK8722 vs. Veh: >0.9999, >0.9999, >0.9999, >0.9999, >0.9999, >0.9999, >0.9999, >0.9999, >0.9999.
Two-Way ANOVA (Sup Fig 5C)	F (8, 54) = 0.2041 F (8, 54) = 0.7101 F (1, 54) = 3.000	P _I =0.9889 P _t =0.6814 P _d =0.0890	MK8722 vs. Veh: >0.9999, >0.9999, >0.9999, >0.9999, >0.9999, >0.9999, >0.9999, >0.9999, >0.9999.
Two-Way ANOVA (Sup Fig 5D)	F (1, 12) = 0.07654 F (1, 12) = 0.02466 F (1, 12) = 0.001398	P _I =0.7867 P _t =0.8778 P _d =0.9708	MK8722 vs Veh: >0.9999, >0.9999.

Table 3.2: Metformin PK study

	ng/ml	ng/g	ng/ml	ng/g	ng/ml	ng/g
	Blood	Brain	Blood	Brain	Blood	Brain
Male	0.5 hr	0.5 hr	1 hr	1 hr	4 hr	4 hr
1	6609	483	2649	726	359	689
2	8143	772	2017	740	495	704
3	9721	747	2961	563	363	484
MEAN	8157.6666 7	667.33333 3	2542.3333 3	676.33333 3	405.66666 7	625.66666 7
SEM	898.38695	92.448784 6	277.67927 1	56.810601 5	44.681589 5	70.965562 9
	ng/ml	ng/g	ng/ml	ng/g	ng/ml	ng/g
	Blood	Brain	Blood	Brain	Blood	Brain
Female	0.5 hr	0.5 hr	1 hr	1 hr	4 hr	4 hr
1	25420	1432	6262	1811	743	2082
2	26223	1255	25785	1342	1659	1139
3	25816	1626	18181	1029	1029	1646

Table 3.2: Metformin PK study

MEAN	25819.666 7	1437.6666 7	16742.666 7	1394	1143.6666 7	1622.3333 3
SEM	231.81338 3	107.13594 7	5681.5046 2	227.23629 4	270.57059 1	272.47772 6
RATIO						
	0.5 HR	1 HR	4 HR			
Male						
1	0.0730821 6	0.2740656 9	1.9192200 6			
2	0.0948053 5	0.3668815 1	1.4222222 2			
3	0.0768439 5	0.1901384 7	1.3333333 3			
MEAN	0.0815771 5	0.2770285 5	1.5582585 4			
SEM	0.0067026 5	0.0510428 2	0.1822957 5			
RATIO						
	0.5 HR	1 HR	4 HR			
Female						
1	0.0563336	0.2892047 3	2.8021534 3			
2	0.0478587 5	0.0520457 6	0.6865581 7			
3	0.0629842	0.0565975 5	1.5996112 7			
MEAN	0.0557255 1	0.1326160 1	1.6961076 2			
SEM	0.0043769 1	0.0783053 8	0.6126226 4			

APPENDIX

SUPPLEMENTAL FIGURES

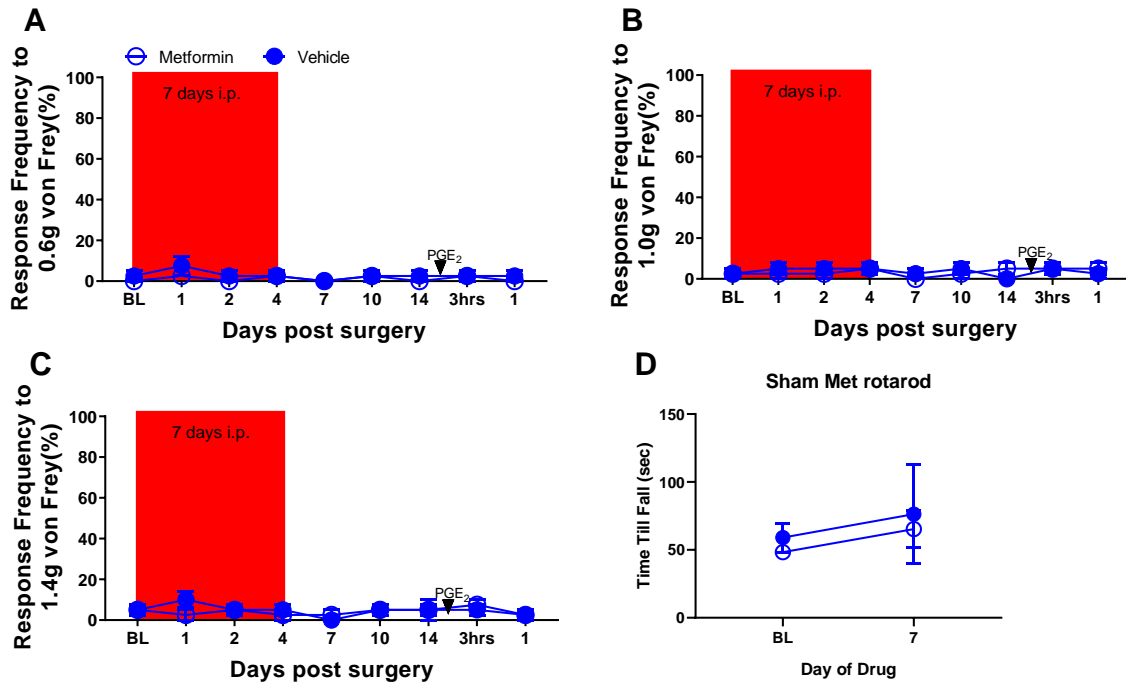


Figure 3.11: Effects of metformin on sham male mice. A-C. Metformin treatment had no effect on the mechanical sensitivity of sham male mice and did not induce hyperalgesic priming. D. Metformin also had no effect on locomotor activity and coordination as indicated by their performance on the rotarod compared to the vehicle group. N = 4 for the metformin (200 mg/kg) group and N = 4 for the vehicle group.

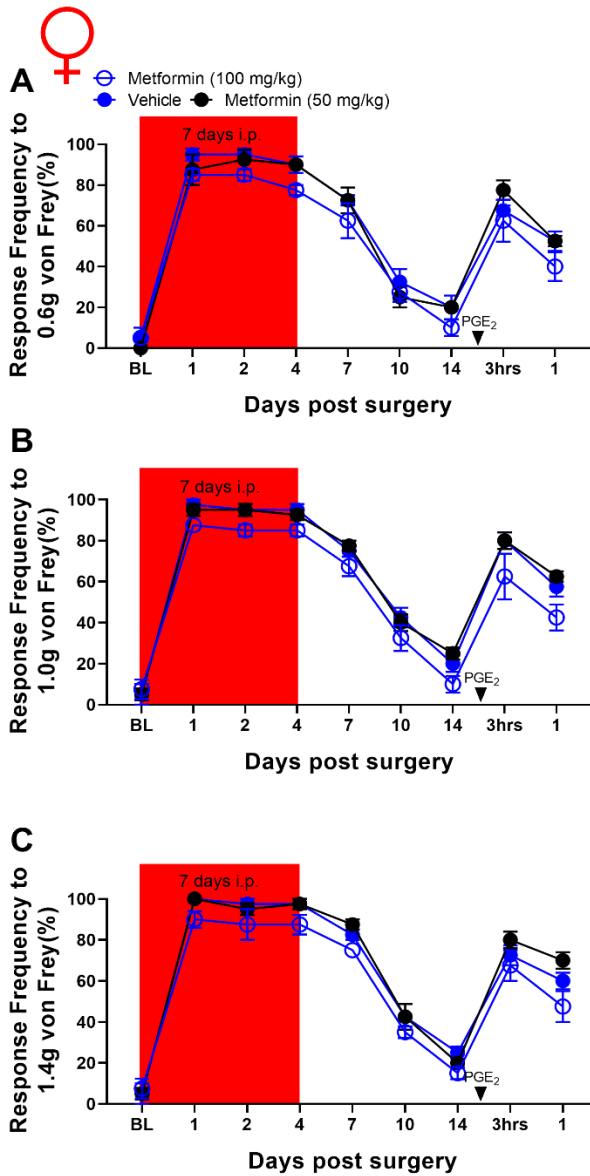


Figure 3.12: Lower doses of metformin treatment failed to attenuate incision-induced mechanical hypersensitivity or blocks hyperalgesic priming in female mice. A-C. Metformin treatment at 100 and 50 mg/kg failed to decrease mechanical hypersensitivity compared to vehicle treated mice. Metformin also failed to prevent plantar incision-induced hyperalgesic priming precipitated by PGE₂ injection. N= 4 for the metformin groups and N= 4 for the vehicle group.

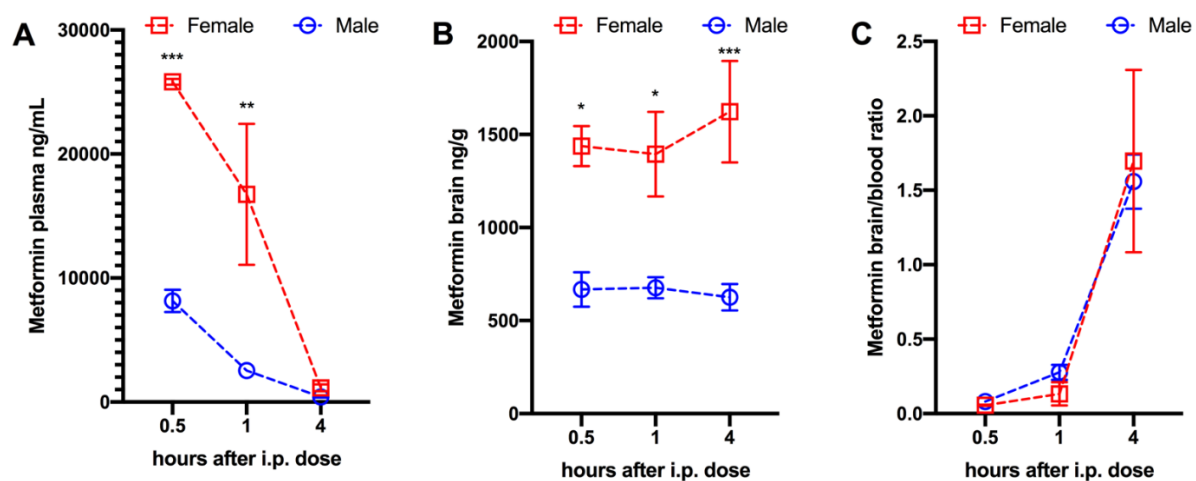


Figure 3.13: Sex differences in pharmacokinetics of metformin. Male and female mice were given metformin (200 mg/kg, i.p.) and then plasma (A) and brain (B) were taken at the indicated time points. (C) Brain to plasma ratios were calculated at each time point per sex and were not different between sexes. Two-way ANOVA with Bonferroni post hoc test. * $p < 0.05$, ** $p < 0.01$; *** $p < 0.001$. $N = 3$ per group.

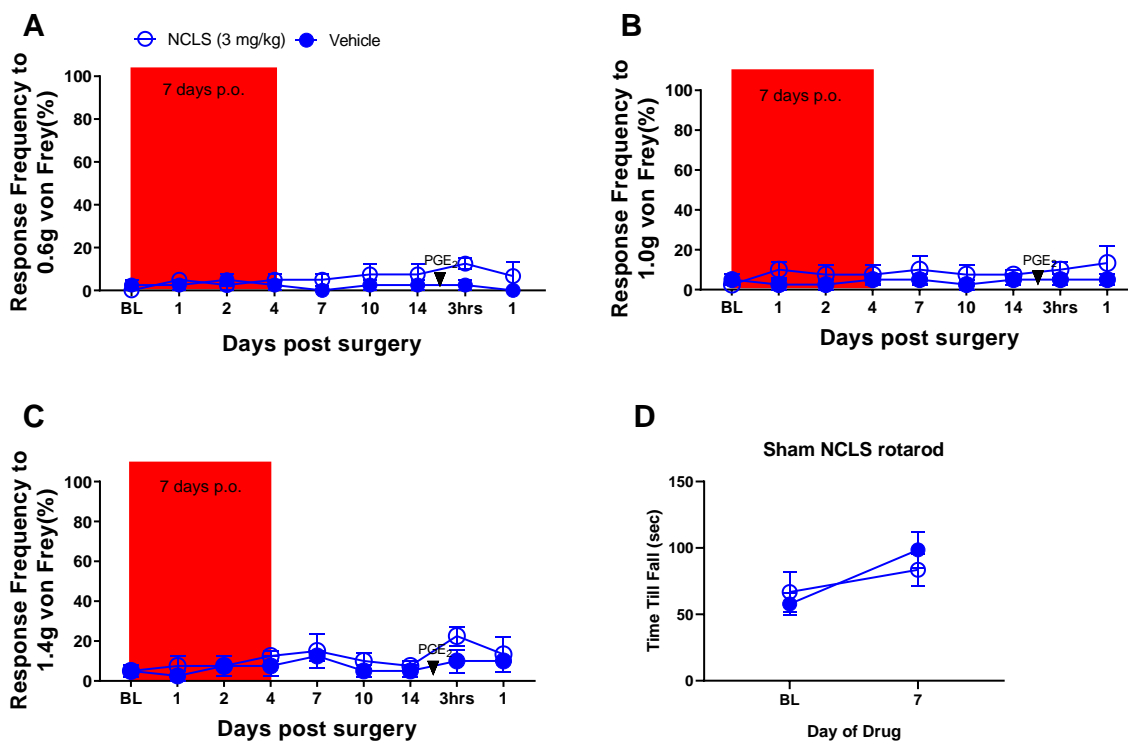


Figure 3.14: Effects of narciclasine on sham male mice. A-C. NCLS treatment had no effect on the mechanical sensitivity of sham male mice and did not induce hyperalgesic priming. D. NCLS also had no effect on locomotor activity and coordination as indicated by their performance on the rotarod compared to the vehicle group. N= 4 for the NCLS group and N= 4 for the vehicle group.

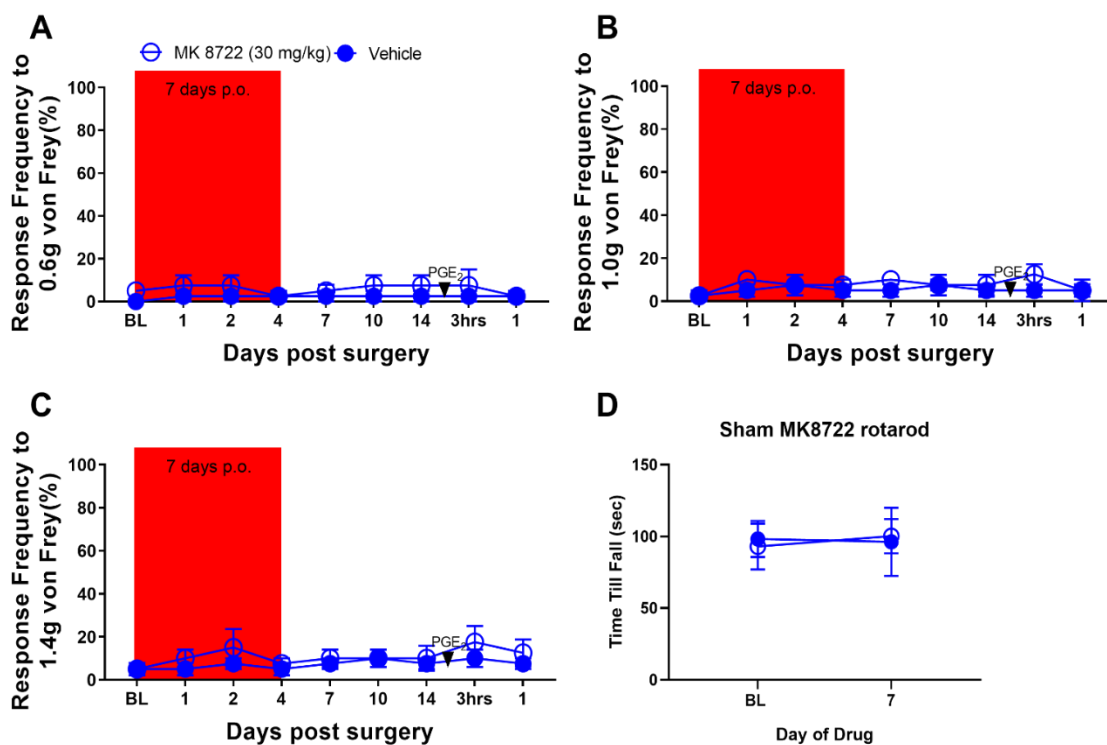


Figure 3.15: Effects of MK8722 on sham male mice. A-C. MK8722 treatment had no effect on the mechanical sensitivity of sham male mice and did not induce hyperalgesic priming. D. MK8722 also had no effect on locomotor activity and coordination as indicated by their performance on the rotarod compared to the vehicle group. N= 4 for the MK8722 group and N= 4 for the vehicle group.

CHAPTER 4

**ALLEVIATION OF PACLITAXEL-INDUCED MECHANICAL HYPERSENSITIVITY
AND HYPERALGESIC PRIMING WITH AMPK ACTIVATORS IN MALE AND FEMALE
MICE**

Kufreobong E Inyang¹, Timothy A McDougal¹, Eric D Ramirez¹, Marisa Williams¹,
Geoffroy Laumet², Annemieke Kavelaars², Cobi J. Heijnen², Michael Burton¹, Gregory
Dussor¹, Theodore J Price^{1*}

¹University of Texas at Dallas, School of Behavioral and Brain Sciences and Center for
Advanced Pain Studies

²MD Anderson Cancer Center, Department of Symptom Research

School of Behavioral and Brain Sciences,

The University of Texas at Dallas

800 W Campbell Rd

Richardson TX 75080

Abstract

AMP-activated protein kinase (AMPK) is an energy-sensing kinase that has emerged as a novel therapeutic target for pain due to its ability to inhibit mechanistic target of rapamycin (mTOR) and mitogen activated protein kinase (MAPK) signaling, two signaling pathways that are linked to pain promotion after injury as well as the development of hyperalgesic priming. MAPK and mTOR signaling are also implicated in chemotherapy induced peripheral neuropathy (CIPN). We conducted a series of experiments to gain further insight into how AMPK activators might best be used to treat pain in both sexes in the setting of CIPN from paclitaxel. We also assessed whether hyperalgesic priming emerges from paclitaxel treatment and if this can be prevented by AMPK targeting. AMPK can be pharmacologically activated indirectly through regulation of upstream kinases like liver kinase B1 (LKB1) or directly using positive allosteric modulators. We used the indirect AMPK activators metformin and narciclasine and the direct AMPK activator MK8722. We previously used these same AMPK activators in the incision post-surgical pain model and saw that metformin was sex specific. Metformin failed to produce an anti-hyperalgesic effect or attenuate priming in female mice. We have also previously seen metformin to be sex specific in the SNI model. Here, the AMPK activators were used in 2 different treatment paradigms. First the drugs were given concurrently with paclitaxel to test whether they prevent mechanical hypersensitivity. Second the AMPK activators were given after the completion of paclitaxel treatment to test whether they reverse established mechanical hypersensitivity. Consistent with our previously published findings with metformin,

narciclasine (1 mg/kg) produced an anti-hyperalgesic effect, preventing paclitaxel-induced neuropathy in outbred mice of both sexes. In contrast to metformin, narciclasine also reversed mechanical hypersensitivity in established CIPN. Both metformin (200 mg/kg) and narciclasine prevented the development of hyperalgesic priming induced by paclitaxel treatment. MK8722 (30 mg/kg) had no effect on mechanical hypersensitivity caused by paclitaxel in either the prevention or reversal treatment paradigms. However, MK8722 did attenuate hyperalgesic priming in male and female mice. We conclude that paclitaxel induces robust hyperalgesic priming that is prevented by AMPK targeting and that narciclasine is a particularly attractive candidate for further development as a CIPN treatment.

Highlights:

- Paclitaxel induces hyperalgesic priming in male and female mice
- AMPK activators attenuate the development of hyperalgesic priming induced by paclitaxel
- Narciclasine prevents and reverses paclitaxel-induced mechanical hypersensitivity and hyperalgesic priming

Introduction

Chemotherapy-induced peripheral neuropathy (CIPN) is characterized by a glove-and-stocking (Seretny, Currie et al. 2014, Ma, Kavelaars et al. 2018) distribution of pain and develops in 30-40% of cancer patients receiving chemotherapy (Pachman, Barton et al. 2011). In these patients, the pain, numbness and tingling in hands and feet develops during treatment and frequently continues even after completion of therapy. This pervasive peripheral neuropathy is a major dose-limiting adverse effect of multiple chemotherapeutic agents, particularly paclitaxel which causes CIPN in as many as 90% of patients (Colvin 2019). Currently, there are no effective treatments for chemotherapy-induced neuropathy (Brown, Sedhom et al. 2019). Therefore, identification of novel or existing drugs that are effective in preventing or reversing CIPN would greatly benefit treatment and quality of life of cancer patients undergoing chemotherapy treatment.

Metformin, a well-known anti-diabetic drug, activates adenosine monophosphate-activated protein kinase (AMPK) indirectly in a liver kinase B1 (LKB1) dependent fashion (Shaw RJ 2005). AMPK detects changes in the AMP/ATP ratio to regulate anabolic processes when cellular energy status is low (Kahn BB 2005). Several studies have shown that AMPK plays a key role in nociceptive sensitization (Song, Han et al. 2015, Song H 2015, Bullón P 2016). Recent findings show that metformin reverses established mechanical allodynia in models of neuropathic pain induced by spinal nerve ligation in rats (Melemedjian, Khoutorsky et al. 2013) and spared nerve injury in mice (Melemedjian and Khoutorsky 2015, Inyang, Szabo-Pardi et al. 2018), but these positive effects are only seen in male animals (Burton, Tillu et al. 2017). On the other hand,

metformin prevents CIPN in female mice but only when given concurrently with the chemotherapeutic treatment (Mao-Ying, Kavelaars et al. 2014). Furthermore, metformin prevents hyperalgesic priming induced by plantar incision, a model of the transition from acute to chronic pain (Reichling and Levine 2009, Price and Inyang 2015), but again, only in male mice (Inyang, Burton et al. 2019). Finally, several recent clinical trials suggest that metformin can be effective for mitigation of pain in humans (Taylor, Westveld et al. 2013, Kialka, Milewicz et al. 2016, El-Fataty, Ibrahim et al. 2018), supporting the clinical translational potential of these preclinical findings. A major unresolved issue is whether the sex-specific effects of metformin are observed across models. Because metformin can prevent CIPN development in female mice (Mao-Ying, Kavelaars et al. 2014), this is an ideal model system to assess the effects of this drug on pain more thoroughly. Another question is whether paclitaxel treatment can produce hyperalgesic priming. The presence of hyperalgesic priming caused by paclitaxel would suggest a long-lasting impact of chemotherapy treatment on the nervous system. Understanding mechanisms causing these changes could reveal new therapeutic options for this important type of neuropathic pain.

Various other AMPK activators have emerged in recent years that are more potent and efficacious than metformin (Cao, Huang et al. 2018, Qin, Qiao et al. 2018). In experiments done to date, none of these other AMPK activators show sex-specific effects on pain outcomes in preclinical models (Inyang, Burton et al. 2019). A particularly promising AMPK activator for therapeutic development is narciclasine. It is a natural compound from the plant *Amaryllidaceae* (Dumont, Ingrassia et al. 2007) that

indirectly activates AMPK (Julien SG 2017) and strongly inhibits incision-evoked mechanical hypersensitivity and hyperalgesic priming in male and female mice (Inyang, Burton et al. 2019). While indirect AMPK activators stimulate upstream kinases that phosphorylate AMPK, another way to activate AMPK is via direct, positive allosteric mechanisms. A highly selective and potent positive allosteric modulator of AMPK called MK8722 was recently described (Feng, Biftu et al. 2018, Weihrauch and Handschin 2018). We have recently compared direct (MK8722) and indirect (metformin and narciclasine) AMPK activators in an incisional pain model. Our findings demonstrate that narciclasine produces more efficacious relief of mechanical hypersensitivity than MK8722 (Inyang, Burton et al. 2019). This likely occurs because the indirect AMPK activator narciclasine is capable of overcoming the suppression of AMPK phosphorylation that is induced by injury (Julien, Kim et al. 2017, Inyang, Burton et al. 2019). Interestingly, while indirect AMPK activators reduce acute mechanical hypersensitivity and attenuate hyperalgesic priming caused by hindpaw incision, direct AMPK activators only attenuate hyperalgesic priming in this model (Inyang, Burton et al. 2019).

Based on the findings described above, we hypothesized that narciclasine would efficaciously prevent mechanical hypersensitivity caused by paclitaxel treatment and that it would ~~block~~ attenuate hyperalgesic priming in male and female mice. We further hypothesized that MK8722 would have little effect on prevention of paclitaxel-induced mechanical hypersensitivity but that it would attenuate hyperalgesic priming in both sexes. Finally, we hypothesized that metformin would show similar effects to

narciclasine in both male and female mice. The experiments described below were designed to test these hypotheses.

Methods

Laboratory animals

Animal procedures were approved by The University of Texas at Dallas Institutional Animal Care and Use Committee and were in accordance with National Institutes of Health Guidelines. All the experiments were performed on male and female ICR outbred mice obtained from Envigo at 4 weeks of age or bred in a colony at University of Texas at Dallas. Mice were housed in the University of Texas at Dallas Animal Care Facility for at least one week prior to the start of behavioral testing. Animals had *ad libitum* access to food and water and were on a 12 hr non-inverted light/dark cycle. Experimenters were blinded to treatment groups in behavioral experiments. Mice were randomized to treatment groups using a random number generator and in such a manner that multiple treatment groups were always found within any individual cage of animals. Male and female mice were housed separately in groups of 4 per cage.

Behavioral testing and drug administration

CIPN was induced using paclitaxel (Sigma Aldrich, 4 mg/kg) given via intraperitoneal injection (i.p.) every other day for one week for a cumulative dose of 16 mg/kg (Megat, Ray et al. 2019). Paclitaxel was dissolved in a 50/50 Kolliphor EL (Sigma Aldrich)/ ethanol solution then further dissolved in 0.9% saline for injections. Mechanical sensitivity was assessed using stimulation of the left hindpaw of the mouse with

calibrated von Frey filaments from Stoelting. We used 0.6, 1.0 and 1.4-gram filaments and measured the response frequency to 10 consecutive stimulations of the hindpaw with each filament with stimulations spaced by at least 5 sec following 45 minutes of habituation to the testing boxes. The number of responses for each filament force was recorded with the tester blinded to the groups and presented as percentage of times responded for each individual filament. Two different treatment paradigms were used in this study. In the prevention paradigm, paclitaxel and an AMPK activator were given concurrently for 1 week. In the reversal paradigm, paclitaxel was given for a week followed by 1 week of AMPK activator treatment. Mice were tested for mechanical hypersensitivity periodically until response frequency returned to baseline levels.

Following the return to baseline, hyperalgesic priming was tested by giving each animal an intraplantar injection of prostaglandin E₂ (PGE₂) (Cayman Chemical, 100 ng/ 25 µL) into the left hindpaw. Response frequency following PGE₂ was tested at time points indicated in graphs. The PGE₂ priming experiments were modeled after previous priming experiments that our lab has done in the plantar incision model (Tillu, Melemedjian et al. 2012, Burton, Tillu et al. 2017, Inyang 2019). The different AMPK activators used in this experiment were metformin i.p. (LKT Laboratories, 200 mg/kg), narciclasine by oral gavage (p.o., Santa Cruz Biotech, 1 mg/kg) (Julien SG 2017) and MK-8722 p.o. (gift from Merck, 30 mg/kg) (Feng, Biftu et al. 2018). Metformin was dissolved in 0.9% saline and narciclasine was made in 45% w/v (2-Hydroxypropyl)-β-cyclodextrin (Sigma Aldrich). MK-8722 was administered in 0.25% methyl cellulose (MC), 5% Tween-80, and 0.02% sodium dodecyl sulfate (SDS) (Feng, Biftu et al. 2018).

Statistics

Data are shown as mean +/- standard error of the mean (SEM) and the number of animals or samples used in each analysis are given in figure legends. GraphPad Prism 8 was used to analyze data for statistical tests, which are given in figure legends.

Repeated measures two-way ANOVAs were used to analyze von Frey data. Post-hoc tests used were the Bonferroni multiple comparisons test. Significance level was set at $\alpha < 0.05$. Values for all test statistics are given in **Table 4.1**.

Results

Paclitaxel induced hyperalgesic priming in male mice.

Our previous work in the hindpaw incision model indicates that indirect AMPK activators reduce acute mechanical hypersensitivity and attenuate hyperalgesic priming whereas direct AMPK activators only attenuate hyperalgesic priming (Inyang, Burton et al. 2019). We hypothesized that similar effects might be seen in a CIPN model, however, no published studies have assessed whether hyperalgesic priming is produced by treatment with chemotherapeutics like paclitaxel. To test whether paclitaxel can cause hyperalgesic priming, we first obtained baseline response frequency measures. Then mice received i.p. paclitaxel or vehicle treatment. Once the mice returned to baseline level mechanical sensitivity, animals received 100 ng PGE₂ into the left hindpaw. Only the mice that received paclitaxel demonstrated mechanical hypersensitivity at the time points tested indicating that paclitaxel causes robust hyperalgesic priming (**Fig 4.1A-C**).

Metformin effects on paclitaxel-induced mechanical hypersensitivity and hyperalgesic priming in male and female mice.

Previous studies have demonstrated that metformin treatment during the course of chemotherapy administration prevents the development of CIPN in female mice. However, if treatment is given after CIPN is established, it fails to reverse the neuropathy (Mao-Ying, Kavelaars et al. 2014). Other studies in the spared nerve injury and incisional models in mice have demonstrated that metformin reverses and prevents, respectively, mechanical hypersensitivity, but only in males (Inyang, Szabo-Pardi et al. 2018, Inyang, Burton et al. 2019). Hence, there is a discrepancy in the efficacy of metformin in male and female mice depending on the model and time point of intervention. Having shown that hyperalgesic priming is present in the paclitaxel CIPN model, we reasoned that metformin might be effective in reversing paclitaxel-induced hyperalgesic priming in both male and female mice.

To test the effects of metformin on paclitaxel-induced mechanical hypersensitivity in male mice, animals were given paclitaxel. These mice were then allocated into metformin (200 mg/kg) and vehicle treatment groups. Consistent with previous results (Mao-Ying, Kavelaars et al. 2014), metformin did not reverse established paclitaxel-induced mechanical hypersensitivity in males. However, metformin did attenuate hyperalgesic priming (**Fig 4.2A-C**). To test whether similar effects would be observed in female mice paclitaxel treatment was given over the course of a week followed by a week of metformin treatment. Like with male mice, metformin had no effect on the mechanical hypersensitivity caused by paclitaxel but did attenuate hyperalgesic priming

(**Fig 4.2D-F**). Therefore, unlike the hindpaw incision model where effects on hyperalgesic priming were only observed in male mice (Inyang, Burton et al. 2019), metformin is effective in reversing paclitaxel-induced hyperalgesic priming in both sexes.

Narciclasine effects on paclitaxel-induced mechanical hypersensitivity and hyperalgesic priming in both sexes.

We then tested the effects of a structurally distinct indirect AMPK activator, narciclasine. Our previous studies in the hindpaw incision model demonstrate that narciclasine dose-dependently inhibits mechanical hypersensitivity and hyperalgesic priming induced by incision in both sexes (Inyang, Burton et al. 2019). In male mice, under the prevention treatment paradigm, narciclasine both prevented mechanical hypersensitivity and attenuated development of hyperalgesic priming following paclitaxel (**Fig 4.3A-C**). Just as in male mice, narciclasine prevented paclitaxel-induced mechanical hypersensitivity in female mice and attenuating paclitaxel-induced priming (**Fig 4.3D-F**). In both sexes, the effect of narciclasine on mechanical hypersensitivity persisted after cessation of treatment.

We then tested narciclasine's ability to reverse paclitaxel-induced mechanical hypersensitivity. Unlike with metformin, narciclasine was able to significantly inhibit mechanical hypersensitivity from paclitaxel in addition to attenuating hyperalgesic priming in males (**Fig 4.4A-C**). In female mice, narciclasine also inhibited paclitaxel-induced mechanical hypersensitivity in the reversal treatment paradigm in addition to

attenuating hyperalgesic priming (**Fig 4.4D-F**). In these experiments, where narciclasine was given after paclitaxel treatment, we also observed a continued effect of the drug even after cessation of treatment. Comparing the prevention to the reversal treatment paradigms, narciclasine was clearly more effective in the prevention paradigm where it almost completely attenuated development of mechanical hypersensitivity in both sexes. In the reversal paradigm, the effect of drug was significant, but there was not a complete reversal of mechanical hypersensitivity or hyperalgesic priming.

MK8722 effects on paclitaxel-induced mechanical hypersensitivity and hyperalgesic priming in male and female mice.

Metformin and narciclasine activate AMPK indirectly via upstream signaling mechanisms. MK8722 is a structurally distinct AMPK activator that binds directly to the kinase to allosterically increase kinase activity. We tested this direct AMPK activator in males and females in paclitaxel CIPN prevention and reversal paradigms. MK8722 did not prevent mechanical hypersensitivity in male mice but did attenuate hyperalgesic priming (**Fig 4.5A-C**). MK8722 also did not prevent paclitaxel-induced mechanical hypersensitivity in female mice when given concurrently with paclitaxel but it did attenuate paclitaxel-induced hyperalgesic priming (**Fig 4.5D-F**).

With another set of male mice, we assessed the ability of MK8722 to reverse paclitaxel-induced neuropathy. These mice received paclitaxel for a week followed by a week of MK8722 treatment. MK8722 was not able to reverse mechanical hypersensitivity induced by paclitaxel but it again attenuated hyperalgesic priming (**Fig 4.6A-C**). In

females, MK8722 also did not reverse established mechanical hypersensitivity but did attenuate hyperalgesic priming (**Fig 4.6D-F**).

Discussion

One of the key findings of this study is that paclitaxel can induce hyperalgesic priming and that this priming effect is strongly attenuated by AMPK activator treatment. All of the direct and indirect AMPK activators used successfully attenuated and/or reversed paclitaxel-induced hyperalgesic priming, even though narciclasine was the only one capable of both preventing and reversing paclitaxel-induced mechanical hypersensitivity. Hyperalgesic priming effects have not been previously explored in models of CIPN, but our work makes it clear that paclitaxel treatment produces a robust hyperalgesic priming effect that is apparent in both male and female mice. Consistent with our previous work in the incisional model, narciclasine, metformin and MK8722 were all capable of inhibiting hyperalgesic priming revealed by mechanical hypersensitivity in response to PGE₂ injection. These findings demonstrate that paclitaxel treatment creates an enduring change in the nervous system that enhances the response to subsequent challenge to a normally non-noxious dose of PGE₂. This finding gives new insight into long-lasting effects of chemotherapeutics on the nociceptive system and demonstrates that a variety of AMPK activators can be used to attenuate and/or reverse this type of plasticity. Since clinical CIPN can be recurring (Ewertz, Qvortrup et al. 2015), hyperalgesic priming may be a useful paradigm for understanding how to break the cycle of pain that can occur in certain patients. Previous studies have shown that CIPN pain resolution is actively regulated by T cells

and interleukin 10 (Krukowski, Eijkelkamp et al. 2016, Laumet, Edralin et al. 2019). Similar observations have been made in inflammatory and post-surgical pain models wherein pain resolution occurs via a mechanism that involves inhibitory G-protein coupled receptors in the spinal cord dorsal horn or nociceptive afferents (Corder, Doolen et al. 2013, Taylor and Corder 2014, Price and Inyang 2015, Walwyn, Chen et al. 2016, Severino, Chen et al. 2018). While it is not known to what extent these pain resolution mechanisms overlap with mechanisms that resolve hyperalgesic priming, it is notable that AMPK activators are effective in reversing hyperalgesic priming in all of these contexts (Tillu, Melemedjian et al. 2012, Burton, Tillu et al. 2017, Inyang, Burton et al. 2019).

It has previously been established that metformin is capable of attenuating the establishment of CIPN as a result of paclitaxel treatment in mice but that this drug does not reverse established CIPN (Mao-Ying, Kavelaars et al. 2014). Our findings are consistent with that previous work insofar as we saw no effect of metformin on established paclitaxel-induced mechanical hypersensitivity in male and female mice. However, we did note an inhibition of hyperalgesic priming in both sexes, indicating that metformin does have effects even when given after cessation of chemotherapy treatment. While the anti-hyperalgesic effects of metformin in male mice are very robust in the SNI and incisional models (Melemedjian OK 2011, Burton, Tillu et al. 2017, Inyang, Szabo-Pardi et al. 2018), our previous observations in female mice have demonstrated a marked sexual dimorphism in the efficacy of metformin (Inyang, Szabo-Pardi et al. 2018) (Inyang, Burton et al. 2019). Surprisingly, in this study, metformin was

just as effective in reversing hyperalgesic priming in females as it was in males. While the mechanistic underpinning of these divergent sex-specific effects are not currently known, several clinical trials with metformin for pain suggest that this drug can be effective in both male and female humans (Taylor, Westveld et al. 2013, Kialka, Milewicz et al. 2016, El-Fataty, Ibrahim et al. 2018). Additional clinical trials will be needed to understand the utility of metformin as a pain therapeutic. Our work provides new information that can be useful in designing those clinical trials.

Narciclasine has shown robust behavioral effects in mice in treatment of acute and chronic pain (Inyang, Burton et al. 2019) as well as combating inflammation (Stark, Schwenk et al. 2019) making it an attractive potential analgesic. One benefit of narciclasine is that it is a natural compound and can be extracted as well as synthesized (Ceriotti 1967). Compared to other AMPK activators, narciclasine stimulates the kinase *in vivo* at low doses and shows efficacy in cancer, metabolic and pain models at doses that coincide with AMPK activation kinetics (Van Goietsenoven, Hutton et al. 2010, Julien SG 2017, Inyang, Burton et al. 2019). Mechanistically, narciclasine increases the adenosine diphosphate (ADP)/ATP ratio in myotubes, which is a potential mechanism through which the compound causes AMPK activation (Hu, Na et al. 2015, Julien, Kim et al. 2017). The mechanism through which narciclasine activates AMPK in sensory neurons is not known, but our previous work demonstrates that the drug stimulates AMPK in dorsal root ganglion neurons *in vitro* and *in vivo* (Inyang, Burton et al. 2019). Interestingly, while narciclasine activates AMPK in skeletal muscle and neurons, it does not activate AMPK in liver (Julien, Kim et al. 2017, Inyang, Burton et al. 2019). The

restricted action of narciclasine on AMPK in certain tissues may be advantageous from a safety perspective. We cannot rule out a potential action of narciclasine on other signaling mechanisms. For instance, narciclasine negatively influences inflammation via downregulation of tumor necrosis factor type 1 receptor (Stark, Schwenk et al. 2019), which would also be expected to have an impact on neuropathic pain. It is possible that the polypharmacology of this compound improves its *in vivo* efficacy.

AMPK activators are likely effective for alleviating pain in CIPN for several reasons. One is that paclitaxel treatment induces enhanced signaling in mTOR and MAPK signaling pathways and activation of AMPK targets both of these signaling mechanisms to reduce nociceptor excitability (Megat, Ray et al. 2019). Another potential target is mitochondrial dysfunction in CIPN. This has recently been comprehensively reviewed by Trecarichi and Flatters (Trecarichi and Flatters 2019) and is clearly a central feature of sensory neuron dysfunction across CIPN types (Ma, Kavelaars et al. 2018). AMPK activation has multiple effects on dysfunctional mitochondria in many different contexts (Hardie, Ross et al. 2012, Burkewitz, Zhang et al. 2014). However, the influence of AMPK activation on mitochondrial dysfunction in CIPN has not been addressed directly.

There are several weaknesses of this study that could be addressed in future experiments. Behavioral measures in this work relied completely on evoked pain measures. Future experiments will focus on the effect of narciclasine on affective components of pain using the conditioned place preference paradigm (King, Vera-Portocarrero et al. 2009, Megat, Ray et al. 2019). Another shortcoming of this study is that it was completely focused on mechanical pain features of CIPN. CIPN is

characterized by other features such as weakness and numbness (Izycki, Niezgoda et al. 2016) that we did not assess. Our previous work with metformin demonstrated that numbness and the loss of intra-epidermal nerve fibers could be prevented by metformin treatment in both sexes (Mao-Ying, Kavelaars et al. 2014). We hypothesize that narciclasine would be similarly effective, but might also reverse these effects once established, unlike our observations with metformin. Finally, and as mentioned above, the common molecular mechanism of the compounds used in this study is AMPK, but we cannot rule out other potential mechanisms of action. It is possible that the differences we observed are due to differential efficacy in AMPK activation *in vivo* for each compound, with narciclasine likely being the most efficacious; but it is also possible that differences arise because AMPK is not the sole target for these compounds.

In conclusion, we observed that hyperalgesic priming is induced by paclitaxel treatment in mice and this priming can be attenuated with diverse types of AMPK activators in both male and female animals. We did find differential effects of these AMPK activators. Most notably, unlike metformin and MK8722, narciclasine both prevented and reversed paclitaxel-induced mechanical hypersensitivity suggesting that this compound can have a unique, disease modifying effect on CIPN. Based on these and other, previously published effects (Julien, Kim et al. 2017, Inyang, Burton et al. 2019, Stark, Schwenk et al. 2019), the natural product narciclasine is a promising lead for further clinical development given its substantial potency and efficacy in multiple preclinical pain models in both sexes.

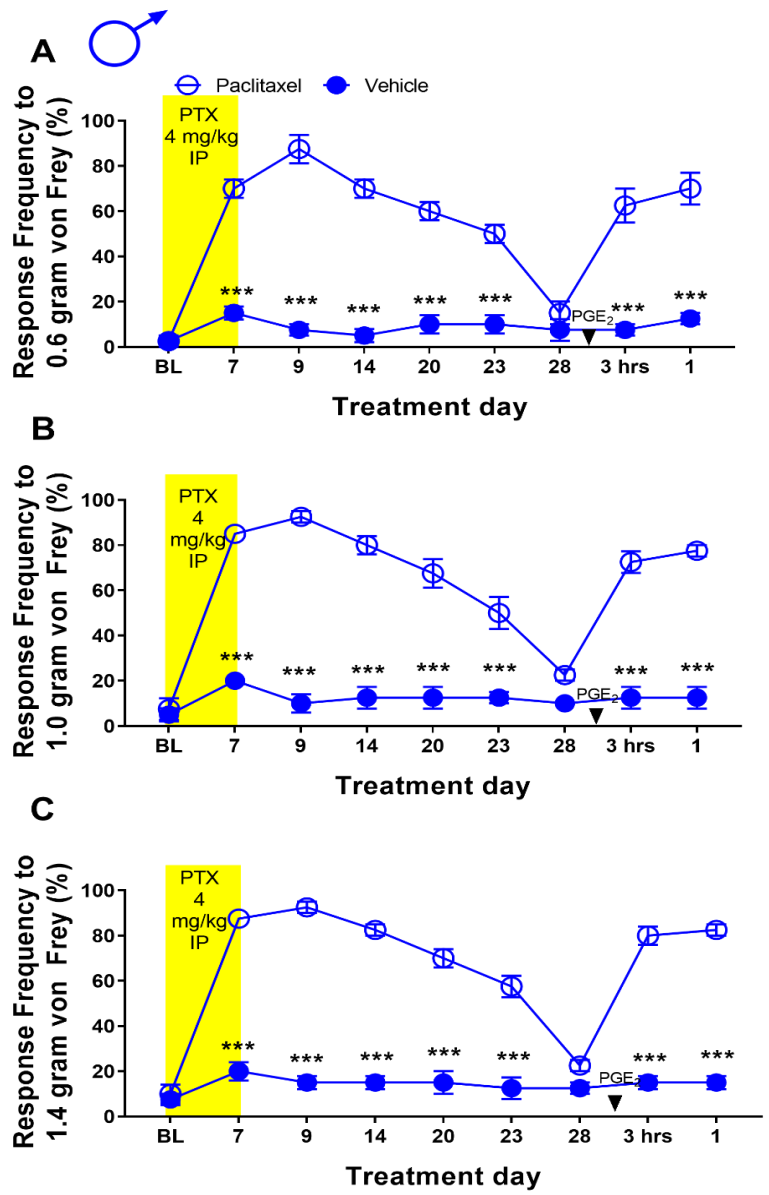


Figure 4.1: Paclitaxel induced hyperalgesic priming in male mice. A-C. Paclitaxel treatment caused an increase in mechanical hypersensitivity. Following resolution of this hypersensitivity, PGE₂ was able to cause an increase in response frequency indicating the presence of hyperalgesic priming. ***p < 0.001; N = 4 per group.

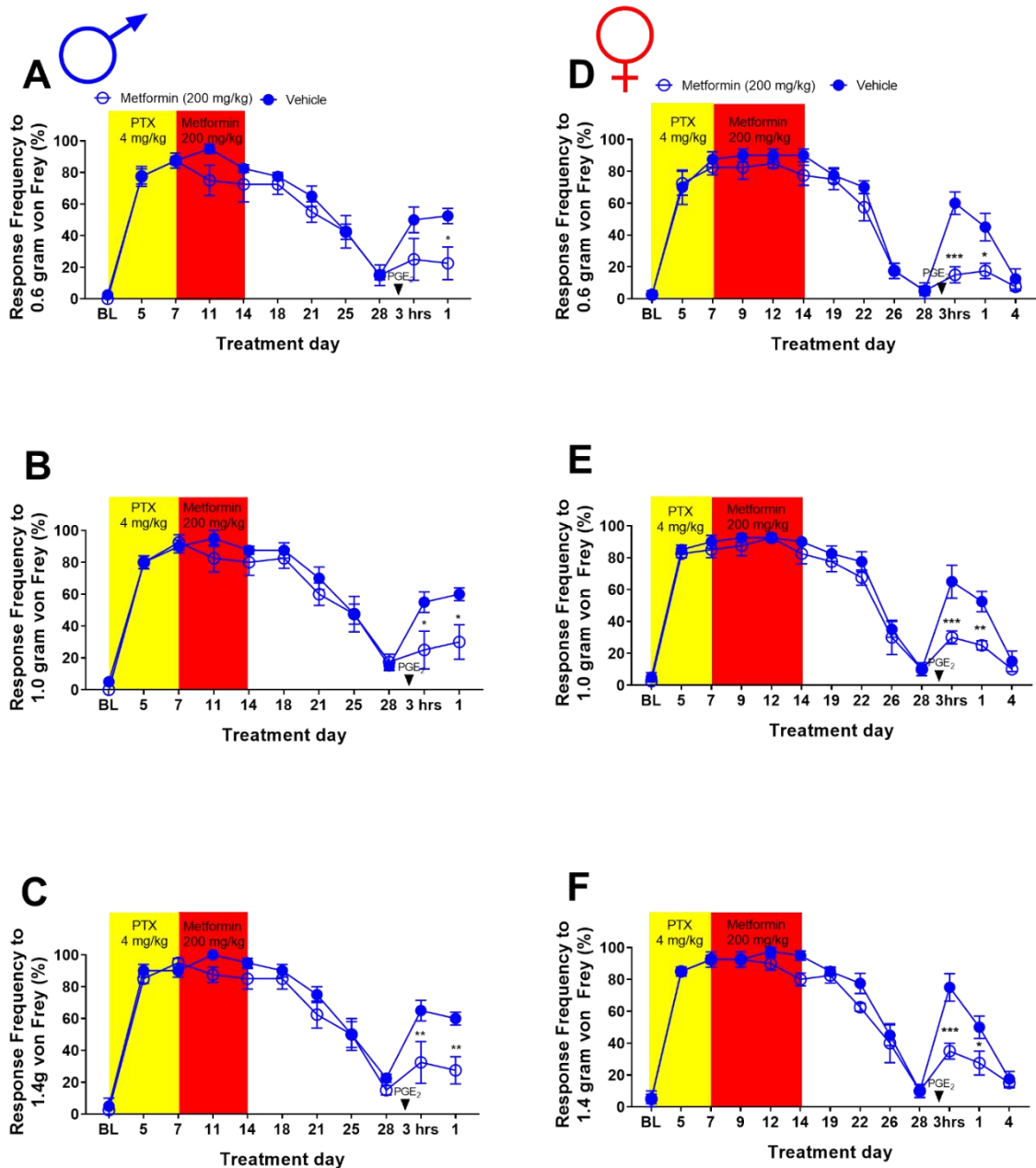


Figure 4.2: Metformin attenuated paclitaxel-induced hyperalgesic priming in male and female mice. A-F. In male and female mice, metformin treatment immediately following a 7-day paclitaxel treatment failed to reverse CIPN but blocked attenuated subsequent hyperalgesic priming precipitated by PGE₂. * $p < 0.05$, ** $p < 0.01$, *** $p < 0.001$; N = 4 per group.

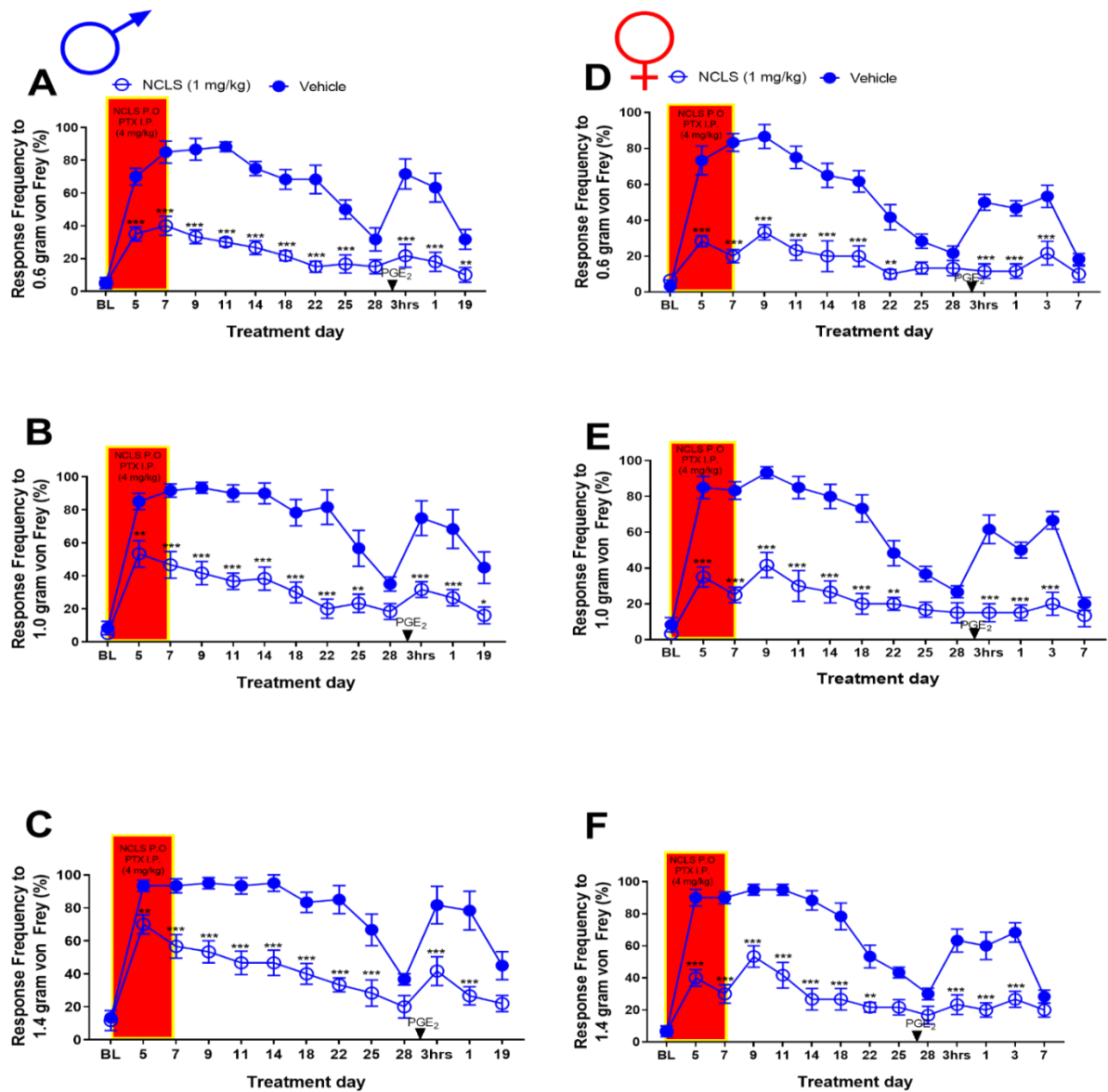


Figure 4.3: Narciclasine (NCLS) blocks attenuated paclitaxel-induced mechanical hypersensitivity and hyperalgesic priming in males and females. A-C. NCLS blocked attenuated the development of CIPN in male mice when give concurrently with paclitaxel and blocked attenuated hyperalgesic priming precipitated by PGE2. *p < 0.05; **p < 0.01; ***p < 0.001; N = 6 for NCLS group and vehicle group. D-F. NCLS prevented CIPN in female mice when given concurrently with paclitaxel treatment and blocked attenuated hyperalgesic priming precipitated by PGE2. *p < 0.05; **p < 0.01; ***p < 0.001; N = 6 for NCLS group and N = 6 for vehicle group.

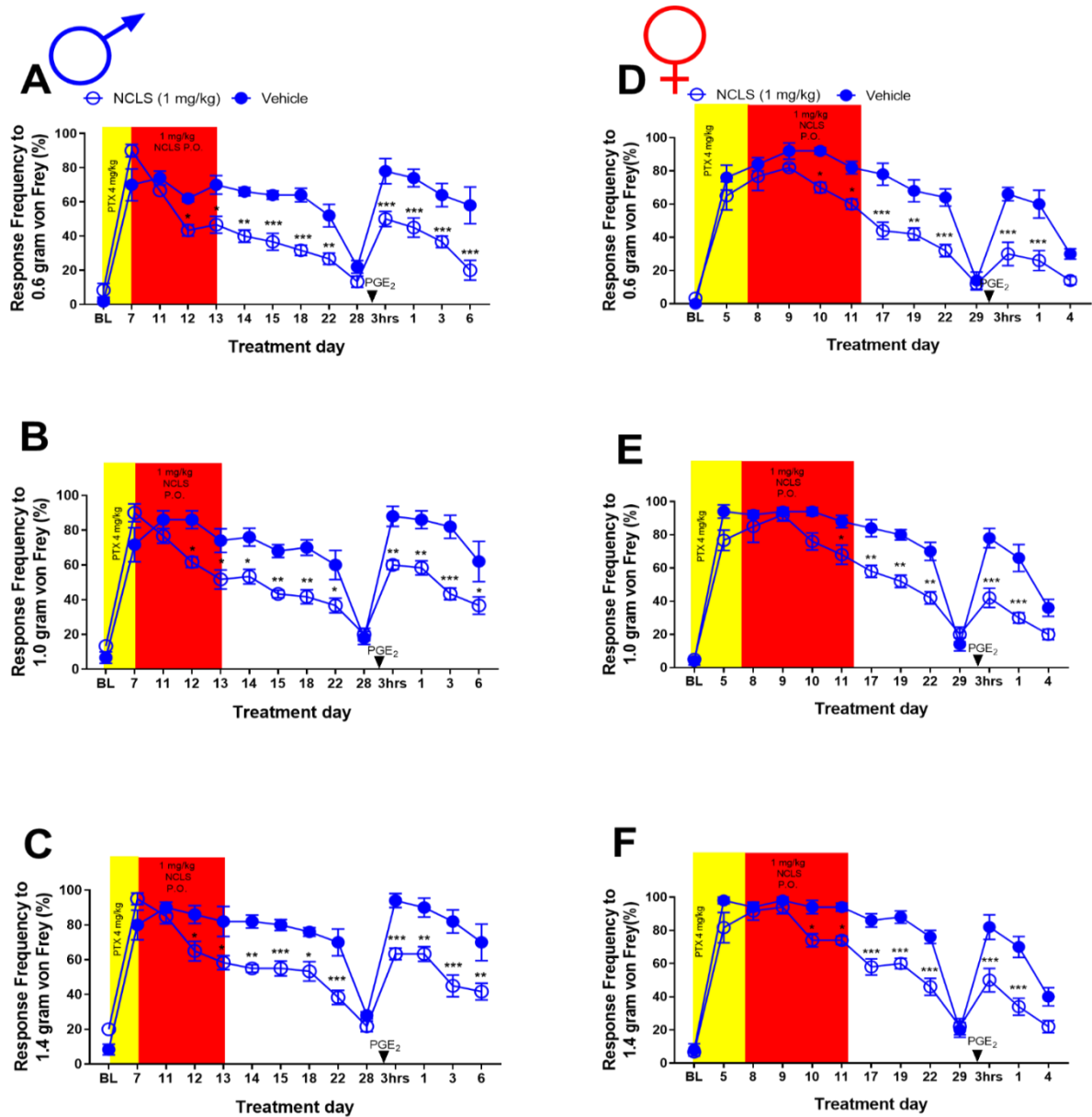


Figure 4.4: Narciclasine partially reverses paclitaxel-induced mechanical hypersensitivity and blocks priming in male and females. A-C. NCLS reverses CIPN in male mice when give immediately following paclitaxel treatment and blocked hyperalgesic priming precipitated by PGE₂. *p < 0.05; **p < 0.01; ***p < 0.001; N = 6 for the NCLS group and N = 6 for the vehicle group. D-F. NCLS reversed CIPN in female mice when given immediately following 7-day paclitaxel treatment and blocked attenuated hyperalgesic priming precipitated by PGE₂. *p < 0.05; **p < 0.01; ***p < 0.001; N = 5 for the NCLS group and N = 5 for the vehicle group.

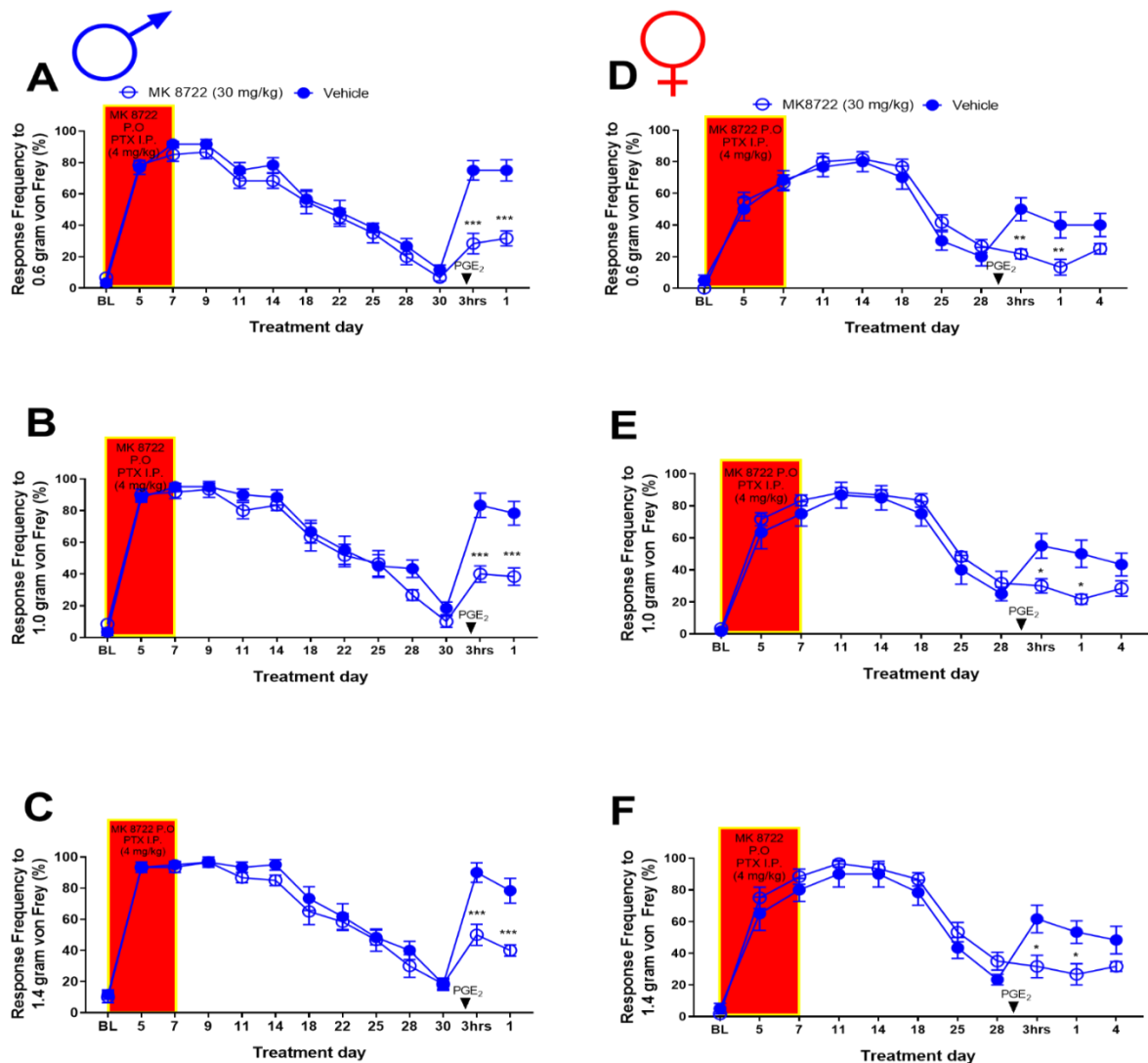


Figure 4.5: MK8722 attenuates paclitaxel-induced hyperalgesic priming in male and female mice when given concurrently with paclitaxel. A-C. MK8722 did not block attenuate the development of CIPN in male mice when give concurrently with paclitaxel but was effective in blocking attenuating hyperalgesic priming precipitated by PGE₂. *** $p < 0.001$; N=6 for MK8722 group and vehicle group. D-F. MK8722 failed to prevent CIPN in female mice when given concurrently with paclitaxel treatment but again attenuated hyperalgesic priming precipitated by PGE₂. * $p < 0.05$; ** $p < 0.01$; *** $p < 0.001$; N= 4 for NCLS and vehicle group.

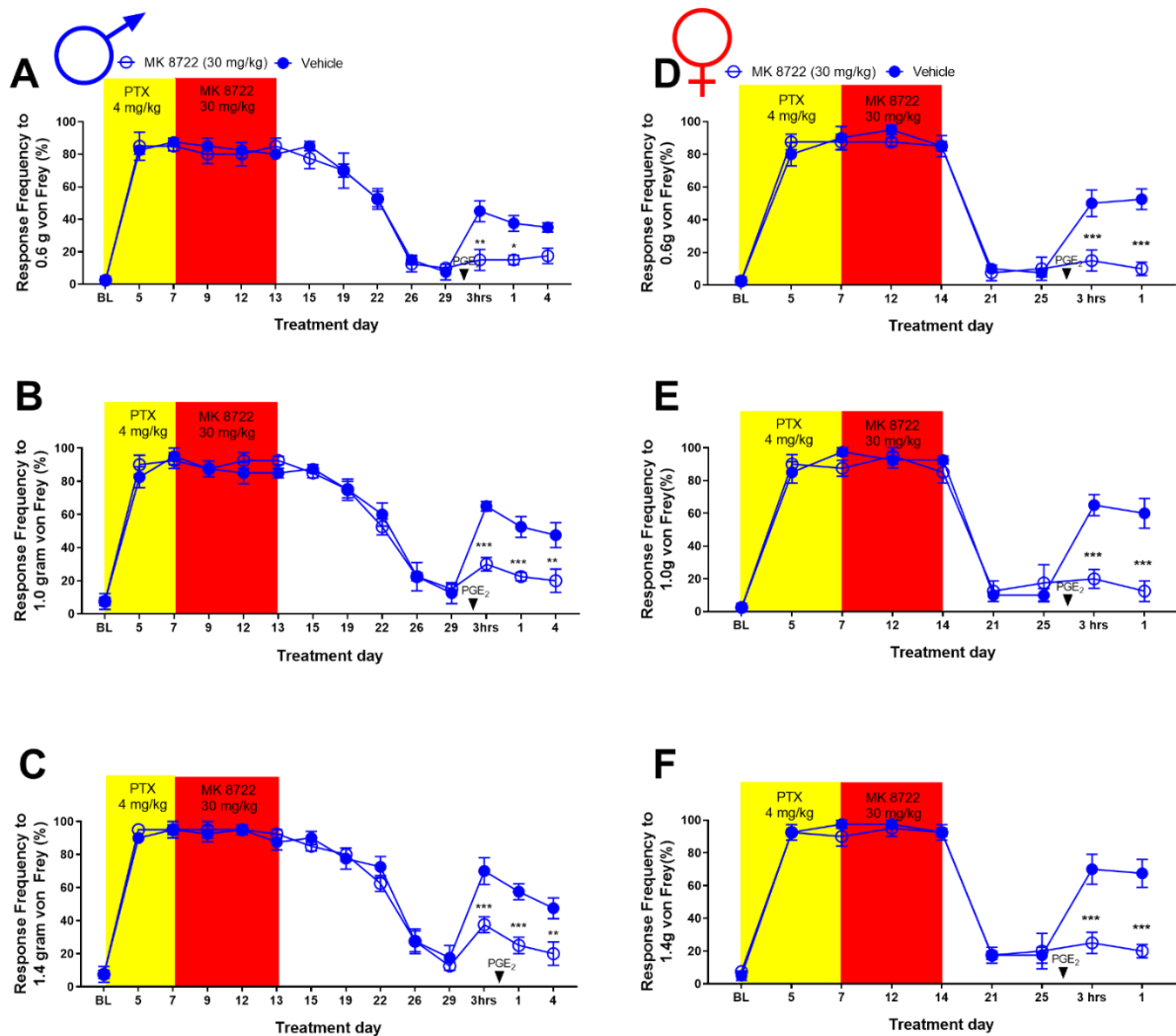


Figure 4.6: MK8722 attenuates paclitaxel-induced hyperalgesic priming in male and female mice when given after paclitaxel treatment. A-C. MK8722 did not reverse CIPN in male mice when given following paclitaxel but was effective in reducing hyperalgesic priming precipitated by PGE2. * $p < 0.05$; ** $p < 0.01$; N = 6 for MK8722 group and vehicle group. D-F. MK8722 failed to reverse CIPN in female mice when given immediately following 7-day paclitaxel treatment but again inhibited hyperalgesic priming precipitated by PGE2. * $p < 0.05$; ** $p < 0.01$; *** $p < 0.001$; N = 4 for MK8722 and vehicle group.

Table 4.1: Statistical test values given by figure number and panel

Test (Factor)	F (df1, df2) interaction F (df1, df2) time F (df1, df2) Drug treatment	P-Value	Adjusted p-value (Post-hoc comparison): BL, days post injection, 3 hrs post PGE₂ and 1-day post.
Two-Way ANOVA (Fig 1A)	F (8, 54) = 17.98 F (8, 54) = 23.52 F (1, 54) = 492.0	P _I <0.0001 P _t <0.0001 P _d <0.0001	PTX vs. Veh: >0.9999, <0.0001, <0.0001, <0.0001, <0.0001, >0.9999, <0.0001, <0.0001.
Two-Way ANOVA (Fig 1B)	F (8, 54) = 21.43 F (8, 54) = 30.40 F (1, 54) = 662.9	P _I <0.0001 P _t <0.0001 P _d <0.0001	PTX vs. Veh: >0.9999, <0.0001, <0.0001, <0.0001, <0.0001, <0.0001, <0.0001, 0.3811, <0.0001, <0.0001.
Two-Way ANOVA (Fig 1C)	F (8, 54) = 30.41 F (8, 54) = 44.04 F (1, 54) = 975.4	P _I <0.0001 P _t <0.0001 P _d <0.0001	PTX vs. Veh: >0.9999, <0.0001, <0.0001, <0.0001, <0.0001, <0.0001, <0.0001, 0.4090, <0.0001, <0.0001.
Two-Way ANOVA (Fig 2A)	F (10, 66) = 1.313 F (10, 66) = 37.80 F (1, 66) = 10.44	P _I =0.2421 P _t <0.0001 P _d =0.0019	Met vs. Veh: >0.9999, >0.9999, >0.9999, 0.3645, 0.9801, >0.9999, 0.9801, >0.9999, >0.9999, 0.1153, 0.0277.
Two-Way ANOVA (Fig 2B)	F (10, 66) = 1.611 F (10, 66) = 44.71 F (1, 66) = 9.757	P _I =0.1229 P _t <0.0001 P _d =0.0027	Met vs. Veh: >0.9999, >0.9999, >0.9999, 0.8834, 0.9973, >0.9999, 0.9728, >0.9999, >0.9999, 0.0186, 0.0186.
Two-Way ANOVA (Fig 2C)	F (10, 66) = 2.018 F (10, 66) = 55.20 F (1, 66) = 16.62	P _I =0.0451 P _t <0.0001 P _d =0.0001	Met vs. Veh: >0.9999, 0.9999, 0.9999, 0.8247, 0.9539, 0.9999, 0.8247, >0.9999, 0.9949, 0.0033, 0.0033.
Two-Way ANOVA (Fig 2D)	F (12, 78) = 2.755 F (12, 78) = 71.69 F (1, 78) = 17.19	P _I =0.0036 P _t <0.0001 P _d <0.0001	Met vs. Veh: >0.9999, >0.9999, >0.9999, 0.9965, >0.9999, 0.8196, >0.9999, 0.8196, >0.9999, >0.9999, <0.0001, 0.0127, >0.9999.

Table 4.1: Statistical test values given by figure number and panel

Two-Way ANOVA (Fig 2E)	F (12, 78) = 2.184 F (12, 78) = 88.84 F (1, 78) = 18.15	P _I =0.0204 P _t <0.0001 P _d <0.0001	Met vs. Veh: >0.9999, >0.9999, 0.9998, 0.9998, >0.9999, 0.9900, 0.9998, 0.9064, 0.9998, >0.9999, <0.0001, 0.0032, 0.9998.
Two-Way ANOVA (Fig 2F)	F (12, 78) = 2.614 F (12, 78) = 82.19 F (1, 78) = 16.98	P _I =0.0056 P _t <0.0001 P _d <0.0001	Met vs. Veh: >0.9999, >0.9999, >0.9999, >0.9999, 0.9926, 0.4591, >0.9999, 0.4591, 0.9999, >0.9999, <0.0001, 0.0412, >0.9999.
Two-Way ANOVA (Fig 3A)	F (12, 128) = 4.608 F (12, 128) = 18.40 F (1, 128) = 310.8	P _I <0.0001 P _t <0.0001 P _d <0.0001	NCLS vs. Veh: >0.9999, 0.0003, <0.0001, <0.0001, <0.0001, <0.0001, <0.0001, <0.0001, 0.0006, 0.4837, <0.0001, <0.0001, 0.1319.
Two-Way ANOVA (Fig 3B)	F (12, 129) = 2.721 F (12, 129) = 15.00 F (1, 129) = 207.4	P _I =0.0026 P _t <0.0001 P _d <0.0001	NCLS vs. Veh: >0.9999, 0.0203, 0.0001, <0.0001, <0.0001, <0.0001, <0.0001, <0.0001, 0.0116, >0.9999, 0.0003, 0.0005, 0.0719.
Two-Way ANOVA (Fig 3C)	F (12, 129) = 2.417 F (12, 129) = 17.85 F (1, 129) = 173.8	P _I =0.0074 P _t <0.0001 P _d <0.0001	NCLS vs. Veh: >0.9999, 0.2287, 0.0031, 0.0004, <0.0001, <0.0001, 0.0002, <0.0001, 0.0017, >0.9999, 0.0009, <0.0001, 0.3313.
Two-Way ANOVA (Fig 3D)	F (13, 140) = 7.154 F (13, 140) = 19.76 F (1, 140) = 290.7	P _I <0.0001 P _t <0.0001 P _d <0.0001	NCLS vs. Veh: >0.9999, <0.0001, <0.0001, <0.0001, <0.0001, <0.0001, <0.0001, 0.0004, 0.5805, >0.9999, <0.0001, <0.0001, 0.0004, >0.9999.
Two-Way ANOVA (Fig 3E)	F (13, 140) = 6.029 F (13, 140) = 21.17 F (1, 140) = 315.0	P _I <0.0001 P _t <0.0001 P _d <0.0001	NCLS vs. Veh: >0.9999, <0.0001, <0.0001, <0.0001, <0.0001, <0.0001, <0.0001, 0.0060, 0.1677, >0.9999, <0.0001, 0.0002, <0.0001, >0.9999.

Table 4.1: Statistical test values given by figure number and panel

Two-Way ANOVA (Fig 3F)	F (13, 140) = 6.055 F (13, 140) = 24.16 F (1, 140) = 306.6	$P_I < 0.0001$ $P_t < 0.0001$ $P_d < 0.0001$	NCLS vs. Veh: > 0.9999 , < 0.0001 , < 0.0001 , < 0.0001 , < 0.0001 , < 0.0001 , 0.0013 , 0.0927 , > 0.9999 , < 0.0001 , < 0.0001 , < 0.0001 , > 0.9999 .
Two-Way ANOVA (Fig 4A)	F (13, 128) = 5.544 F (13, 128) = 32.46 F (1, 128) = 101.4	$P_I < 0.0001$ $P_t < 0.0001$ $P_d < 0.0001$	NCLS vs. Veh: > 0.9999 , 0.0503 , > 0.9999 , 0.1305 , 0.0175 , 0.0048 , 0.0025 , 0.0002 , 0.0067 , > 0.9999 , 0.0017 , 0.0010 , 0.0025 , < 0.0001 .
Two-Way ANOVA (Fig 4B)	F (13, 128) = 4.907 F (13, 128) = 34.25 F (1, 128) = 80.36	$P_I < 0.0001$ $P_t < 0.0001$ $P_d < 0.0001$	NCLS vs. Veh: > 0.9999 , 0.1511 , > 0.9999 , 0.0191 , 0.0448 , 0.0390 , 0.0165 , 0.0030 , 0.0294 , > 0.9999 , 0.0035 , 0.0041 , < 0.0001 , 0.0122 .
Two-Way ANOVA (Fig 4C)	F (13, 128) = 5.245 F (13, 128) = 36.37 F (1, 128) = 92.65	$P_I < 0.0001$ $P_t < 0.0001$ $P_d < 0.0001$	NCLS vs. Veh: > 0.9999 , 0.4363 , > 0.9999 , 0.0599 , 0.0188 , 0.0039 , 0.0102 , 0.0294 , 0.0003 , > 0.9999 , 0.0006 , 0.0046 , < 0.0001 , 0.0020 .
Two-Way ANOVA (Fig 4D)	F (12, 107) = 3.125 F (12, 107) = 53.52 F (1, 107) = 86.17	$P_I = 0.0008$ $P_t < 0.0001$ $P_d < 0.0001$	NCLS vs. Veh: > 0.9999 , > 0.9999 , > 0.9999 , > 0.9999 , 0.0541 , 0.0541 , 0.0002 , 0.0101 , 0.0006 , > 0.9999 , < 0.0001 , 0.0002 , 0.4612 .
Two-Way ANOVA (Fig 4E)	F (12, 107) = 3.826 F (12, 107) = 68.56 F (1, 107) = 81.94	$P_I < 0.0001$ $P_t < 0.0001$ $P_d < 0.0001$	NCLS vs. Veh: > 0.9999 , 0.1485 , > 0.9999 , > 0.9999 , 0.1546 , 0.0695 , 0.0045 , 0.0016 , 0.0016 , > 0.9999 , < 0.0001 , < 0.0001 , 0.3238 .
Two-Way ANOVA (Fig 4F)	F (12, 107) = 3.571 F (12, 107) = 71.54 F (1, 107) = 90.17	$P_I = 0.0002$ $P_t < 0.0001$ $P_d < 0.0001$	NCLS vs. Veh: > 0.9999 , 0.1952 , > 0.9999 , > 0.9999 , 0.0592 , 0.0592 , 0.0012 , 0.0012 , 0.0004 , > 0.9999 , 0.0001 , < 0.0001 , 0.1352 .

Table 4.1: Statistical test values given by figure number and panel

Two-Way ANOVA (Fig 5A)	F (12, 130) = 5.288 F (12, 130) = 65.61 F (1, 130) = 28.83	$P_I < 0.0001$ $P_t < 0.0001$ $P_d < 0.0001$	MK8722 vs. Veh: >0.9999, >0.9999, >0.9999, >0.9999, >0.9999, >0.9999, >0.9999, >0.9999, >0.9999, >0.9999, >0.9999, <0.0001, <0.0001.
Two-Way ANOVA (Fig 5B)	F (12, 130) = 3.887 F (12, 130) = 57.85 F (1, 130) = 20.69	$P_I < 0.0001$ $P_t < 0.0001$ $P_d < 0.0001$	MK8722 vs. Veh: >0.9999, >0.9999, >0.9999, >0.9999, >0.9999, >0.9999, >0.9999, >0.9999, >0.9999, 0.4261, >0.9999, <0.0001, <0.0001.
Two-Way ANOVA (Fig 5C)	F (12, 130) = 3.540 F (12, 130) = 64.53 F (1, 130) = 21.37	$P_I = 0.0001$ $P_t < 0.0001$ $P_d < 0.0001$	MK8722 vs. Veh: >0.9999, >0.9999, >0.9999, >0.9999, >0.9999, >0.9999, >0.9999, >0.9999, >0.9999, >0.9999, >0.9999, <0.0001, <0.0001.
Two-Way ANOVA (Fig 5D)	F (10, 110) = 3.052 F (10, 110) = 43.53 F (1, 110) = 2.572	$P_I = 0.0019$ $P_t < 0.0001$ $P_d = 0.1116$	MK8722 vs. Veh: >0.9999, >0.9999, >0.9999, >0.9999, >0.9999, >0.9999, >0.9999, >0.9999, 0.0050, 0.0102, 0.6392.
Two-Way ANOVA (Fig 5E)	F (10, 110) = 2.608 F (10, 110) = 41.98 F (1, 110) = 0.6676	$P_I = 0.0070$ $P_t < 0.0001$ $P_d = 0.4157$	MK8722 vs. Veh: >0.9999, >0.9999, >0.9999, >0.9999, >0.9999, >0.9999, >0.9999, >0.9999, 0.0491, 0.0148, 0.9272.
Two-Way ANOVA (Fig 5F)	F (10, 110) = 2.906 F (10, 110) = 41.14 F (1, 110) = 0.3700	$P_I = 0.0029$ $P_t < 0.0001$ $P_d = 0.5442$	MK8722 vs. Veh: >0.9999, >0.9999, >0.9999, >0.9999, >0.9999, >0.9999, >0.9999, >0.9999, 0.0143, 0.0447, 0.7628.
Two-Way ANOVA (Fig 6A)	F (13, 84) = 2.118 F (13, 84) = 83.14 F (1, 84) = 9.035	$P_I = 0.0210$ $P_t < 0.0001$ $P_d = 0.0035$	MK8722 vs. Veh: >0.9999, >0.9999, >0.9999, >0.9999, >0.9999,

Table 4.1: Statistical test values given by figure number and panel

			>0.9999, >0.9999, >0.9999, >0.9999, >0.9999, >0.9999, 0.0009, 0.0304, 0.2231.
Two-Way ANOVA (Fig 6B)	F (13, 84) = 4.009 F (13, 84) = 76.95 F (1, 84) = 8.930	P _I <0.0001 P _t <0.0001 P _d =0.0037	MK8722 vs. Veh: >0.9999, >0.9999, >0.9999, >0.9999, >0.9999, >0.9999, >0.9999, >0.9999, >0.9999, >0.9999, >0.9999, <0.0001, 0.0009, 0.0033.
Two-Way ANOVA (Fig 6C)	F (13, 84) = 3.729 F (13, 84) = 83.95 F (1, 84) = 13.70	P _I =0.0001 P _t <0.0001 P _d <0.0004	MK8722 vs. Veh: >0.9999, >0.9999, >0.9999, >0.9999, >0.9999, >0.9999, >0.9999, >0.9999, >0.9999, >0.9999, >0.9999, 0.0002, 0.0002, 0.0026.
Two-Way ANOVA (Fig 6D)	F (8, 54) = 5.910 F (8, 54) = 114.3 F (1, 54) = 13.71	P _I <0.0001 P _t <0.0001 P _d =0.0005	MK8722 vs. Veh: >0.9999, >0.9999, >0.9999, >0.9999, >0.9999, >0.9999, >0.9999, <0.0001, <0.0001.
Two-Way ANOVA (Fig 6E)	F (8, 54) = 6.832 F (8, 54) = 90.87 F (1, 54) = 14.51	P _I <0.0001 P _t <0.0001 P _d =0.0004	MK8722 vs. Veh: >0.9999, >0.9999, >0.9999, >0.9999, >0.9999, >0.9999, >0.9999, <0.0001, <0.0001.
Two-Way ANOVA (Fig 6F)	F (8, 54) = 6.828 F (8, 54) = 93.30 F (1, 54) = 17.48	P _I <0.0001 P _t <0.0001 P _d =0.0001	MK8722 vs. Veh: >0.9999, >0.9999, >0.9999, >0.9999, >0.9999, >0.9999, >0.9999, <0.0001, <0.0001.

CHAPTER 5

DISCUSSION

Sex differences observed with metformin in some but not all animal models

One of the first key findings of this study was the sexually dimorphic effects of metformin in the SNI and incision models. For male mice, metformin was effective in blocking hyperalgesic priming in the incision and paclitaxel models as well as preventing SNI-induced mechanical hypersensitivity. Metformin was not effective in females in the incision or SNI models in females. However, metformin was effective in both sexes in preventing (Mao-Ying, Kavelaars et al. 2014) CIPN as well as blocking hyperalgesic priming from paclitaxel-induced neuropathic pain. While the mechanistic explanations of these apparent divergent sex-specific effects are not sufficiently understood, several clinical trials with metformin for pain suggest that this drug can be effective in both male and female humans (El-Fatratry et al. 2018; Taylor et al. 2013; Kialka et al. 2016). This leads us to believe that the sex differences we are seeing with metformin could be an artifact of the mouse models we are using and/or a sex difference that is specific to mice.

Additionally, we used several different AMPK activators in this study and saw no sex differences with any compound other than metformin. Narciclasine, MK 8722 and ZLN 024 all produced behavioral effects in males that were identical to those in females. Other pain studies involving AMPK activators such as resveratrol used in females showed robust anti-hyperalgesic effects (Song et al. 2015; Zhu et al. 2017; Tao et al.

2016). This suggests that not only are the sex differences seemingly specific to particular pain models, they appear to be completely specific to metformin. There is an overwhelming amount of evidence showing AMPK activators to be effective in female mice (Calder et al. 2017; Galdieri et al. 2016; Chakrabarti et al. 2015) and humans (Petti et al. 2012).

Microglia activation linked to male chronic pain exclusively

Another key finding of this studying was confirmation that microglia play different roles in males and females in pain. In vitro, metformin caused an increase in phospho-ACC staining corresponding to AMPK activation in male and female DRG neurons as well as microglia. However, we saw a different result when in our in vivo metformin experiments. For males, there is a clear link between microglial activation given the reduction in the number of activated microglia in the ipsilateral dorsal horn in metformin treatment mice when compared to vehicle. Drugs that target and inhibit activated microglia such as minocycline have previously been shown to decrease mechanical hypersensitivity in male mice in the SNI (Sorge et al. 2015) and incision (Moriarty et al. 2019) models without having an effect on female pain. Meanwhile, T cells appear to play a more prominent role in pain in female mice (Sorge and Totsch 2017). While metformin caused a reduction in the amount of activated microglia in the dorsal horn of lumbar spinal cords of male SNI mice, we saw no reduction in the number of activated microglia in females. This supports the idea that activated microglia are crucial for mechanical hypersensitivity and cold allodynia experienced in surgery-induced neuropathy in males. The mechanisms that underlie the sex differences in immune cell

proliferation in response to pain have not yet been completely explained, particularly with respect to their dependence on genetic or hormonal causes, even if there seem to be no gender differences at the transcriptional level in genes related to nociception (Lopes et al. 2017)

Coupled with these findings is the previously mentioned effectiveness of metformin in the paclitaxel model. There is a well-established link between paclitaxel-induced neuropathy and CD8+ T cells (Krukowski et al. 2016) and the proliferation of the T cells is required for a resolution of CIPN (Laumet et al. 2019). Based on the results of our study, it can be assumed that metformin is capable of acting on T cells as well since the drug has shown to be capable of preventing CIPN (Mao-Ying, Kavelaars et al. 2014) and paclitaxel-induced hyperalgesic priming. While this does provide a potential explanation for metformin's effectiveness in the CIPN paclitaxel model, this does not sufficiently explain all of the results that we have presented here. Metformin was also effective in a preclinical model of myasthenia gravis, another pathology known for T cell dysfunction (Cui et al. 2019). In this study as well as our paclitaxel experiments, metformin was effective in female rodents. It has been well-established that T-cells play a larger role in the maintenance of hypersensitivity associated with chronic pain in females (Sorge et al. 2015). It would have been reasonable to hypothesize that metformin would produce an anti-hyperalgesic effect in females in the SNI and incision models if they are both T cell dependent given that metformin is effective in several models that also involve T cells (Kim et al. 2019; Kunisada et al. 2017). This was not the case. Our lack of a sufficient explanation for this observed phenomenon is a weakness of this study.

Suggestions for where to go with metformin now

At this point, we can confidently say that there is a sex difference between males and females following metformin treatment in the SNI and plantar incision model. This sex difference is absent in the paclitaxel model of CIPN. Metformin was able to prevent CIPN and block priming in this model. There currently exists an overwhelmingly large amount of preclinical work done with metformin in a wide variety of pain models from nerve injury (Melemedjian et al. 2011; Ge et al. 2018; Weng et al. 2019; Tao et al. 2016) to inflammatory pain (Russe et al. 2013; Pecikoza et al. 2017) in general with multiple showing its effectiveness in CIPN (Mao-Ying et al. 2014; Ling et al. 2017). These studies show that metformin can prevent CIPN when given concurrently with chemotherapy drugs (Mao-Ying, Kavelaars et al. 2014). Metformin also has not shown to be sex specific in humans. Metformin is effective in reducing the negative effects of type II diabetes in men and women (Knowler et al. 2002) is currently the most widely prescribed drug in the world. Several recent studies showing metformin's effectiveness for pain in humans that have also shown no sex specificity (El-Fataty et al. 2018; Kialka et al. 2016). Because metformin is safe and efficacious in reversing paclitaxel-induced neuropathy in both males and females, we believe our findings warrant further investigation of metformin as a drug for preventing the chronic aspects of CIPN in humans. The transition from preclinical rodent studies to clinical CIPN experiments in humans has already begun. In a recent study, colon cancer patients undergoing oxaliplatin, a chemotherapy drug known to induce CIPN (Cavaletti, Nicolini et al. 2008), saw a reduction in pain score in the metformin treated arm compared to the untreated

contralateral arm used as a control (El-Fatraty et al. 2018). While this supports our hypothesis that metformin could be a very effective drug for treating CIPN in humans, more experiments need to be done. However, enough work has been done with metformin in animal models related to pain that a move to clinical trials would be appropriate at this point.

Comparative effect direct and indirect AMPK activators in chronic pain models

Perhaps the most impactful finding of this study is that indirect AMPK activators are effective for acute as well as chronic aspects of pain. This was evident by narciclasine reducing and reversing mechanical hypersensitivity in both the incision model and the paclitaxel model while also blocking hyperalgesic priming in both models. Similar results have been seen with metformin (Burton et al. 2017; Inyang 2019) in the incision model. We have also seen indirect AMPK activator resveratrol (Dasgupta and Milbrandt, Shin, Cho et al. 2009) have acute effects in the incision model while also blocking hyperalgesic priming (Tillu et al. 2012). It is possible that the upstream targets like LKB1 for metformin (Shaw et al. 2005) and resveratrol (Hu and Liu 2016) or potentially cAMP for narciclasine (Hu et al. 2015; Julien SG 2017) according to existing literature also need to be activated for an acute anti-hyperalgesic effect to be seen. While the current literature lists cAMP as the direct target of narciclasine upstream of AMPK, we do not believe that is the case as we detail later in this chapter.

Contrastingly, the direct AMPK activators we have used have shown a consistent ability to block PGE2 -induced hyperalgesic priming without producing acute analgesic effects.

These drugs like ZLN-024 (Zhang, Zhou et al. 2009) and MK-8722 (Feng et al. 2018; Weihrauch and Handschin 2018) are very specific to and directly modulate AMPK. Activating AMPK directly does not appear to be sufficient to have an acute analgesic effect in pain models. This is likely due to the dependence of these compounds on the presence of phospho-AMPK to work. We have shown that injury, specifically incision causes a decrease in p-AMPK in sensory neurons. Activating AMPK using positive allosteric modulators and the resulting translation inhibition does seem to be enough to prevent the chronic aspects of pain. This is not ideal for an analgesic since most people expect an acute analgesic effect when taking such a drug. While acute anti-hyperalgesic effects are not seen with positive allosteric modulators, there is evidence that they are capable of having acute effects on inflammation. A769662 is a direct AMPK activator that has been shown to have anti-inflammatory effects against lipopolysaccharide (LPS) -induced (Rameshrad et al. 2016) as well as inflammatory aspects of arthritis (Guma, Wang et al. 2015).

While direct AMPK activators do not seem to have acute in models of pain, these compounds have shown to be robustly effective in other preclinical models. MK8722 was used in a rat model of diabetic nephropathy where it produced an improvement in renal function (Zhou et al. 2019) which is similar to what has been seen in with metformin (Zhang L 2019). ZLN-024 also has been shown to have acute AMPK related effects in vitro. At a dose of 15 mg/kg, ZLN-024 caused a significant decrease in total cholesterol while improving glucose tolerance (Zhang, Xu et al. 2013). As a diabetes drug, metformin also has a history of being used to improve glucose tolerance

(Numbenjapon et al. 2010; Hostalek, Gwilt, and Hildemann 2015). Metformin's ability to combat diabetes and regulate glucose has been long attributed to its AMPK related activity (Zhou et al. 2001). Since MK8722 and ZLN-024 are pharmacologically distinct from metformin other than their collective abilities activate AMPK, it is safe to assume that their impact on diabetes symptoms are AMPK related and that all of these drugs are capable of activating AMPK acutely. The inability of direct AMPK activators to sufficiently increase the concentration of pAMPK appears to be specific to pain states resulting in no acute anti-hyperalgesia.

What we now understand about why direct AMPK activators are unlikely to be the best drugs to use

Similar results have been seen with other drugs that have been able to block hyperalgesic priming without having an acute effect (Asiedu et al. 2011; Price and Inyang 2015). This leads us to believe that directly activating AMPK is not sufficient to produce short term analgesia. Our current explanation for this behavioral difference we saw between the indirect AMPK activators and positive allosteric modulators is the decrease in pAMPK in the DRG observed in the incision model (Inyang et al. 2019) as well as following diabetic neuropathy models (Atef et al. 2019). Positive allosteric modulators of AMPK are thought to rely on the presence of phosphorylated AMPK to increase subsequent AMPK activity. It is reasonable to conclude that an injury-induced decrease in the amount of pAMPK would likely cause a decrease efficacy in drugs reliant on the presence of pAMPK. The only incidence of a positive allosteric modulator having an acute effect is A769662 in the Hargreaves model for thermal sensitivity at a

very high dose and only for a short amount of time (Asiedu, Han et al. 2017). This is not an issue for indirect AMPK activators since they produce an increase in pAMPK through upstream targets that combats the decrease in pAMPK caused by the injury (Melemedjian et al. 2011). While a block in the chronic aspects of pain is beneficial, the inability for direct AMPK activators to illicit an acute effect makes them inferior to indirect AMPK activators.

It may be possible to create a direct AMPK activator that has dual action on a kinase upstream of AMPK like LKB1 that could potentially have some sort of acute analgesic effect. If it were possible to create drugs like this, valuable information could be gained about the details of the mechanism. If a compound like this could be produced, we might be able to learn if AMPK activation is necessary but not sufficient to decrease pain, and if an increase in other kinases is required for a full disease modifying effect.

Narciclasine is robustly effective in several pain models in both sexes

One of the most significant findings of this study is the effectiveness of narciclasine in several different animal pain models in both sexes. NCLS prevented mechanical hypersensitivity in both the incision and paclitaxel model and was able to block hyperalgesic priming. NCLS has previously been established as an AMPK activator (Julien SG 2017; Cao et al. 2018) and a drug capable of reversing inflammation (Lubahn et al. 2012; Stark et al. 2019). Here we show that it is capable of functioning as an anti-hyperalgesic with a similar level of efficacy as metformin. In addition to a lack of sex specificity, NCLS is also effective at much lower doses than metformin. We saw

anti-hyperalgesic effects with as low as 1 mg/kg in males and females with NCLS compared to 200 mg/kg with metformin under an identical time course (Inyang 2019). The key behavioral difference between narciclasine and positive allosteric modulators is that narciclasine caused an acute decrease in mechanical hypersensitivity within a few days of treatment in addition to blocking hyperalgesic priming. Prior to these studies very little had been done with narciclasine in pain despite its ability to activate AMPK and reduce inflammation.

What is narciclasine and what is its pharmacological history

Narciclasine is a natural compound named for the plant genus Amaryllidaceous narcissus which includes the daffodil (Furst 2016). The compound was first isolated in 1967 as part of a project looking for antigrowth factors (Ceriotti 1967) and the structure of the molecule was determined a few years later (Immirizi A 1972). Earliest uses of narciclasine were for preclinical anti-tumor studies due to its ability to block protein synthesis and mitotic activity (Ceriotti 1967). High doses of have been shown to cause apoptotic cancer cell death via activation of the Fas and death receptor 4 (DR4) death-inducing complex (Asiedu, Han et al. 2017) and the subsequent recruitment of caspase-8 (Dumont et al. 2007). Lower doses have been shown to impair tumor cell growth without causing cell death (Lefranc, Sauvage et al. 2009). Following a period without very many published papers related to narciclasine outside of a study showing the drug's anti-viral capabilities at high doses (Gabrielsen, Monath et al. 1992), the compound seemed to reemerge in the late 1990s. In 1999, narciclasine was first shown to decrease paw swelling in a model of rat arthritis as well as causing a suppression of

the inflammatory cytokine tumor necrosis factor alpha (TNF α) (Mikami et al. 1999). Following this study, subsequent studies showed the ability of narciclasine and derivative compounds to inhibit pro-inflammatory cytokines (Lubahn et al. 2012; Fuchs et al. 2015). More recently, narciclasine was determined to be an AMPK activator (Julien SG 2017; Cao et al. 2018) which led to our initial interest in the compound for pain. Narciclasine has also been shown to be able to counter obesity (Julien, Kim et al. 2017) which is similar to what has previously been seen with metformin (Seifarth, Schehler, and Schneider 2013; Yerevanian and Soukas 2019; Mead et al. 2016).

There are many advantages of narciclasine over many of the other AMPK activators that we have used in the past. In addition to be effective in models that the other drugs are not effective in, NCLS is effective at low doses compared to other AMPK activators. Table 5.1 compares the efficacy of NCLS to other AMPK activators in the incision model. NCLS is a plant-based compound that can be isolated rather than synthesized (Ceriotti 1967). Natural compounds provide a solid starting point for pharmaceutical chemists attempting to optimize compounds for future analgesics. If subsequent AMPK activators were to be created, NCLS would be a good molecule to start with and improve from since it is a molecule that is already known to work and is potent. Another key positive aspect of NCLS is its ability to produce a strong effect on AMPK when given orally without effecting AMPK activation in the liver (Julien SG 2017). Narciclasine only activating AMPK in specific tissues has strong positive implications on the potential safety of the drug.

How we think narciclasine actually works

As with most natural compounds, the exact mechanism of action for narciclasine is not fully understood. We know that it is an AMPK activator, but it is unknown what the direct target of the compound is, what the off-target effects are, and if AMPK activation is what causes the observed analgesic effects. Current literature suggests that narciclasine activates AMPK through the activation of cAMP (Julien SG 2017). While we do not doubt that narciclasine may influence cAMP, we do not believe that this is what is causing AMPK activation and the subsequent analgesic effects. Activation of cAMP results in the activation of cAMP-dependent protein kinase or protein kinase A (PKA) (Pierce, Premont et al. 2002). The implications of this kinase are well known. PKA plays a significant role in the establishment (Taiwo et al. 1989; Taiwo and Levine 1990; England, Bevan, and Docherty 1996) and maintenance of inflammatory pain (Aley and Levine 1999), so it would be unlikely for a drug to decrease mechanical hypersensitivity if increasing cAMP and PKA is its main mechanistic effects.

One potential target for narciclasine is Ca (2+)/calmodulin-dependent protein kinase kinase β (CaMKK β). CaMKK is a serine/threonine-directed kinase that is activated following increases in intracellular Ca²⁺ and exists in isoforms, CaMKK α and CaMKK β (Green et al. 2011). Previous studies have shown that LKB1 and CaMKK β are 2 of the main upstream kinases of phosphorylating AMPK (Kahn et al. 2005). It is known which one of these kinases could be directly related to narciclasine's activation of AMPK. This could be investigated through multiple experiments. One useful experiment would involve the use of transgenic mice. Our lab previously possessed mice with the gene for CaMKK β knocked out. These mice could be treated with narciclasine in the incision

model as previously done with naïve ICR mice. If there is an anti-hyperalgesic effect from narciclasine in the CaMKK β -knockout mice, that would eliminate CaMKK β as an upstream target for narciclasine. Another set of experiments that could elucidate the potential mechanism of narciclasine's AMPK related activity is using western blotting. Proteins taken from NCLS-treated DRG neuron cultures could be stained with CaMKK β and LKB1 antibodies as well as a pAMPK antibody see NCLS has an effect on either of these upstream kinases.

The future of narciclasine in pain (where do we go from here?)

This study provides interesting insight into the direction of future AMPK drug development. Based on our results, it appears that indirect AMPK activators are generally more effective than positive allosteric modulators. It would make the most sense to model future compounds after those. Narciclasine lacks the sex specificity in the incision model that is seen in metformin, so a drug that more closely resembles narciclasine would be more ideal. There are a few things that need to be more thoroughly investigated before narciclasine can truly replace metformin as the most commonly used AMPK activator of the pain field. First, the mechanisms of action for narciclasine is not fully understood as it relates to AMPK and translation control of pain (Cao et al. 2018). A greater understanding of some of narciclasine's off-target effects and how they might relate to pain resolution would be crucial to understanding the drug and effective ways to simultaneously prevent the acute and chronic aspects of pain. This could be investigated using genetic models. For example, the action of metformin and similar drugs are blocked by an inactivation of LKB1 (Shackelford, Abt et al. 2013).

If metformin and narciclasine were given side by side in a behavioral experiment in LKB1 knockout mice and only narciclasine was effective, it would provide insight into the role of LKB1 in chronic pain prevention as well as show that narciclasine is LKB1-independent.

Metformin has been used safely and proven to be effective in a wide range of pain models as show Table 1.1 in the introductory chapter. Most notably, metformin has been shown to reduce mechanical hypersensitivity in the models of neuropathic pain from nerve injury such as spared nerve injury (Myers et al.) (Melemedjian et al. 2011), chronic constriction injury (Kola et al.) (Augusto et al. 2019) and spared nerve ligation (SNL) (Weng et al. 2019). Whether narciclasine can match metformin's efficacy in these models is unknown and leaves a sizeable hole in our knowledge of the compound effectiveness as a potential analgesic. Our preliminary data with narciclasine in the SNI model showed no significant reduction in mechanic hypersensitivity but a significant reduction in cold allodynia in response to acetone. More experiments need to be done with narciclasine in nerve injury models (**Fig 5.1**). It is possible that the dose of narciclasine used in our preliminary experiments (3 mg/kg) was too low. In the incision model, we saw narciclasine to be safe and effective at 6 mg/kg. Given that a lower dose of narciclasine was able to reverse cold allodynia, we hypothesize that 7 days of narciclasine at 6 mg/kg will cause a decrease in SNI-induced mechanical hypersensitivity in both male and female mice. A similar reduction in mechanical hypersensitivity should correspond with a decrease in activated microglia. We also

hypothesize that narciclasine would be effective in reducing hypersensitivity in the SNL and CCI models as well in both sexes.

Another set of experiments that would benefit AMPK research would be ones that optimize the synthesis of narciclasine. NCLS was initially isolated in 1967 from *Narcissus* bulbs (Ceriotti 1967) but the first synthesis was not successfully performed until 1997 (Rigby J 1997). Current methods of synthesis are multi-stepped and do not provide particularly high yields (Ghavre et al. 2016). This likely contributes the high cost of the compound. Currently, 1 mg of the compound costs about \$150 which is somewhat prohibitive for in vivo studies even at small doses. Finding more efficient ways to synthesize the compound should help decrease this cost and increase the amount of work that could be done with narciclasine. Refining the synthesis process could not only make the drug more affordable but also lead to more derivative drugs. While narciclasine is a modestly soluble drug (Weniger et al. 1995), derivatives like sodium narcistatin have been created to be more water soluble (Pettit et al. 2003). Sodium narcistatin (SNS) is structurally similar to narciclasine but it has been made more water soluble due to the addition of a cyclic phosphate group (Pettit et al. 2003). SNS has already been used preclinically to combat inflammation in models of arthritis (Lubahn et al. 2012) which is a model that narciclasine was also effective in (Mikami et al. 1999). One potential difference between narciclasine and SNS is potency. A slightly higher dose SNS was required to produce an anti-inflammatory response (Stark et al. 2019; Lubahn et al. 2012). A decrease in potency has been a recurring theme in the development of narciclasine-like drugs. Natural enantiomers, or mirror image molecule,

of narciclasine have a similar level of efficacy to the original molecule while synthetic versions of the enantiomer was very weakly active (Matveenko et al. 2009). While both are effective in combating inflammation, it would be ideal to produce a narciclasine-derived drug that is water soluble but is as potent as narciclasine. A better understanding of narciclasine's synthesis could lead to more derivatives with increased solubility and potentially greater AMPK specificity.

Additionally, some experiments exploring potential synergistic or additive effects of narciclasine and exercise could be beneficial for the understanding of AMPK activation in pain. AMPK can be activated in many non-pharmacological ways most notably through exercise. Exercise leads to an increase in ATP consumption and intracellular AMP resulting in the activation of AMPK in a time-dependent manner in rodents (Winder and Hardie 1996) as well as humans (Wojtaszewski et al. 2000). In addition to activating AMPK, exercise has been shown to have analgesic effects as well as reverse inflammation and reverse microglial activation (Mee-Inta, Zhao et al. 2019) similar to what we have shown with pharmacological activators of AMPK. It is unclear how these two distinct forms of AMPK activation impact each other. Potential future experiments include repeating some of the previous performed pain experiments with narciclasine with an exercise task added. For example, 1 mg/kg NCLS was shown to have a preventative effect against paclitaxel-induced neuropathy. This experiment could be repeated with additional treatment groups doing an exercise task with and without NCLS treatment. There exists data suggesting that AICAR has a small, non-significant analgesic effect on mice in conjunction with treadmill running when compared to mice

that only exercised (King-Himmelreich, Moser et al. 2017). Contrastingly, a clinical study with prediabetic men and women showed that metformin somewhat dampened the effect of exercise training on insulin sensitivity (Malin et al. 2012) casting some doubt in whether we would see synergy in a preclinical pain study. This could be due to increased incidence of lactic acidosis which is a side effect of metformin treatment (Bruijstens et al. 2008; Salpeter et al. 2010; Asif, Bennett, and Marakkath 2019) which is not known to be a side effect of narciclasine. Lactic acidosis is a buildup of lactic acid in the bloodstream and is known to cause a decrease in athletic performance (Robergs, Ghasvand et al. 2004) and increase in fatigue (Cairns 2006). A decrease in athletic performance caused by metformin is likely causing an impairment in exercise-induced AMPK activation. Nevertheless, we hypothesize that this will have an additive and possibly synergistic AMPK activation effect and increased analgesia with AMPK activators other than metformin.

What we've learned about AMPK activators in pain

In conclusion, AMPK activators inhibit eIF4F-dependent translation causing a decrease in mechanical hypersensitivity in the SNI, incision, and paclitaxel-induced neuropathy models and cold allodynia in the SNI model. Metformin specifically caused a reduction in nerve injury-induced microglial activation in males. While metformin appears to have some sex specific effects in the SNI and incisional pain models but not paclitaxel-induced neuropathy, other AMPK activators that we used have shown no signs of sex-specificity. Metformin also produced a sex-specific decrease in microglial response to neuropathic pain supporting the notion that microglia play differing roles in the

maintenance of male and female pain. Additionally, while we saw that all the AMPK activators that we used were able to block chronic aspects of pain indicated through a block in hyperalgesic priming, only indirect upstream AMPK activators showed an ability to acutely decrease mechanical hypersensitivity. Of the indirect AMPK activators used, narciclasine's ability to reverse mechanical hypersensitivity in the paclitaxel model of chemotherapy-induced peripheral neuropathy, apparent complete lack of sex specificity and its effectiveness at a comparatively low dose sets it apart from metformin. While the future of AMPK activators as analgesics has not fully explored and understood, narciclasine shows particular promise as a compound for potential clinical use moving forward.

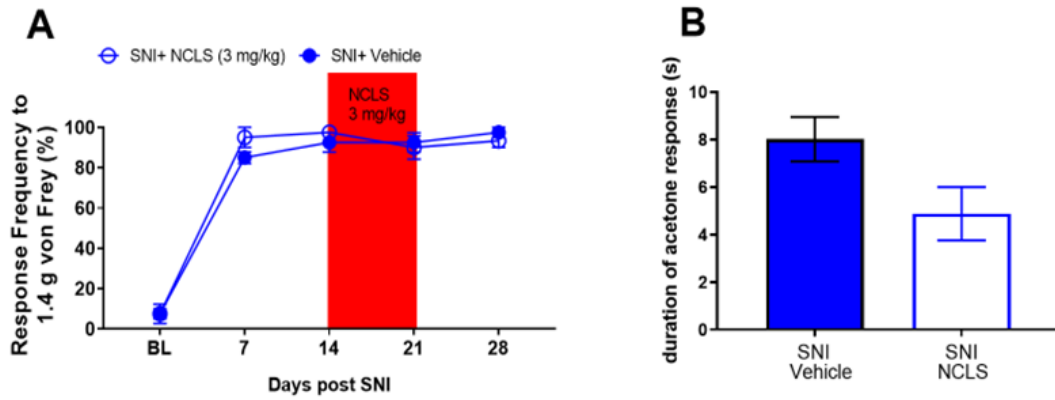


Figure 5.1: Narciclasine reduced SNI-induced cold allodynia. Two weeks post-SNI, 7-day narciclasine treatment failed to reduce mechanical hypersensitivity (A) but caused a reduction in cold allodynia (B).

Table 5.1. Systemic AMPK activators in the incision model

Drug	Dose	Acute effect?	Priming blocked?
Metformin (Burton, Tillu et al. 2017)	200 mg/kg	Yes (in males)	Yes (in males)
Narciclasine	3 mg/kg	Yes	Yes
ZLN-024	30 mg/kg	No	Yes
MK 8722	30 mg/kg	No	Yes
R419 (Mejia, Asiedu et al. 2016)	20 mg/kg	Yes	No

BIBLIOGRAPHY

- Afshari, K., A. Dehdashtian, N. S. Haddadi, A. Haj-Mirzaian, A. Iranmehr, M. A. Ebrahimi, S. M. Tavangar, H. Faghir-Ghanesefat, F. Mohammadi, N. Rahimi, A. N. Javidan and A. R. Dehpour (2018). "Anti-inflammatory effects of Metformin improve the neuropathic pain and locomotor activity in spinal cord injured rats: introduction of an alternative therapy." Spinal Cord **56**(11): 1032-1041.
- Aley, K. O. and J. D. Levine (1999). "Role of protein kinase A in the maintenance of inflammatory pain." J Neurosci **19**(6): 2181-2186.
- Areti, A., P. Komirishetty, A. K. Kalvala, K. Nellaiappan and A. Kumar (2018). "Rosmarinic Acid Mitigates Mitochondrial Dysfunction and Spinal Glial Activation in Oxaliplatin-induced Peripheral Neuropathy." Mol Neurobiol **55**(9): 7463-7475.
- Asiedu, M. N., C. Han, S. D. Dib-Hajj, S. G. Waxman, T. J. Price and G. Dussor (2017). "The AMPK Activator A769662 Blocks Voltage-Gated Sodium Channels: Discovery of a Novel Pharmacophore with Potential Utility for Analgesic Development." PLoS One **12**(1): e0169882.
- Asiedu, M. N., D. V. Tillu, O. K. Melemedjian, A. Shy, R. Sanoja, B. Bodell, S. Ghosh, F. Porreca and T. J. Price (2011). "Spinal Protein Kinase M ζ Underlies the Maintenance Mechanism of Persistent Nociceptive Sensitization." The Journal of Neuroscience **31**(18): 6646-6653.
- Atef, M. M., N. M. El-Sayed, A. A. M. Ahmed and Y. M. Mostafa (2018). "Donepezil improves neuropathy through activation of AMPK signalling pathway in streptozotocin-induced diabetic mice." Biochem Pharmacol.
- Atef, M. M., N. M. El-Sayed, A. A. M. Ahmed and Y. M. Mostafa (2019). "Donepezil improves neuropathy through activation of AMPK signalling pathway in streptozotocin-induced diabetic mice." Biochem Pharmacol **159**: 1-10.
- Augusto, P. S. A., A. V. Braga, F. F. Rodrigues, M. I. Morais, M. Dutra, C. R. A. Batista, I. S. F. Melo, S. Costa, F. A. Goulart, M. M. Coelho and R. R. Machado (2019). "Metformin antinociceptive effect in models of nociceptive and neuropathic pain is partially mediated by activation of opioidergic mechanisms." Eur J Pharmacol **858**: 172497.
- Banik, R. K., A. R. Subieta, C. Wu and T. J. Brennan (2005). "Increased nerve growth factor after rat plantar incision contributes to guarding behavior and heat hyperalgesia." Pain **117**(1): 68-76.
- Banik RK, W. Y., Park SS, Brennan TJ. (2006). "Strain and sex influence on pain sensitivity after plantar incision in the mouse." Anesthesiology **105**(6): 1246-1253.

- Barragan-Iglesias, P., V. H. Oidor-Chan, E. Loeza-Alcocer, J. B. Pineda-Farias, I. Velazquez-Lagunas, A. B. Salinas-Abarca, E. Hong, A. Sanchez-Mendoza, R. Delgado-Lezama, T. J. Price and V. Granados-Soto (2018). "Evaluation of the neonatal streptozotocin model of diabetes in rats: Evidence for a model of neuropathic pain." Pharmacol Rep **70**(2): 294-303.
- Bennett, G. J. and Y. K. Xie (1988). "A peripheral mononeuropathy in rat that produces disorders of pain sensation like those seen in man." Pain **33**(1): 87-107.
- Boerner, K. E., K. A. Birnie, L. Caes, M. Schinkel and C. T. Chambers (2014). "Sex differences in experimental pain among healthy children: a systematic review and meta-analysis." Pain **155**(5): 983-993.
- Bonica, J. J. and J. F. Hoffman (1954). "The Management of Pain with Special Emphasis on the Use of Analgesic Blocks in Diagnosis, Prognosis, and Therapy." Anesthesia & Analgesia **34**(5): 57-58.
- Brown, T. J., R. Sedhom and A. Gupta (2019). "Chemotherapy-Induced Peripheral Neuropathy." JAMA Oncol.
- Bullón P, A.-G. E., Carrión AM, Marín-Aguilar F, Garrido-Maraver J, Román-Malo L, Ruiz-Cabello J, Culic O, Ryffel B, Apetoh L, Ghiringhelli F, Battino M, Sánchez-Alcazar JA, Cordero MD (2016). "AMPK Phosphorylation Modulates Pain by Activation of NLRP3 Inflammasome." Antioxid Redox Signal **24**(3): 157-170.
- Burkewitz, K., Y. Zhang and W. B. Mair (2014). "AMPK at the nexus of energetics and aging." Cell Metab **20**(1): 10-25.
- Burton, M. D., D. V. Tillu, K. Mazhar, G. L. Mejia, M. N. Asiedu, K. Inyang, T. Hughes, B. Lian, G. Dussor and T. J. Price (2017). "Pharmacological activation of AMPK inhibits incision-evoked mechanical hypersensitivity and the development of hyperalgesic priming in mice." Neuroscience **359**: 119-129.
- Cairns, S. P. (2006). "Lactic acid and exercise performance : culprit or friend?" Sports Med **36**(4): 279-291.
- Cao, C., W. Huang, N. Zhang, F. Wu, T. Xu, X. Pan, C. Peng and B. Han (2018). "Narciclasine induces autophagy-dependent apoptosis in triple-negative breast cancer cells by regulating the AMPK-ULK1 axis." Cell Prolif **51**(6): e12518.
- Cavaletti, G., G. Nicolini and P. Marmiroli (2008). "Neurotoxic effects of antineoplastic drugs: the lesson of pre-clinical studies." Front Biosci **13**: 3506-3524.
- Cerioti, G. (1967). "Narciclasine: an antimetabolic substance from Narcissus bulbs." Nature **213**(5076): 595-596.
- Clauw, D. J. (2015). "Fibromyalgia and related conditions." Mayo Clin Proc **90**(5): 680-692.

- Clayton, J. A. and F. S. Collins (2014). "Policy: NIH to balance sex in cell and animal studies." Nature **509**(7500): 282-283.
- Colvin, L. A. (2019). "Chemotherapy-induced peripheral neuropathy: where are we now?" Pain **160 Suppl 1**: S1-s10.
- Corder, G., S. Doolen, R. R. Donahue, M. K. Winter, B. L. Jutras, Y. He, X. Hu, J. S. Wieskopf, J. S. Mogil, D. R. Storm, Z. J. Wang, K. E. McCaeson and B. K. Taylor (2013). "Constitutive mu-opioid receptor activity leads to long-term endogenous analgesia and dependence." Science **341**(6152): 1394-1399.
- Cusi, K., A. Consoli and R. A. DeFronzo (1996). "Metabolic effects of metformin on glucose and lactate metabolism in noninsulin-dependent diabetes mellitus." J Clin Endocrinol Metab **81**(11): 4059-4067.
- Dart, R. C., S. G. Severtson and B. Bucher-Bartelson (2015). "Trends in opioid analgesic abuse and mortality in the United States." N Engl J Med **372**(16): 1573-1574.
- Das, V., J. S. Kroin, M. Moric, R. J. McCarthy and A. Buvanendran (2019). "Antihyperalgesia effect of AMP-activated protein kinase (AMPK) activators in a mouse model of postoperative pain." Reg Anesth Pain Med.
- Dasgupta, B. and J. Milbrandt (2007). "Resveratrol stimulates AMP kinase activity in neurons." Proc Natl Acad Sci U S A **104**(17): 7217-7222.
- Decosterd, C. J. W. (2000). "Spared nerve injury: an animal model of persistent peripheral neuropathic pain." Pain(87): 149-158.
- Decosterd, I. and C. J. Woolf (2000). "Spared nerve injury: an animal model of persistent peripheral neuropathic pain." Pain **87**(2): 149-158.
- Dina, O. A., P. G. Green and J. D. Levine (2008). "Role of interleukin-6 in chronic muscle hyperalgesic priming." Neuroscience **152**(2): 521-525.
- Dorn, S. D., P. D. Meek and N. D. Shah (2011). "Increasing frequency of opioid prescriptions for chronic abdominal pain in US outpatient clinics." Clin Gastroenterol Hepatol **9**(12): 1078-1085.e1071.
- Dumont, P., L. Ingrassia, S. Rouzeau, F. Ribaucour, S. Thomas, I. Roland, F. Darro, F. Lefranc and R. Kiss (2007). "The Amaryllidaceae isocarboxystiril narciclasine induces apoptosis by activation of the death receptor and/or mitochondrial pathways in cancer cells but not in normal fibroblasts." Neoplasia **9**(9): 766-776.
- El-Fataty, B. M., O. M. Ibrahim, F. Z. Hussien and T. M. Mostafa (2018). "Role of metformin in oxaliplatin-induced peripheral neuropathy in patients with stage III colorectal cancer: randomized, controlled study." Int J Colorectal Dis **33**(12): 1675-1683.

- England, S., S. Bevan and R. J. Docherty (1996). "PGE2 modulates the tetrodotoxin-resistant sodium current in neonatal rat dorsal root ganglion neurones via the cyclic AMP-protein kinase A cascade." J Physiol **495 (Pt 2)**: 429-440.
- Ewertz, M., C. Qvortrup and L. Eckhoff (2015). "Chemotherapy-induced peripheral neuropathy in patients treated with taxanes and platinum derivatives." Acta Oncol **54(5)**: 587-591.
- Feng, D., T. Biftu, F. A. Romero, A. Kekec, J. Dropinski, A. Kassick, S. Xu, M. M. Kurtz, A. Gollapudi, Q. Shao, X. Yang, K. Lu, G. Zhou, D. Kemp, R. W. Myers, H. P. Guan, M. E. Trujillo, C. Li, A. Weber and I. K. Sebat (2018). "Discovery of MK-8722: A Systemic, Direct Pan-Activator of AMP-Activated Protein Kinase." ACS Med Chem Lett **9(1)**: 39-44.
- Finnerup NB, A. N., Haroutounian S, McNicol E, Baron R, Dworkin RH, Gilron I, Haanpää M, Hansson P, Jensen TS, Kamerman PR, Lund K, Moore A, Raja SN, Rice AS, Rowbotham M, Sena E, Siddall P, Smith BH, Wallace M (2015). "Pharmacotherapy for neuropathic pain in adults: a systematic review and meta-analysis." Lancet Neurol **14(2)**: 162-173.
- Furst, R. (2016). "Narciclasine - an Amaryllidaceae Alkaloid with Potent Antitumor and Anti-Inflammatory Properties." Planta Med **82(16)**: 1389-1394.
- Gabrielsen, B., T. P. Monath, J. W. Huggins, D. F. Kefauver, G. R. Pettit, G. Groszek, M. Hollingshead, J. J. Kirsi, W. M. Shannon, E. M. Schubert and et al. (1992). "Antiviral (RNA) activity of selected Amaryllidaceae isoquinoline constituents and synthesis of related substances." J Nat Prod **55(11)**: 1569-1581.
- Ge, A., S. Wang, B. Miao and M. Yan (2018). "Effects of metformin on the expression of AMPK and STAT3 in the spinal dorsal horn of rats with neuropathic pain." Mol Med Rep **17(4)**: 5229-5237.
- Gilron, I., R. Baron and T. Jensen (2015). "Neuropathic pain: principles of diagnosis and treatment." Mayo Clin Proc **90(4)**: 532-545.
- Goode, A. P., R. R. Coeytaux, J. McDuffie, W. Duan-Porter, P. Sharma, H. Mennella, A. Nagi and J. W. Williams, Jr. (2016). "An evidence map of yoga for low back pain." Complement Ther Med **25**: 170-177.
- Grossman, C. J., G. A. Roselle and C. L. Mendenhall (1991). "Sex steroid regulation of autoimmunity." J Steroid Biochem Mol Biol **40(4-6)**: 649-659.
- Gui, Y., L. Chen, S. Duan, G. Li, J. Tang and A. Li (2018). "Methyl cinnamate alleviated CCI-induced upregulation of spinal AMPA receptors and pain hypersensitivity by targeting AMPK." Eur J Pharmacol **833**: 183-189.
- Gui, Y., A. Li, F. Chen, H. Zhou, Y. Tang, L. Chen, S. Chen and S. Duan (2015). "Involvement of AMPK/SIRT1 pathway in anti-allodynic effect of troxerutin in CCI-induced neuropathic pain." Eur J Pharmacol **769**: 234-241.

- Guma, M., Y. Wang, B. Viollet and R. Liu-Bryan (2015). "AMPK Activation by A-769662 Controls IL-6 Expression in Inflammatory Arthritis." PLoS One **10**(10): e0140452.
- Guo, X., X. Tao, Q. Tong, T. Li, D. Dong, B. Zhang, M. Zhao and T. Song (2019). "Impaired AMPKCGRP signaling in the central nervous system contributes to enhanced neuropathic pain in highfat dietinduced obese rats, with or without nerve injury." Mol Med Rep **20**(2): 1279-1287.
- Hardie (2007). "AMP-activated/SNF1 protein kinases: conserved guardians of cellular energy." Nature Reviews Molecular Cell Biology **8**: 774-785.
- Hardie, D. G., F. A. Ross and S. A. Hawley (2012). "AMPK: a nutrient and energy sensor that maintains energy homeostasis." Nat Rev Mol Cell Biol **13**(4): 251-262.
- Haroutiunian S, N. L., Finnerup NB, Jensen TS (2013). "The neuropathic component in persistent postsurgical pain: a systematic literature review." Pain **154**: 95-102.
- Hayter, S. M. and M. C. Cook (2012). "Updated assessment of the prevalence, spectrum and case definition of autoimmune disease." Autoimmun Rev **11**(10): 754-765.
- Hu, M. and B. Liu (2016). "Resveratrol via activation of LKB1-AMPK signaling suppresses oxidative stress to prevent endothelial dysfunction in diabetic mice." Clin Exp Hypertens **38**(4): 381-387.
- Hu, Y., X. Na, J. Li, L. Yang, J. You, X. Liang, J. Wang, L. Peng and Y. Bi (2015). "Narciclasine, a potential allelochemical, affects subcellular trafficking of auxin transporter proteins and actin cytoskeleton dynamics in Arabidopsis roots." Planta **242**(6): 1349-1360.
- Hylands-White, N., R. V. Duarte and J. H. Raphael (2017). "An overview of treatment approaches for chronic pain management." Rheumatology International **37**(1): 29-42.
- Ikhlas, S. and M. Ahmad (2017). "Metformin: Insights into its anticancer potential with special reference to AMPK dependent and independent pathways." Life Sci **185**: 53-62.
- Immirizi A, F. C. (1972). "The crystal and molecular structure of narciclasine tetra-acetate." J Chem Soc Chem Commun **4**(240).
- Institute of Medicine Committee on Advancing Pain Research, C. and Education (2011). The National Academies Collection: Reports funded by National Institutes of Health. Relieving Pain in America: A Blueprint for Transforming Prevention, Care, Education, and Research. Washington (DC), National Academies Press (US)
- National Academy of Sciences.
- Inyang, K., M. D. Burton, T. Szabo-Pardi, E. Wentworth, T. A. McDougal, E. D. Ramirez, G. Pradhan, G. Dussor and T. Price (2019). "Indirect AMPK activators prevent incision-induced hyperalgesia and block hyperalgesic priming while positive allosteric modulators only block priming in mice." J Pharmacol Exp Ther.

- Inyang, K., Burton, Michael D, Szabo-Pardi, Thomas, Wentworth, Emma, McDougal, Timothy A, Ramirez, Eric D, Pradhan, Grishma, Dussor, Gregory, Price, Theodore (2019). "Indirect AMPK activators prevent incision-induced hyperalgesia and block hyperalgesic priming while positive allosteric modulators only block priming in mice." Journal of Pharmacology and Experimental Therapeutics: jpet.119.258400.
- Inyang, K. E., T. Szabo-Pardi, E. Wentworth, T. A. McDougal, G. Dussor, M. D. Burton and T. J. Price (2018). "The antidiabetic drug metformin prevents and reverses neuropathic pain and spinal cord microglial activation in male but not female mice." Pharmacol Res **139**: 1-16.
- Izycki, D., A. Niezgoda, M. Kazmierczak and E. Nowak-Markwitz (2016). "Chemotherapy-induced peripheral neuropathy - epidemiology and pathogenesis." Ginekol Pol **87**(4): 293-299.
- Jimenez-Diaz, L., S. M. Geranton, G. M. Passmore, J. L. Leith, A. S. Fisher, L. Berliocchi, A. K. Sivasubramaniam, A. Sheasby, B. M. Lumb and S. P. Hunt (2008). "Local translation in primary afferent fibers regulates nociception." PLoS One **3**(4): e1961.
- Julien, S. G., S. Y. Kim, R. Brunmeir, J. R. Sinnakannu, X. Ge, H. Li, W. Ma, J. Yaligar, B. P. Kn, S. S. Velan, P. V. Roder, Q. Zhang, C. K. Sim, J. Wu, M. Garcia-Miralles, M. A. Pouladi, W. Xie, C. McFarlane, W. Han and F. Xu (2017). "Narciclasine attenuates diet-induced obesity by promoting oxidative metabolism in skeletal muscle." PLoS Biol **15**(2): e1002597.
- Julien SG, K. S.-Y., Brunmeir R, Sinnakannu JR, Ge X, Li H, et al (2017). "Narciclasine attenuates diet-induced obesity by promoting oxidative metabolism in skeletal muscle." PLoS Biol **15**(2).
- Kahn BB, A. T., Carling D, Hardie DG (2005). "AMP-activated protein kinase: ancient energy gauge provides clues to modern understanding of metabolism." Cell Metabolism **1**(1): 15-25.
- Kehlet, H., T. S. Jensen and C. J. Woolf (2006). "Persistent postsurgical pain: risk factors and prevention." Lancet **367**(9522): 1618-1625.
- Kehlet H, J. T., Woolf CJ (2006). "Persistent postsurgical pain: risk factors and prevention." Lancet Neurol **367**: 1618-1625.
- Kialka, M., T. Milewicz, K. Sztefko, I. Rogatko and R. Majewska (2016). "Metformin increases pressure pain threshold in lean women with polycystic ovary syndrome." Drug Des Devel Ther **10**: 2483-2490.
- Kimura N, M. S., Tanihara Y, Ueo H, Okuda M, Katsura T, Inui K. (2005). "Metformin is a superior substrate for renal organic cation transporter OCT2 rather than hepatic OCT1." Drug Metabolism and Pharmacokinetics **20**(5): 378-386.

- King-Himmelreich, T. S., C. V. Moser, M. C. Wolters, J. Schmetzer, Y. Schreiber, N. Ferreiros, O. Q. Russe, G. Geisslinger and E. Niederberger (2017). "AMPK contributes to aerobic exercise-induced antinociception downstream of endocannabinoids." Neuropharmacology **124**: 134-142.
- King, T., L. Vera-Portocarrero, T. Gutierrez, T. W. Vanderah, G. Dussor, J. Lai, H. L. Fields and F. Porreca (2009). "Unmasking the tonic-aversive state in neuropathic pain." Nature neuroscience **12**(11): 1364-1366.
- Krukowski, K., N. Eijkelkamp, G. Laumet, C. E. Hack, Y. Li, P. M. Dougherty, C. J. Heijnen and A. Kavelaars (2016). "CD8+ T Cells and Endogenous IL-10 Are Required for Resolution of Chemotherapy-Induced Neuropathic Pain." J Neurosci **36**(43): 11074-11083.
- Laumet, G., J. D. Edralin, R. Dantzer, C. J. Heijnen and A. Kavelaars (2019). "Cisplatin educates CD8+ T cells to prevent and resolve chemotherapy-induced peripheral neuropathy in mice." Pain.
- Lefranc, F., S. Sauvage, G. Van Goietsenoven, V. Megalizzi, D. Lamoral-Theys, O. Debeir, S. Spiegl-Kreinecker, W. Berger, V. Mathieu, C. Decaestecker and R. Kiss (2009). "Narciclasine, a plant growth modulator, activates Rho and stress fibers in glioblastoma cells." Mol Cancer Ther **8**(7): 1739-1750.
- Ling, Y. Z., Z. Y. Li, H. D. Ou-Yang, C. Ma, S. L. Wu, J. Y. Wei, H. H. Ding, X. L. Zhang, M. Liu, C. C. Liu, Z. Z. Huang and W. J. Xin (2017). "The inhibition of spinal synaptic plasticity mediated by activation of AMP-activated protein kinase signaling alleviates the acute pain induced by oxaliplatin." Exp Neurol **288**: 85-93.
- Liu, Y., J. Li, H. Li, Y. Shang, Y. Guo, Z. Li and Z. Liu (2019). "AMP-Activated Protein Kinase Activation in Dorsal Root Ganglion Suppresses mTOR/p70S6K Signaling and Alleviates Painful Radiculopathies in Lumbar Disc Herniation Rat Model." Spine (Phila Pa 1976) **44**(15): E865-e872.
- Lovich-Sapola, J., C. E. Smith and C. P. Brandt (2015). "Postoperative pain control." Surg Clin North Am **95**(2): 301-318.
- Lu, Y., H. M. Xu, Y. Han and Y. L. Zhang (2019). "Analgesic effect of resveratrol on colitis-induced visceral pain via inhibition of TRAF6/NF-kappaB signaling pathway in the spinal cord." Brain Res **1724**: 146464.
- Lubahn, C., J. A. Schaller, E. Shewmacker, C. Wood, D. L. Bellinger, D. Byron, N. Melody, G. R. Pettit and D. Lorton (2012). "Preclinical efficacy of sodium narcistatin to reduce inflammation and joint destruction in rats with adjuvant-induced arthritis." Rheumatol Int **32**: 3751-3760.
- Ma, J., A. Kavelaars, P. M. Dougherty and C. J. Heijnen (2018). "Beyond symptomatic relief for chemotherapy-induced peripheral neuropathy: Targeting the source." Cancer **124**(11): 2289-2298.

- Ma, J., H. Yu, J. Liu, Y. Chen, Q. Wang and L. Xiang (2015). "Metformin attenuates hyperalgesia and allodynia in rats with painful diabetic neuropathy induced by streptozotocin." Eur J Pharmacol **764**: 599-606.
- Maixner, D. W., X. Yan, M. Gao, R. Yadav and H. R. Weng (2015). "Adenosine Monophosphate-activated Protein Kinase Regulates Interleukin-1beta Expression and Glial Glutamate Transporter Function in Rodents with Neuropathic Pain." Anesthesiology **122**(6): 1401-1413.
- Mao-Ying, Q. L., A. Kavelaars, K. Krukowski, X. J. Huo, W. Zhou, T. J. Price, C. Cleeland and C. J. Heijnen (2014). "The anti-diabetic drug metformin protects against chemotherapy-induced peripheral neuropathy in a mouse model." PLoS One **9**(6): e100701.
- Mapplebeck, J. C., S. Beggs and M. W. Salter (2017). "Molecules in pain and sex: a developing story." Mol Brain **10**(1): 9.
- Mee-Inta, O., Z. W. Zhao and Y. M. Kuo (2019). "Physical Exercise Inhibits Inflammation and Microglial Activation." Cells **8**(7).
- Megat, S., P. R. Ray, J. K. Moy, T. F. Lou, P. Barragan-Iglesias, Y. Li, G. Pradhan, A. Wanghzou, A. Ahmad, M. D. Burton, R. Y. North, P. M. Dougherty, A. Khoutorsky, N. Sonenberg, K. R. Webster, G. Dussor, Z. T. Campbell and T. J. Price (2019). "Nociceptor Translational Profiling Reveals the Regulator-Rag GTPase Complex as a Critical Generator of Neuropathic Pain." J Neurosci **39**(3): 393-411.
- Mejia, G. L., M. N. Asiedu, Y. Hitoshi, G. Dussor and T. J. Price (2016). "The potent, indirect adenosine monophosphate- activated protein kinase activator R419 attenuates mitogen-activated protein kinase signaling, inhibits nociceptor excitability, and reduces pain hypersensitivity in mice." Pain Rep **1**(1).
- Melemedjian OK, A. M., Tillu DV, Sanoja R, Yan J, Lark A, Khoutorsky A, Johnson J, Peebles KA, Lepow T, Sonenberg N, Dussor G, Price TJ. (2011). "Targeting adenosine monophosphate-activated protein kinase (AMPK) in preclinical models reveals a potential mechanism for the treatment of neuropathic pain." Molecular Pain.
- Melemedjian, O. K., M. N. Asiedu, D. V. Tillu, R. Sanoja, J. Yan, A. Lark, A. Khoutorsky, J. Johnson, K. A. Peebles, T. Lepow, N. Sonenberg, G. Dussor and T. J. Price (2011). "Targeting adenosine monophosphate-activated protein kinase (AMPK) in preclinical models reveals a potential mechanism for the treatment of neuropathic pain." Mol Pain **7**: 70.
- Melemedjian, O. K. and A. Khoutorsky (2015). "Translational control of chronic pain." Prog Mol Biol Transl Sci **131**: 185-213.
- Melemedjian, O. K., A. Khoutorsky, R. E. Sorge, J. Yan, M. N. Asiedu, A. Valdez, S. Ghosh, G. Dussor, J. S. Mogil, N. Sonenberg and T. J. Price (2013). "mTORC1 inhibition induces pain via IRS-1-dependent feedback activation of ERK." Pain **154**(7): 1080-1091.

- Melemedjian, O. K., Tillu, D. V., Moy, J. K., Asiedu, M. N., Mandell, E. K., Ghosh, S., Dussor, G., Price, T. J (2014). "Local translation and retrograde axonal transport of CREB regulates IL-6-induced nociceptive plasticity." Mol Pain **10**(45).
- Mersfelder, T. L. and W. H. Nichols (2016). "Gabapentin: Abuse, Dependence, and Withdrawal." Ann Pharmacother **50**(3): 229-233.
- Merskey H, B. N. (1986). "Classification of chronic pain. Descriptions of chronic pain syndromes and definitions of pain terms. Prepared by the International Association for the Study of Pain, Subcommittee on Taxonomy." Pain Suppl **3**: S1-226.
- Merskey H, B. N. (1994). "Classification of Chronic Pain: Descriptions of Chronic Pain Syndromes and Definitions of Pain Terms, 2nd Edition." International Association for the Study of Pain (IASP) Press.
- Mifflin, K. A. and B. J. Kerr (2017). "Pain in autoimmune disorders." J Neurosci Res **95**(6): 1282-1294.
- Miller, C. and S. E. Newton (2006). "Pain perception and expression: the influence of gender, personal self-efficacy, and lifespan socialization." Pain Manag Nurs **7**(4): 148-152.
- Myers, R. W., H. P. Guan, J. Ehrhart, A. Petrov, S. Prahalada, E. Tozzo, X. Yang, M. M. Kurtz, M. Trujillo, D. Gonzalez Trotter, D. Feng, S. Xu, G. Eiermann, M. A. Holahan, D. Rubins, S. Conarello, X. Niu, S. C. Souza, C. Miller, J. Liu, K. Lu, W. Feng, Y. Li, R. E. Painter, J. A. Milligan, H. He, F. Liu, A. Ogawa, D. Wisniewski, R. J. Rohm, L. Wang, M. Bunzel, Y. Qian, W. Zhu, H. Wang, B. Bennet, L. LaFranco Scheuch, G. E. Fernandez, C. Li, M. Klimas, G. Zhou, M. van Heek, T. Biftu, A. Weber, D. E. Kelley, N. Thornberry, M. D. Erion, D. M. Kemp and I. K. Sebhat (2017). "Systemic pan-AMPK activator MK-8722 improves glucose homeostasis but induces cardiac hypertrophy." Science **357**(6350): 507-511.
- Neyaz, O., L. Sumila, S. Nanda and S. Wadhwa (2019). "Effectiveness of Hatha Yoga Versus Conventional Therapeutic Exercises for Chronic Nonspecific Low-Back Pain." J Altern Complement Med.
- Ngo, S. T., F. J. Steyn and P. A. McCombe (2014). "Gender differences in autoimmune disease." Front Neuroendocrinol **35**(3): 347-369.
- Nozu, T., S. Miyagishi, S. Kumei, R. Nozu, K. Takakusaki and T. Okumura (2019). "Metformin inhibits visceral allodynia and increased gut permeability induced by stress in rats." J Gastroenterol Hepatol **34**(1): 186-193.
- Pachman, D. R., D. L. Barton, J. C. Watson and C. L. Loprinzi (2011). "Chemotherapy-induced peripheral neuropathy: prevention and treatment." Clin Pharmacol Ther **90**(3): 377-387.
- Pecikoza, U. B., M. A. Tomic, A. M. Micov and R. M. Stepanovic-Petrovic (2017). "Metformin Synergizes With Conventional and Adjuvant Analgesic Drugs to Reduce Inflammatory Hyperalgesia in Rats." Anesth Analg **124**(4): 1317-1329.

- Peltier, A., S. A. Goutman and B. C. Callaghan (2014). "Painful diabetic neuropathy." Bmj **348**: g1799.
- Pierce, K. L., R. T. Premont and R. J. Lefkowitz (2002). "Seven-transmembrane receptors." Nat Rev Mol Cell Biol **3**(9): 639-650.
- Price TJ, B. A., Bresnahan J, Chambers JF, de Koninck Y, Edwards RR, Ji RR, Katz J, Kavelaars A, Levine JD, Porter L, Schechter N, Sluka KA, Terman GW, Wager TD, Yaksh TL, Dworkin RH (2018). "Transition to chronic pain: opportunities for new therapeutics." Nature Reviews Neuroscience in press.
- Price, T. J. and S. M. Geranton (2009). "Translating nociceptor sensitivity: the role of axonal protein synthesis in nociceptor physiology." Eur J Neurosci **29**(12): 2253-2263.
- Price, T. J. and K. E. Inyang (2015). "Commonalities between pain and memory mechanisms and their meaning for understanding chronic pain." Prog Mol Biol Transl Sci **131**: 409-434.
- Qin, X., H. Qiao, S. Wu, J. Cheng, Q. Wan and R. Liu (2018). "Curcumin Inhibits Monocyte Chemoattractant Protein-1 Expression in TNF-alpha induced Astrocytes Through AMPK Pathway." Neurochem Res **43**(4): 775-784.
- Reichling, D. B. and J. D. Levine (2009). "Critical role of nociceptor plasticity in chronic pain." Trends Neurosci **32**(12): 611-618.
- Rena, G., D. G. Hardie and E. R. Pearson (2017). "The mechanisms of action of metformin." Diabetologia **60**(9): 1577-1585.
- Rigby J, M. M. (1997). "Total Synthesis of (+)-Narciclasine." J. Am. Chem. Soc. **119**(51): 12655-12656.
- Riley, J. L., 3rd, G. H. Gilbert and M. W. Heft (1998). "Orofacial pain symptom prevalence: selective sex differences in the elderly?" Pain **76**(1-2): 97-104.
- Robergs, R. A., F. Ghiasvand and D. Parker (2004). "Biochemistry of exercise-induced metabolic acidosis." Am J Physiol Regul Integr Comp Physiol **287**(3): R502-516.
- Russe, O. Q., C. V. Moser, K. L. Kynast, T. S. King, H. Stephan, G. Geisslinger and E. Niederberger (2013). "Activation of the AMP-activated protein kinase reduces inflammatory nociception." J Pain **14**(11): 1330-1340.
- Sato, Y. and T. Ohshima (2000). "The expression of mRNA of proinflammatory cytokines during skin wound healing in mice: a preliminary study for forensic wound age estimation (II)." International Journal of Legal Medicine **113**(3): 140-145.
- Seifarth, C., B. Schehler and H. J. Schneider (2013). "Effectiveness of metformin on weight loss in non-diabetic individuals with obesity." Exp Clin Endocrinol Diabetes **121**(1): 27-31.

- Seretny, M., G. L. Currie, E. S. Sena, S. Ramnarine, R. Grant, M. R. MacLeod, L. A. Colvin and M. Fallon (2014). "Incidence, prevalence, and predictors of chemotherapy-induced peripheral neuropathy: A systematic review and meta-analysis." Pain **155**(12): 2461-2470.
- Severino, A., W. Chen, J. K. Hakimian, B. L. Kieffer, C. Gaveriaux-Ruff, W. Walwyn and J. C. G. Marvizon (2018). "Mu-opioid receptors in nociceptive afferents produce a sustained suppression of hyperalgesia in chronic pain." Pain **159**(8): 1607-1620.
- Shackelford, D. B., E. Abt, L. Gerken, D. S. Vasquez, A. Seki, M. Leblanc, L. Wei, M. C. Fishbein, J. Czernin, P. S. Mischel and R. J. Shaw (2013). "LKB1 inactivation dictates therapeutic response of non-small cell lung cancer to the metabolism drug phenformin." Cancer Cell **23**(2): 143-158.
- Shaw RJ, L. K., Vasquez D, Koo SH, Bardeesy N, Depinho RA, Montminy M, Cantley LC. (2005). "The kinase LKB1 mediates glucose homeostasis in liver and therapeutic effects of metformin." Science **310**(5754): 1642-1646.
- Shiers, S., G. Pradhan, J. Mwirigi, G. Mejia, A. Ahmad, S. Kroener and T. Price (2018). "Neuropathic Pain Creates an Enduring Prefrontal Cortex Dysfunction Corrected by the Type II Diabetic Drug Metformin But Not by Gabapentin." J Neurosci **38**(33): 7337-7350.
- Shin, S. M., I. J. Cho and S. G. Kim (2009). "Resveratrol protects mitochondria against oxidative stress through AMP-activated protein kinase-mediated glycogen synthase kinase-3beta inhibition downstream of poly(ADP-ribose)polymerase-LKB1 pathway." Mol Pharmacol **76**(4): 884-895.
- Simon, L. S. (2012). "RELIEVING PAIN IN AMERICA: A BLUEPRINT FOR TRANSFORMING PREVENTION, CARE, EDUCATION, AND RESEARCH." Journal of Pain & Palliative Care Pharmacotherapy **26**(2): 197-198.
- Singh, A. K. and M. Vinayak (2017). "Resveratrol alleviates inflammatory hyperalgesia by modulation of reactive oxygen species (ROS), antioxidant enzymes and ERK activation." Inflamm Res **66**(10): 911-921.
- Sonenberg, N. and A. G. Hinnebusch (2009). "Regulation of translation initiation in eukaryotes: mechanisms and biological targets." Cell **136**(4): 731-745.
- Song, H., Y. Han, C. Pan, X. Deng, W. Dai, L. Hu, C. Jiang, Y. Yang, Z. Cheng, F. Li, G. Zhang, X. Wu and W. Liu (2015). "Activation of Adenosine Monophosphate-activated Protein Kinase Suppresses Neuroinflammation and Ameliorates Bone Cancer Pain: Involvement of Inhibition on Mitogen-activated Protein Kinase." Anesthesiology **123**(5): 1170-1185.
- Song H, H. Y., Pan C, Deng X, Dai W, Hu L, Jiang C, Yang Y, Cheng Z, Li F, Zhang G, Wu X, Liu W (2015). "Activation of Adenosine Monophosphate-activated Protein Kinase Suppresses Neuroinflammation and Ameliorates Bone Cancer Pain: Involvement of Inhibition on Mitogen-activated Protein Kinase." Anesthesiology **123**(5): 1170-1185.

- Sorge, R. E. and S. K. Totsch (2017). "Sex Differences in Pain." J Neurosci Res **95**(6): 1271-1281.
- Stark, A., R. Schwenk, G. Wack, G. Zuchtriegel, M. G. Hatemler, J. Brautigam, A. Schmidtko, C. A. Reichel, I. Bischoff and R. Furst (2019). "Narciclasine exerts anti-inflammatory actions by blocking leukocyte-endothelial cell interactions and down-regulation of the endothelial TNF receptor 1." Faseb j **33**(8): 8771-8781.
- Szigethy, E., M. Knisely and D. Drossman (2018). "Opioid misuse in gastroenterology and non-opioid management of abdominal pain." Nat Rev Gastroenterol Hepatol **15**(3): 168-180.
- Takaishi, Y., M. Okada, D. Fujiwara, A. Uyama, T. Kondoh and A. Arai (2019). "[Surgical Results of Lumbar Degenerative Disease with Foot Drop]." No Shinkei Geka **47**(8): 851-857.
- Tao, L., Q. Ding, C. Gao and X. Sun (2016). "Resveratrol attenuates neuropathic pain through balancing pro-inflammatory and anti-inflammatory cytokines release in mice." Int Immunopharmacol **34**: 165-172.
- Taylor, A., A. H. Westveld, M. Szkudlinska, P. Guruguri, E. Annabi, A. Patwardhan, T. J. Price and H. N. Yassine (2013). "The use of metformin is associated with decreased lumbar radiculopathy pain." J Pain Res **6**: 755-763.
- Taylor, B. K. and G. Corder (2014). "Endogenous analgesia, dependence, and latent pain sensitization." Curr Top Behav Neurosci **20**: 283-325.
- Tillu, D. V., O. K. Melemedjian, M. N. Asiedu, N. Qu, M. De Felice, G. Dussor and T. J. Price (2012). "Resveratrol engages AMPK to attenuate ERK and mTOR signaling in sensory neurons and inhibits incision-induced acute and chronic pain." Mol Pain **8**: 5.
- Tillu, D. V., O. K. Melemedjian, M. N. Asiedu, N. Qu, M. De Felice, G. Dussor and T. J. Price (2012). "Resveratrol engages AMPK to attenuate ERK and mTOR signaling in sensory neurons and inhibits incision-induced acute and chronic pain." Mol Pain **8**(5): 1744.
- Tillu DV, M. O., Asiedu MN, Qu N, De Felice M, Dussor G, Price TJ (2012). "Resveratrol engages AMPK to attenuate ERK and mTOR signaling in sensory neurons and inhibits incision-induced acute and chronic pain." Mol Pain **8**(5): 1744-8069.
- Treacarichi, A. and S. J. L. Flatters (2019). "Mitochondrial dysfunction in the pathogenesis of chemotherapy-induced peripheral neuropathy." Int Rev Neurobiol **145**: 83-126.
- Trigunaite, A., J. Dimo and T. N. Jorgensen (2015). "Suppressive effects of androgens on the immune system." Cell Immunol **294**(2): 87-94.
- Tsuda, M. (2016). "Microglia in the spinal cord and neuropathic pain." J Diabetes Investig **7**(1): 17-26.

- Turner R, C. C., Holman R (1998). "United Kingdom Prospective Diabetes Study 24: A 6-Year, Randomized, Controlled Trial Comparing Sulfonylurea, Insulin, and Metformin Therapy in Patients with Newly Diagnosed Type 2 Diabetes That Could Not Be Controlled with Diet Therapy." Annals of Internal Medicine **128**(3): 165-175.
- Van Goietsenoven, G., J. Hutton, J. P. Becker, B. Lallemand, F. Robert, F. Lefranc, C. Pirker, G. Vandebussche, P. Van Antwerpen, A. Evidente, W. Berger, M. Prevost, J. Pelletier, R. Kiss, T. G. Kinzy, A. Kornienko and V. Mathieu (2010). "Targeting of eEF1A with Amaryllidaceae isocarboxtyrils as a strategy to combat melanomas." Faseb j **24**(11): 4575-4584.
- Victorri-Vigneau, C., M. Guerlais and P. Jolliet (2007). "Abuse, dependency and withdrawal with gabapentin: a first case report." Pharmacopsychiatry **40**(1): 43-44.
- Walwyn, W. M., W. Chen, H. Kim, A. Minasyan, H. S. Ennes, J. A. McRoberts and J. C. Marvizon (2016). "Sustained Suppression of Hyperalgesia during Latent Sensitization by mu-, delta-, and kappa-opioid receptors and alpha2A Adrenergic Receptors: Role of Constitutive Activity." J Neurosci **36**(1): 204-221.
- Wang, L., H. Shan, B. Wang, N. Wang, Z. Zhou, C. Pan and F. Wang (2018). "Puerarin Attenuates Osteoarthritis via Upregulating AMP-Activated Protein Kinase/Proliferator-Activated Receptor-gamma Coactivator-1 Signaling Pathway in Osteoarthritis Rats." Pharmacology **102**(3-4): 117-125.
- Weihrauch, M. and C. Handschin (2018). "Pharmacological targeting of exercise adaptations in skeletal muscle: Benefits and pitfalls." Biochem Pharmacol **147**: 211-220.
- Weng, W., C. Yao, K. Poonit, X. Zhou, C. Sun, F. Zhang and H. Yan (2019). "Metformin relieves neuropathic pain after spinal nerve ligation via autophagy flux stimulation." J Cell Mol Med **23**(2): 1313-1324.
- Wieland, L. S., N. Skoetz, K. Pilkington, R. Vempati, C. R. D'Adamo and B. M. Berman (2017). "Yoga treatment for chronic non-specific low back pain." Cochrane Database Syst Rev **1**: Cd010671.
- Winder, W. W. and D. G. Hardie (1996). "Inactivation of acetyl-CoA carboxylase and activation of AMP-activated protein kinase in muscle during exercise." Am J Physiol **270**(2 Pt 1): E299-304.
- Wu, W., S. Wang, Q. Liu, T. Shan and Y. Wang (2018). "Metformin Protects against LPS-Induced Intestinal Barrier Dysfunction by Activating AMPK Pathway." Mol Pharm **15**(8): 3272-3284.
- Xiang, H. C., L. X. Lin, X. F. Hu, H. Zhu, H. P. Li, R. Y. Zhang, L. Hu, W. T. Liu, Y. L. Zhao, Y. Shu, H. L. Pan and M. Li (2019). "AMPK activation attenuates inflammatory pain through inhibiting NF-kappaB activation and IL-1beta expression." J Neuroinflammation **16**(1): 34.

- Xie, W., J. A. Strong and J. M. Zhang (2017). "Active Nerve Regeneration with Failed Target Reinnervation Drives Persistent Neuropathic Pain." eNeuro **4**(1).
- Yui, S., M. Mikami, Y. Mimaki, Y. Sashida and M. Yamazaki (2001). "Inhibition effect of Amaryllidaceae alkaloids, lycorine and lycoricidinol on macrophage TNF-alpha production." Yakugaku Zasshi **121**: 167-171.
- Zhang, B. B., G. Zhou and C. Li (2009). "AMPK: an emerging drug target for diabetes and the metabolic syndrome." Cell Metab **9**(5): 407-416.
- Zhang L, N. J., Zhang X, He W (2019). "Metformin Can Alleviate the Symptom of Patient with Diabetic Nephropathy Through Reducing the Serum Level of Hcy and IL-33." Open Med (Wars) **14**: 625-628.
- Zhang, L. N., L. Xu, H. Y. Zhou, L. Y. Wu, Y. Y. Li, T. Pang, C. M. Xia, B. Y. Qiu, M. Gu, T. C. Dong, J. Y. Li, J. K. Shen and J. Li (2013). "Novel small-molecule AMP-activated protein kinase allosteric activator with beneficial effects in db/db mice." PLoS One **8**(8): e72092.
- Zhu, H., J. Ding, J. Wu, T. Liu, J. Liang, Q. Tang and M. Jiao (2017). "Resveratrol attenuates bone cancer pain through regulating the expression levels of ASIC3 and activating cell autophagy." Acta Biochim Biophys Sin (Shanghai) **49**(11): 1008-1014.

BIOGRAPHICAL SKETCH

Kufreobong Inyang was born in Dallas, Texas but moved to Huntsville, Texas at the age of 3. After completing his schoolwork at Huntsville High School, Kufre attended Cornell University in Ithaca, New York in the Fall of 2008. He received a bachelor's in Science and Technology Studies in the Spring of 2012. During the next year, Kufre attended Sam Houston State University as a post-baccalaureate student before starting graduate school at The University of Texas at Dallas in the Fall of 2013. Kufre began working in Dr. Price's pain lab in May 2014. He received a master's degree in Applied Cognition and Neuroscience in the Spring of 2015. In August 2015, Kufre returned to The University of Texas at Dallas to pursue a doctorate degree in neuroscience.

CURRICULUM VITAE

Kufreobong E Inyang

Research Interests

My current dissertation research is focused on the use of AMPK activators to prevent the transition from acute to chronic pain.

Academic History

University of Texas at Dallas **Richardson, Texas**
PhD, Cognition and Neuroscience *December 2019*

University of Texas at Dallas **Richardson, Texas**
Master of Science, Applied Cognition and Neuroscience *May 2015*

Cornell University **Ithaca, New York**
Bachelor of Arts, Science and Technology Studies *May 2012*

Research/Teaching Experience

Research Assistant **Richardson, Texas**
University of Texas at Dallas *May 2014 – present*

- This involves running behavioral experiments, biochemical experiments, confocal microscopy and data analysis as well as teaching lab skills to undergraduate lab technicians.

Teaching Assistant **Richardson, Texas**
University of Texas at Dallas *August 2015 – present*

- This involves leading weekly review sessions, grading exams, running experiments and holding office hours with students.

Professional Experience

Supervisor

Richardson, Texas

University of Texas at Dallas Activity Center

October 2013 – December 2014

- My duties included managing building staff employees to ensure gym safety.

Presentations

Society for Neuroscience 2019

Optimizing pharmacological targeting of AMPK for treatment of paclitaxel-induced peripheral neuropathy

Kufreobong E Inyang¹, Timothy McDougal¹, Eric Ramirez¹, Marisa Williams¹, Annemieke Kavelaars², Cobi Heijnen², Geoffroy Laumet², Michael Burton¹, Gregory Dussor¹, Theodore J Price¹

International Association for the Study of Pain 2018

The AMPK activator narciclasine prevents and reverses paclitaxel-induced peripheral neuropathy

Kufreobong E Inyang, Eric Ramirez, Marisa Williams, Michael Burton, Gregory Dussor, Theodore J Price

Society for Neuroscience 2017

Metformin reverses neuropathic and post-surgical pain and spinal microglial activation specifically in male mice.

Inyang KE, Burton MD, Szabo-Pardi T, Wentworth E, Dussor G, Price TJ

American Pain Society 2016

Treatment of Chronic pain: long term effects of metformin on chronic neuropathic pain and microglial activation

Inyang K, Szabo-Pardi T, Price TJ

Publications

Alleviation of paclitaxel-induced mechanical hypersensitivity and hyperalgesic priming with AMPK activators in male and female mice.

Inyang KE, McDougal TA, Ramirez ED, Williams M, Laumet G, Kavelaars A, Heijnen CJ, Burton M, Dussor G, Price TJ. *Neurobiol Pain*. 2019 Sep 27;6:100037. doi: 10.1016/j.ynpai.2019.100037

Indirect AMPK activators prevent incision-induced hyperalgesia and block hyperalgesic priming while positive allosteric modulators only block priming in mice.

Inyang, K., Burton, Michael D, Szabo-Pardi, Thomas, Wentworth, Emma, McDougal, Timothy A, Ramirez, Eric D, Pradhan, Grishma, Dussor, Gregory, Price, Theodore (2019). Journal of Pharmacology and Experimental Therapeutics: jpet.119.258400.

The antidiabetic drug metformin prevents and reverses neuropathic pain and spinal cord microglial activation in male but not female mice.

Inyang KE, Szabo-Pardi T, Wentworth E, McDougal TA, Dussor G, Burton MD, Price TJ.

Pharmacol Res. 2019 Jan;139:1-16.

Pharmacological activation of AMPK inhibits incision-evoked mechanical hypersensitivity and the development of hyperalgesic priming in mice.

Burton MD, Tillu DV, Mazhar K, Mejia GL, Asiedu MN, **Inyang K**, Hughes T, Lian B, Dussor G, Price TJ.

Neuroscience. 2017 Jul 17. pii: S0306-4522(17)30490-6

(309) Treatment of Chronic pain: long term effects of Metformin on chronic neuropathic pain and microglial activation.

Inyang K, Szabo-Pardi T, Price T.

J Pain. 2016 Apr;17(4S):S53.

Commonalities between pain and memory mechanisms and their meaning for understanding chronic pain.

Price TJ, **Inyang KE**.

Prog Mol Biol Transl Sci. 2015;131:409-34.